**جمهورية العراق**
**وزارة التعليم العالي والبحث العلمي**
**جامعة بابل/ كلية العلوم**
**قسم الفيزياء**

# تصميم و تمثيل نظام حصاد الطاقة من الترددات الراديوية المحيطة

أطروحة مقدمة إلى

مجلس كلية العلوم في جامعة بابل

وهي جزء من متطلبات نيل درجة دكتوراه فلسفة في العلوم // الفيزياء

من قبل

**ابتسام عمران راضي حمادي**

بكالوريوس علوم فيزياء 1998

ماجستير علوم فيزياء 2005

إشراف

**ا.م.د. سميرة عدنان مهدي** **ا.د.حسن جاسم مطلك**

**1443هـ** **2022 م**

**Republic of Iraq**
**Ministry of Higher Education and Scientific Research**
**University of Babylon**
**College of Science**
**Department of Physics**

# Design and Implementation of Energy Harvesting from an Ambient Radio Frequencies

***A Thesis***

***Submitted to the Council of the College of Science, University of Babylon in Partial Fulfillment of the Requirements for the Degree of Doctorate of Philosophy in Physics***

***by***

**Ibtesam Omran Radi Hamadi**

**B.Sc. in Physics / 1998**

**M.Sc. in Physics / 2005**

**Asst. Prof. Dr.** **Samira Adnan Mahdi**

**Prof. Dr.** **Hassan Jassim Motlak**

**2022 A.D** **1443 A.H**

بسم الله الرحمن الرحيم

" قَالُوا سُبْحَانَكَ لَا عِلْمَ لَنَا إِلَّا مَا عَلَّمْتَنَا
إِنَّكَ أَنْتَ العَلِيمُ الحَكِيمُ "

صدق الله العلي العظيم

سورة البقرة الآية (٣٢)

"

# *Dedication*

*To everyone  who has ever taught me a letters*

*To my father and mother : May Almighty Allah have mercy you*

*To all my cherished brothers and sisters*

*To my devoted husband and my two kids, Ahmed and Mustafa*

*Thank you to everyone who has helped and supported me, even if it has simply been with a nice word.*

*Ibtasam*

# Acknowledgments

In The Name of Allah, The Most Beneficent, The Most Merciful. All praise and thanks to Allah, the Lord of the universe. Prayers and peace be upon his prophet, Mohammed, and his progeny.

First of all, I would like to express my deepest thanks and appreciation to my supervisors, Assist. Prof. Dr. Samira Adnan Mahdi and Prof. Dr. Hassan Jassim Motlak for their supervision and their valuable directions and opinions

I am greatly indebted to the staff of the physics department in the college of sciences at Babylon University for their provision of facilities and continuous support .

My deep thanks and grateful to Mr. Ali shaban for his scientific help and advice. I would like to express my deep appreciation to all members of my family for their material and spiritual support .

Last but not least, I'd like to express my gratitude to all my friend who provided me with encouragement, assistance, and constant contact.

Ibtasam

# Summary

The appropriate Radio frequency (RF )source is the foundation of any RF energy harvesting model. In this work a thorough examination of the various radio frequency sources Digital television, Global system for mobile communications, and Wireless fidelity (DTV, GSM, WiFi) has been presented. As a renewable energy sources that are available in the frequency range 400MHz - 3GHz of an electromagnetic signals

To convert the energy of electromagnetic (EM ) waves into a direct current ( DC )voltage, In this work an electronic circuits have been built using several electronic components such as diodes, capacitors, and an antenna. The relationship between the output voltage and the charging time of the capacitor was determined using various types of multi-voltage circuits consisting of a voltage doubling circuit for stages ranging (3, 5, 7,10,and 12).

Using a series of voltage doubling circuits, the output power of the electric current was measured. The relationship between the number of phases and the output power was set . Parallel circuits were built for a three-phase voltage doubling circuit consisting of two parallel circuits to eight circuits in order to boost the efficiency of the voltage doubling circuits. The ambient radio frequency was measured according to the city of Hilla, where it is in Iraq.

The voltage doubling circuit was simulated using ADS (Advanced Design System 2020 64-bit Simulations) software. The output voltages of the three, five, seven, ten, and twelve voltage doubling circuit were (5.6, 9, 11, 13, and 12) Volt respectively. The results showed that the output voltage of the stages (3 ,5, 7) is significant, but there is a steep slope of the output voltage of the phases 10 and 12.

The efficiency of the stage circuits (3, 5, 7,10,and12) which was calculated. The results have been plotted as a function of the input power under the frequency ranges (400-680) MHz, (700-900) MHz, and (2.5) GHz, respectively. Demonstration that at three stages, more efficient, with max value( 15.4) % for frequency (2.5) GHz at load (4)KΩ. And as the number of steps increases, the efficiency decreases. The greatest efficiency in a five-phase circuit was (3, 4, and 5)% for all frequency ranges respectively. In a seven-phase circuit, the highest efficiency values were (3, 4, and 5)%. In a ten-phase and twelve-phase circuits, the efficiency is very low .

To maximize the amplification circuits efficiency, a model of an energy harvesting system has been designed as a parallel stages (two , three , four, five , six, seven, and eight) stages for a voltage doubling circuit with three phases. The circuit becomes more efficient as the parallel phases of a three-phase voltage- doubling circuit grow. This is the result of putting the current values together. As a result, the output voltage rises while the load decreases.

In practically, testing the circuit for three phases yielded the maximum voltage of (2.1) Volt and an efficiency of (4.8 ) % within the frequency range (850-960) MHz. The maximum voltage value within the frequency range of (2.11-2.17) GHz was (2.3) Volt, while the efficiency value was (5.3) %.

A two-phase parallel circuit was implemented for a three-stage circuit, yielding a (26) % efficiency.

# Chapter One

# Introduction

## 1-1: Introduction

Energy-harvesting low-power systems considered as a remarkable and valuable hotspot of an expanding both energy efficiency and spectral efficiency. Radio Frequency (RF) energy is currently broadcasted from billions of radio transmitters around the world, including mobile telephones, handheld radios, mobile base stations, and television and radio broadcast stations. There are a number of alternative ways to extract energy from the surroundings and convert it into electrical energy. To feed the low power electronic circuits directly or gather then for later on use for example, an energy from the radio frequency[1].

The major concern for these devices is typically the battery life and replacement. The ability to harvest RF energy from ambient or dedicated sources enables wireless charging of low-power devices and has resultant benefits to produce design usability and reliability. Battery-based systems can be trickled charged to eliminate battery replacement or extend the operating life of systems using disposable batteries. Battery-free devices can be designed to operate upon demand or when a sufficient charge is accumulated. In both cases, these devices can be free of connectors, cables, and battery access panels, and have freedom of placement and mobility during charging and usage. However, since the power density of the ambient RF power is extremely small. It is very challenging to design RF energy-harvesting systems with satisfying RF-to-D.C power conversion efficiencies (PCEs) [2,3].

The decrease in electronic components consumption has led to the development of wireless devices. Unlike most energy sources, the Electromagnetic ( EM ) or Radio Frequency (RF) energy sources are continuously available when multiple RF energy sources are available. The amount of energy harvested can be increased if the system is designed to work over a wide frequency band. Ambient RF energy is present in various frequency bands As shown in the Table1.1 [4].

**Table(1.1): Ambient RF energy in various frequency bands[4].**

| Meaning | Abbreviations | Range of frequency |
|---|---|---|
| **Digital television** | **DTV** | **(550-600)MHz** |
| **Long term evolution** | **LTE** | **(750-800)MHz** |
| **Global system for mobile communications** | **GSM900** | **(850-910)MHz** |
| | **GSM1800** | **(1850-1900)MHz** |
| **Universal mobile telecommunications system** | **UMTS** | **(2150-2200)MHz** |
| **Wireless fidelity** | **Wi-Fi** | **(2.4-2.45)GHz** |
| **Band for radio and television** | | **(900MHz–2GHz)** |
| **Industrial, Scientific, and Medical** | **ISM** | **(2.1–2.6)GHz** |
| **Wireless local area network** | **WLAN** | **(3.1–4.4)GHz** |

The RF harvester measurements show that the proposed stacked multi-band RF harvester is able to supply typical electronic devices. It can charge low power devices such as watches, calculator (10) $\mu$Watt, Hearing aids, temperature sensors (100) $\mu$Watt, Active Radio-frequency Identification (RFID) 1 mW [5]. Finite electrical battery life encourages businesses and engineers to develop innovative concepts and inventions to

power portable electronic devices over an indefinite or extended period of time [2,3].

Wind, solar, vibration, thermoelectric, temperature gradient, radio frequency (RF), acoustic, and other external atmospheric energy sources are the most often considered and used for energy harvesting [5]. In fact, due to the high receiver sensitivity of cell phone antennas, only a few milliwatts of RF power can be scavenged from the environment for mobile communication. The main cause of such a drastic decrease in transmitted power is absorption by a obstacles in the direction of the RF waves, as well as power loss in the form of heat in materials where it is absorbed. Most portable machines, such as cell phones, use only a few microwatts or milliwatts of power in their sleep and active modes, respectively [2,3].

## 1-2: Literature survey

In (2010) **Bouchouicha D.*et al.*,**[6] measured ambient RF power density for two systems: the first is a broadband device without a matching circuit, and the second is a narrow band (1.8-1.9) GHz system with a matching circuit. The power density fluctuation in the ( 680MHz-3.5GHz) range is determined to be between (-60 and -14.5) $dBm/m^2$, ($1nW/m^2$ and 35.5 $W/m^2$) .This power density was tested at its highest in the (1.8-1.9) GHz range. The total of all observed power densities indicates a higher power density of about (12) $dBm/m^2$. The gain is more than 2.5dBi over the whole frequency range (1-3) GHz. At a frequency of 3 GHz, the gain can approach (7) dBi. The efficiency of the rectifier is in the range of (0.6)%.

In the same year **Ojaroudi M. *et al.*,**[ 7] presented A new printed monopole antenna for ultra-wide band applications. The suggested antenna is made up of a square radiating patch with an inverted T-shaped slot and a ground plane with an inverted T-shaped conductor-backed plane. From (2.9 to 14.1) GHz, the manufactured antenna meets the (10) dB return loss criterion. By severing a modified inverted T-shaped slot with changeable size from the radiating patch and inserting an inverted T-shaped. At (4 and 10) GHz, as well as (12.2 and 14.4) GHz, there is reasonable agreement between models and observations.

In(2011) **Mikeka C. *et al.*,**[8] studied a design architecture for a micro power RF energy harvesting in the Digital TV (DTV) band. Given a single tone excitation at( 550) MHz, the rectifying antenna (rectenna) has a measured conversion efficiency of 0.4 percent for (-40) dBm input and (18.2 )% for (-20) dBm input, respectively. Along with this rectenna, a DC boost converter circuit is designed and built.

Also in this year **Arrawatia M. *et al.*,**[9] studied an experimental RF energy harvesting device is being capture energy from cell towers. A square microstrip antenna that is linked has a gain of (9.1) dB with a bandwidth ranging from (877 to 998) MHz. A single stage voltage doubler and a six-stage voltage doubler based on Schottky diodes have also been built for DC voltage production. The measured findings reveal that at a distance of (10)m from the cell tower, a voltage of (2.78)V is obtained, and at a distance of (50) m, a voltage of (0.87)V is obtained.

In(2012) **Md Din N. *et al.*,**[3] studied an RF energy harvesting system that can harvest energy from the ambient surroundings at the downlink radio frequency range of the GSM-900 band. The system design

consists of three modules: a single wideband 377- E-shaped patch antenna, a pi matching network, and a 7-stage voltage doubler circuit. These three modules were fabricated on a single printed circuit board. The antenna and Pi matching network have been optimized through electromagnetic simulation software in the Agilent advanced design system (ADS) 2009 environment. The DC voltage obtained from the harvester system in the field test at an approximate distance of (50) m from the GSM cell tower was (2.9) V.

In same year **Nintanavongsa P. *et al.*,** [10] they propose a dual-stage energy harvesting circuit composed of a seven-stage and ten-stage design for Villard multiplier and Dickson multiplier simulation is a modified voltage multiplier of HSMS-2852 and MSP430G2553. Each stage is organized into series. The operational point for these two stages, is between the high (20 ) dBm and low power ( -20 ) dBm extremities . run out designed on a printed circuit board to demonstrate how such a circuit can run a commercial Mica2 sensor mote. Throughout the (-20 to 7) dBm range, the suggested prototype delivers a greater voltage than the power cast P1100. The power cast P1100's output voltage remains constant at (3.3) V at (20 ) dBm. This is due to the power cast P1100's built-in voltage regulator, which begins to regulate its output voltage at (7) dBm at a voltage of (3.3) V.

In (2013) **Hong S. *et al.*,**[11] suggested rectenna architecture which consists of a receiving antenna attached to a rectifying circuit. A seven stage Cockroft-Walton voltage multiplier optimized for low input power (below 0 dBm) is proposed. The prototype was fabricated on an RT/Duroid 5880 (RO5880) printed circuit board( PCB) substrate with a dielectric constant and loss tangent of (2.2) and (0.0009) respectively.

Experimental results show that( 2 )V output voltage can be harvested from an operating frequency of (2.48 ) GHz.

Also in this year (2013) **Barroca N. *et al*.**,[ 12] determine spectrum possibilities for RF energy harvesting to power wireless sensor nodes in real-world indoor/outdoor settings. power density observations ranging from (350) MHz to (3 ) GHz It is proposed to use a dual-band band printed antenna working at GSM bands (900/1800), with gains on the order of 1.8-(2.06) dBi and an efficiency of (77.6-84)%. They discussed the recommendations for building energy harvesting circuits in a situation where a wireless body area network (WBAN) is supported by a TX91501 power east RF dedicated transmitter and a five-stage Dickson voltage multiplier responsible for collecting the RF energy. The range input power ranges from ( -27 -37 ) dBm .

In (2014) **Ali E.*et al.,***[13] studied design of voltage doubler stages for RF energy harvesting device based on the HSMS-2850 Schottky diode. The architecture is based on the Villard voltage doubler circuit, which is optimized for the 900 MHz frequency range. They made simulations of a three-stage Schottky diode voltage doubler circuit by using ADS software .They obtained output voltage of (6.335 )V, which is considered optimal for GSM applications.

In same year **Akter N.*et al.,***[14] provided an improvement of the voltage doublers stages in an energy conversion module for Radio Frequency (RF) energy harvesting system at (950) MHz band is presented. An ADS simulator was used to design a 10-stage voltage multiplier RF energy harvesting circuit, which produces approximately (5) Volt at (0 ) dBm and amaximum of (36.489) %. Two 10 stage voltage multipliers were

designed and the Agilent diode HSMS-2850 and HSMS-2822 were compared, and finally, it was confirmed that the HSMS-2850 works much better than the HSMS-2822 diode. The proposed system can be used to power low power sensors in sensor networks ultimately in place of batteries.

In(2015)**Siddhesh S. and Roshan L.**,[15]designed an antenna for the frequency range of (2110-2170)MHz. A rectifier circuit with (12 ) stages of a voltage doubler circuit was simulated and built. The voltage output of the voltage doubler circuit was calculated to be (3.764)V. The measured voltage, on the other hand, was (1.53)V. The reason for the loss in power is the use of the SMA connector **(**SubMiniature version A, connectors are semi-precision coaxial RF connectors*).*

Also in this year **Lee T. *et al.*,**[16] studied energy harvesting applications requiring low input power levels, an efficient rectifier operating at (2.45 )GHz is used. For functioning at low input power levels, a single diode shunt-mounted architecture is used. At( -20) dBm of input power, the efficiency is (27.7) %, (39.2 )% at (-15) dBm, and (51.2) percent at (-10 ) dBm. At (-0.4 ) dBm input power, the maximum efficiency of (61.7)% is achieved.

In (2016) **Zeng M. *et al.*,**[17] suggested two rectifiers (differential serial rectifier and differential doubler rectifier) at GSM 1800 band (1.83) GHz. The rectifiers with Schottky diodes (SMS7630) are fabricated on aTeflon substrate. The proposed rectifiers are compact, low-cost, power sensitive, and can be used in the RF energy harvesting system. Measured maximum efficiencies of two rectifiers are (49% ) at (0) dBm

and (53)% at (2) dBm, and the highest output voltage (1.9, 3.17)V respectively.

Also in this year **Bakkali A. *et al.,***[18] suggested a novel dual-band rectenna ,This rectenna is created from a dual-band antenna and a dual-band rectifier which operates at GSM bands (900 MHz and 1800 MHz). The printed monopole antenna is miniaturized by two meander-lines. The received signal from the receiving antenna is rectified by a voltage double using a Schottky diode, SMS-7630. The output voltage ranges from (183-415) mV.

In (2017) **Shanpu S. *et al.,***[19] proposed a broadband design L-probe microstrip patch rectenna for ambient RF energy harvesting. The antenna L-probe microstrip patch has a wide band capability. For power harvesting, ambient radio frequency signals from the UMTS-2100 band (2110-2170) MHz and WLAN spectrum (2400-2500) MHz are received. In advance, wideband antenna L-probe microstrip patch simulation and measurement effects. It indicates that the RF-DC efficiency over the UMTS-2100 band and WLAN band are around( 25- 20)%, providing good dual-band characteristics of the rectifier under low input power.

In same year **Song C. *et al.,***[20] studied a novel rectenna with a wide , operates at four different frequency bands from (1.1 to 2.8) GHz. Over (60)% energy conversion efficiency is achieved for the desired frequency band, rectenna a much-simplified structure and reduced cost. The capacitors are typical (100 ) nF chip capacitors from Murata, the rectifying diodes are Schottky diodes HSMS2852 from Avago, and a typical (2000) n resistor is used as the load.

In(2018) **Amjad O. *et al.*,**[21] shows the design and analysis of a dual-band microstrip patch antenna working at (2.4 and 5.8) GHz, an impedance matching network, a 4-stage voltage doubler, and a storage circuit for RF energy harvesting. The antenna was developed with ADS Agilent and sonnet suite software, and it has a directivity of (5.5) dBi at (2.4) GHz and (6.3) dBi at (5.8) GHz. The constructed antenna's measured findings correspond well with the simulated results. Simulated findings demonstrate that for a (10 ) mW input received power, the proposed system can deliver (4.5) mW power at the output of a 4-stage voltage rectifier with a (45 )% overall efficiency at a (10) KOhm output resistance.

Also in this year **Sedeek A.*et al.*,**[22 ] presented a( 2.45 ) GHz low power rectifier that harvests radio frequency (RF) energy via a 180° hybrid junction. When compared to a standard Greinacher voltage doubler rectifier, this rectifier has higher efficiency at low input power levels. The proposed rectifier has two rectifying branches and two output ports.Each rectifying branch is based on the Greinacher voltage doubler arrangement, however each branch has just one rectifying diode and only one diode. It is simulated using (ADS). The maximum power conversion efficiency (PCE) of (70)% is compared to a maximum PCE of( 51)% for the conventional voltage doubler circuit.

In(2019) **Filiz S. and Yunus U.**,[23] studied Voltage multiplier circuits (Villard, Dickson, and Greinacher) without impedance matching . the impacts of load resistance, input power, and input frequency are examined and compared. (ADS) is a simulation tool. These voltage multipliers are built with HSMS 2852 Schottky diodes and capacitors. The results demonstrate that identifying load resistance is crucial for assessing high efficiency; efficiency differences of up to (33) % are achieved for the

Dickson voltage multiplier at 100 MHz input frequency. the Greinacher voltage multiplier achieves the highest efficiency for low input frequencies of less than (1) GHz, while no significant variations are seen for high frequencies. The Greinacher voltage multiplier is the ideal choice for achieving high efficiency in low frequency RF harvesting applications.

In same year **Park S.*et al.*,**[24] studied avoltage multiplier that is a hybrid of a Cockcroft-Walton multiplier and a Dickson charge pump . As the number of multiplier stages rises in the Cockcroft-Walton construction, the output voltage drops significantly under load. This is due to the fact that all coupling capacitors are linked in series. The Dickson charge pump solves this problem by connecting all capacitors in parallel. The suggested hybrid structure organizes certain capacitors in parallel and others in series, resulting in a minimal output voltage drop and low capacitor voltage stress. They were test of hybrid multipliers. They also show a (60 - 2.25 ) KV D.C-D.C converter based on a 16-stage hybrid voltage multiplier with a voltage gain of (12.8) and a maximum capacitor voltage stress of (660) V.

In (2020) **Nguyen C. *et al.*,** [25] studied a hybrid solar-radio frequency (RF) harvesting system capable of supplying electricity for the continuous and efficient operation of electrically propelled wheelchairs This system can gather electricity from both an RF and a solar source that are both available in the surrounding environment. The standalone solar system is equipped with a maximum power point tracking (MPPT) and a boost converter, whilst the standalone RF system is outfitted with a 9-stage Voltage Multiplier (VM). The charging voltage level is calculated by

summing the output voltages of each source. producing a charging current of (16) Amps and a voltage of (24 )Volts.

Also in this year **Tafekirt H. *et al.*,**[26] studied a triple-band power receiver for RF energy harvesting systems where GSM-900, GSM-1800, and Wi-Fi-2450 bands are available. Using the improved impedance matching technique, which consists of three parallel branches Each branch contains a narrowband matching network . Each branch is connected by a single voltage doubler made of HSMS-28 52 Schottky diodes. A rectifier circuit was built and tested to compare its performance to the Simulation findings. The observed RF to DC conversion efficiency is (33.7, 21.8, and 20 )% at (0.9, 1.8, and 2.45) GHz, respectively, with an optimal load resistance of (3.8) KOhm at (-10) dBm input power level. Under (0 ) dBm input power, the efficiency is more than (46.5) % for all bands of interest.

In (2021) **Ali E. *et al.*,** [27] investigate an analytical novel mode designed for RF energy harvesting systems to investigate the voltage and current output of rectifier stages for efficiency optimization. A seven-stage voltage multiplier rectification circuit is included in the design. For the circuit modeling voltage multiplier circuit, the Schottky diode HSMS 285C was chosen. The equations of the theoretical model derived with MATLAB code were validated using ADS simulation. The manufactured system was tested throughout a (10) W to (100 ) mW input power range, with a maximum output power of (0.2577) mW and a maximum efficiency of (29.85)%.

In same year **Yalcin A.** and **Filiz S.**,[28] designed a multi-band RF energy harvesting circuit. The output voltage and power of the system built at frequencies of (900, 1800, and 2450) MHz are revealed. The (ADS)

2017 program is used for all simulations. The load resistances that provide the most power at each frequency are determined, and the appropriate load is chosen for all three frequencies. Then, using the selected load, a multi-stage Dickson Voltage Multiplier (DVM) with two to six stages is designed, and the number of stages providing the maximum power for each frequency is determined. L type and type impedance matching have been used to achieve the highest output power in a DVM design with this number of stages and two Schottky diode models (HSMS-2852). Finally, Thus efficiency of the triple band reaches (83.37)% where it reaches approximately (44, 32 and 30 )% efficiency for (900, 1800 and 2450 ) MHz respectively.

In(2022) **Surender, *et al.***,[29] suggested a single band circularly polarized (CP) rectenna for smart city applications that operates at a (2.45) GHz Wi-Fi band and employs a hexagonal form of a microstrip radiator and a voltage doubler rectifier. The suggested antenna exhibits omnidirectional radiation behavior, which aids in the collection of RF energy from its surroundings. The SMS7630-005 LF diode is used in a voltage doubler configuration to design a rectifier circuit with a maximum conversion efficiency of (65.1) % and an output voltage of (1.65) V at an input power of ( 0) dBm for a load resistance value of (4.1) KOhm, which is very much suitable for powering low power sensing devices.

In same year **Roy, S. *et al.*,[30]** introduced a novel impedance matching network is with novel broadband rectifying components to better align the usable RF signals with comparatively lower RF power density levels. The highly sensitive full-wave rectifier circuit is intended to strengthen the low power sensitivity. The simulated and measured performances have shown that the harvester has a maximum D.C.

rectification efficiency of about (52 )% for (−20) dBm input RF power from (0.9 to 2.6) GHz. Measurement in an ambient RF setting shows that the proposed harvester is able to harvest dc energy at (−20) dBm up to (0.678) V. This harvester can be used for ambient wireless RF energy scavenging for a huge number of wireless devices and network applications.

## 1-3:Aim of the study

The main aims of this research are:

1-Obtaining a source of renewal energy.

2-Searching ambient frequencies in space for getting an electrical energy.

3-Identify the frequencies that can be received and useful for high energies.

4-Using different types of voltage multiplier to obtain the highest value of voltages.

# Chapter Two

# Theoretical Part

## 2-1:Introduction

Wireless networking has become increasingly common in the electronic world in recent years. These RF signals can be used and converted into DC power. The growing number of RF transmission sources has provided an explosion of ambient microwave energy sources, which has sparked widespread interest in Frequency modulation (FM ) radio stations and TV transmitters. Radio Frequency radiation is generated from sources that produce strong electromagnetic waves, such as TV broadcasts, cellular radio networks, and mobile phone towers, and we are surrounded by it. There are over a billion mobile phones in use today, thousands of radio and television stations, and numerous home Wi-Fi systems emitting RF radiation into the environment [31,32].

E.M harvesting has potential for stimulation of low-power electronic devices circuits, In order to eliminate the need for batteries, this principle needs an active antenna as well as a circuit qualified for translating RF signals into direct current ( DC) voltage [33,3,34]. Antenna systems cannot only meet the applications of multi-functional electronic and cellular devices, but the number of compact antenna designs is growing to meet user and safety specifications [35,36].

## 2-2: Architecture of RF energy harvesting network

An energy harvester is usually made up of four parts: an antenna, matching circuit, a rectifier, a storage or load component, and a to

maximize power transfer. The various components are shown in Figure 2.1. Each component of the construction will be discussed in detail in the sub-chapters that follow [37,38, 18].

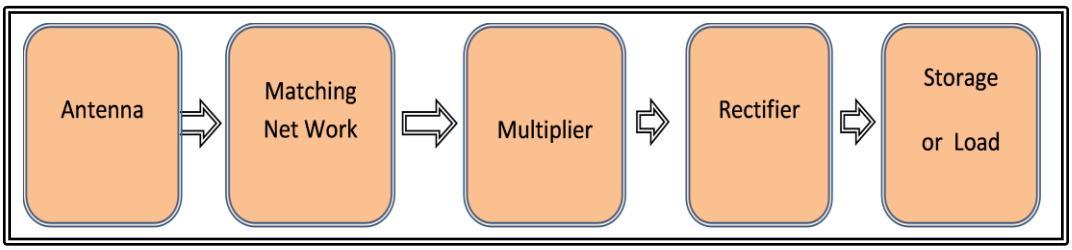


**Figure2.1:Typical energy harvesting circuit layout.**

1-The antenna can be configured to operate on a single frequency or several bands frequency, allowing the network node to collect from a single or numerous sources at the same time. Nonetheless, because the energy density of RF signals varies with frequency, the RF energy harvester generally functions over a wide range of frequencies.

2-The impedance matching circuit is a resonator circuit that operates at the specified frequency to enhance power transmission between the antenna and the multiplier. At the specified frequency, the impedance matching is highly efficient**.**

3-The diodes of the rectifying circuit, which transform RF signals alternating current (AC) signals in nature into DC voltage, are the essential component of the voltage multiplier. In general, diodes with a lower built-in voltage have greater conversion efficiency. The capacitor guarantees that electricity is delivered to the load in a smooth and consistent manner. Furthermore, if RF energy is not accessible, the capacitor can be used as a temporary reserve.

The RF energy harvester's efficiency is determined by the antenna's efficiency, the precision of the antenna-to-voltage-multiplier impedance matching, and the power efficiency of the voltage multiplier that transforms the received RF signals to DC voltage.

## 2-3: The RF sources

RF sources may be divided into two categories: dedicated RF sources and ambient RF sources.

### 2-3-1:Dedicated RF sources

When a more consistent energy supply is required, dedicated RF sources can be installed to deliver energy to network nodes. For RF energy transfer, dedicated RF sources can utilize the license-free ISM frequency bands. The Powercaster transmitter [5,39].Which operates on (915) MHz with (1 or 3) W transmit power, is an example of a marketed dedicated RF source. However, establishing dedicated RF sources might be expensive for the network. Furthermore, due to concerns about RF radiation safety and health, laws such as the Federal Communications Commission (FCC) must restrict the output power of RF emitters. For example, the highest threshold in the (900) MHz spectrum is (4)W [40].

Even at this maximum level, the received power is just (10) W at a reasonable distance of (20) meters. Due to this restriction, a large number of specialized RF sources may be required to fulfill customer demand. Because the RF energy harvesting process using dedicated RF sources is entirely controlled, it is more suited to support Quality of Service (QoS) - constrained applications. It's worth noting that the specialized RF sources

might be movable, with the ability to travel and transmit RF energy to network nodes on a regular basis [39,40-42].

## 2-3-2:**Ambient RF sources**

Ambient RF sources are RF transmitters that are not designed to convey RF energy. This radio frequency energy is virtually unrestricted. Ambient RF sources have a wide range of transmitting power, ranging from about (106) W for TV towers to around (10) W for cellular and RFID systems to around (0.1) W for mobile communication devices and WiFi systems. Static and dynamic ambient RF sources are the two types of ambient RF sources. The frequency range of ambient RF transmission is (0.8–3) GHz, and this includes most of the radiations from domestic appliances (e.g., television, Bluetooth, WiFi) [5,42,43].

### 2-3-2-1:Static ambient RF sources

These are transmitters that emit relatively steady power throughout time, such as TV and radio towers. Although static ambient RF sources can supply predictable RF energy, long-term and short-term variations may occur owing to service scheduling (e.g., TV and radio) and fading, respectively. Typically, the power density of ambient RF sources in various frequency bands is low. As a result, a high gain antenna is necessary for all frequency bands. Furthermore, the rectifier must be built for a broad spectrum [5,43].

### 2-3-2-2: Dynamic ambient RF sources

It is RF transmitters that operate on a regular basis or employ time-varying transmit power (e.g., a WiFi access point and licensed users in a cognitive radio network). To seek energy harvesting possibilities in a

certain frequency band, RF energy harvesting from dynamic ambient RF sources must be adaptable and perhaps intelligent to search for energy harvesting opportunities in a certain frequency range. A secondary user can harvest RF energy from a secondary user is sufficiently remote from main users or when the adjacent primary users are inactive, it can harvest RF energy from nearby transmitting primary users and send data [42,43].

The most important criteria for the energy harvesting circuit [44,45].

1- Ability to function with low input RF power.

2- Choosing the right antenna and it may be set up to work on a single frequency or several frequencies.

3-Diodes with the lowest possible turn on voltage are preferred since the peak voltage of the AC signal produced at the antenna is typically significantly lower than the diode threshold .

4- Because the energy harvesting circuit operates at high frequencies, highly fast switching diodes are required. Instead of a semiconductor–semiconductor junction, Schottky diodes(a metal–semiconductor junction ) are used. This enables the junction to function significantly quicker, with a forward voltage drop as low as (0.15) V.

5- Another key element influencing diode efficiency is saturation current. Diodes having a high saturation current, low junction capacitance, and low Equivalent Series Resistance are preferred (ESR). Furthermore, diodes that have a greater saturation current have a higher forward current. which is beneficial for load driving.

## 2-4: Schottky diode

A P-N junction is produced when a p-type and an n-type semiconductor are connected together as shown in Figure 2.2. The p-n junction diode works well as a rectifier and switching device at low frequencies (50 to 400 ) Hz, but its performance as a rectifier suffers greatly at high frequencies due to the existence of stored charge carriers in the junction. When reverse voltage is supplied, It has the effect of temporarily enabling current to flow in the other direction. This problem becomes increasingly difficult when the frequency of the alternating current source is raised and the periodic time of the applied voltage decreases. To obviate these issues, utilize a diode with a metal semiconductor contact instead of a p-n junction. It is advantageous for load driving when metals such as aluminum or platinum replace P-type semiconductors [46]. Metal-Semiconductor (M-S) or schottky diode is formed. The Schottky diode is named after the German physicist Walter H. Schottky [47]. Construction of Schottky diode as shown in Figure 2.3.

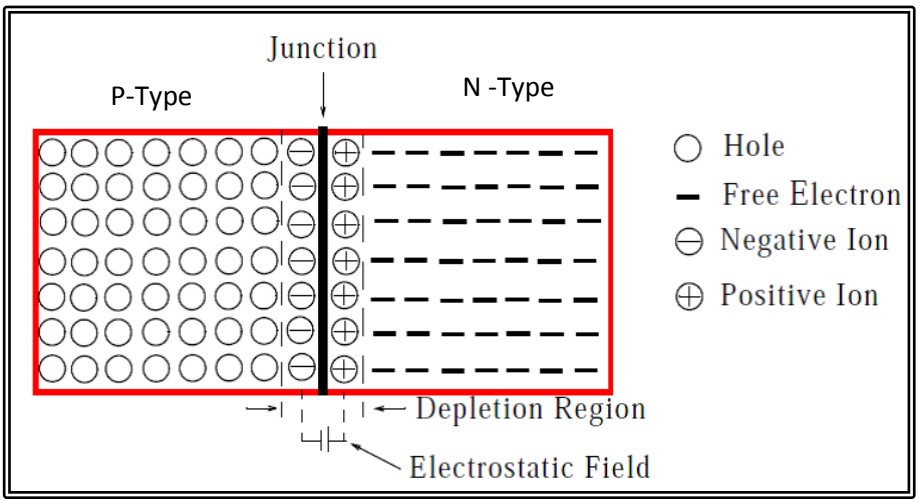


Figure 2.2:PN Junction[48]

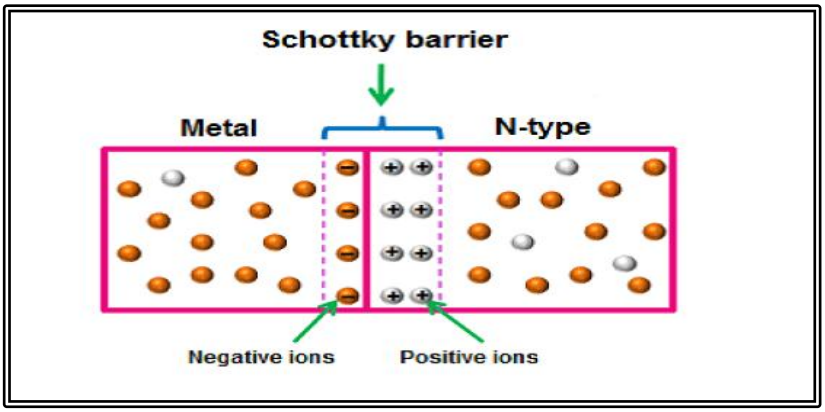


**Figure 2.3:Construction of Schottky diode[48].**

In terms of switching ON and OFF speed, the Schottky diode better than the p-n junction diode. When the Schottky diode is forward biased, electrons travel from the n-type material to the metal and quickly lose energy. Because there are no minority carriers (holes), conduction comes to a halt fast and switches to reverse bias. It also produces less unwanted noise. Because of, these characteristics, it is excellent for use as a rectifier for high frequency transmissions. A conducting Schottky diode generally has a forward voltage drop of (0.3 to 0.5 )Volts, as opposed to (0.6 to 0.8) Volts in a silicon junction [45,46].

Current begins to flow forward when a sufficient voltage is applied to the Schottky diode. As a result of this current flow, a small voltage drop occurs between the terminals of the Schottky diode. This voltage loss is referred to as voltage drop. A Schottky diode has a voltage loss of (0.2 to 0.3) Volts. Voltage loss or voltage drop is the amount of voltage wasted when turning on a diode. The voltage necessary to activate a Schottky diode is the same as the voltage required to activate a germanium diode. However, because its switching speed is significantly slower than that of Schottky diodes, germanium diodes are rarely used. The depletion region of a Schottky diode is insignificant. As a result, the Schottky diode will

quickly flip from ON to OFF. Additionally, the Schottky diode has very low capacitance. The diode is an important building block when designing a rectifier. SMS7630-079LF is the diode used in this project. These diodes feature a low forward voltage, rapid switching, and have been designed for energy harvesting circuits. [47-49]. The symbol of the Schottky diode is shown in Figure 2.4. Datasheet of diode notes is shown in Table 2.1.

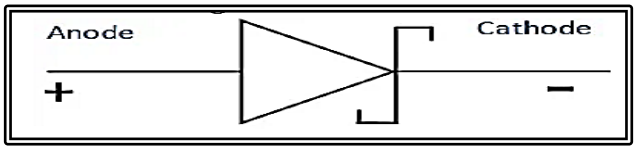


**Figure 2.4: Symbol of the Schottky diode.**

**Table2.1: Datasheet of diode SMS7630-079LF[50]**

| Schottky diode SMS 7630-079LF | | | |
|---|---|---|---|
| **Meaning** | **Symbols** | **Value** | **Unit** |
| **Saturation current** | $I_S$ | $5*10^{-6}$ | **A** |
| **Series resistance** | $R_S$ | **20** | **Ω** |
| **Emission coefficient** | **N** | **1.05** | **-** |
| **Transit time** | **TT** | $1*10^{-11}$ | **s** |
| **Zero –basic junction capacitance** | $C_{JO}$ | **0.14** | **pF** |
| **Grading coefficient** | **M** | **0.4** | **-** |
| **Energy gap** | $E_G$ | **0.69** | **eV** |
| **Forward-bias depilation capacitance coefficient** | **FC** | **0.5** | **-** |
| **Reverse breakdown voltage** | $B_V$ | **2** | **V** |
| **Reverse breakdown current** | $I_{BV}$ | $10^{-4}$ | **A** |
| **Junction voltage drop** | $V_J$ | **0.34** | **V** |
| **$I_S$ temperature exponent** | **XTI** | **2** | **-** |
| **Series inductance** | $L_S$ | **0.7** | **nH** |

## 2-5: Radio Frequency Signals

As a result of several high-frequency technology, ambient RF radiation is abundant in metropolitan surroundings. Wi-Fi, radio transmission, television, RFID tags, and mobile phones are all examples of applications that employ the radio frequency band, As shown in Figure 2.5, RF energy is the energy carried by the radio spectrum ,which ranges from (3) KHz to (300) GHz. Amplitude modulate (AM) radio (535-1705) KHz, (FM) radio (88-108) MHz, microwave ovens (2.45) GHz,and Wi-Fi are examples of specific frequency bands utilized for various purposes (2.41-2.46) GHz, and (5.18-5.82) GHz. Because of the low power density of ambient RF energy, collecting a usable quantity of energy is a difficult undertaking that necessitates meticulous research and design of both the antenna and processing circuitry[ 51,52].

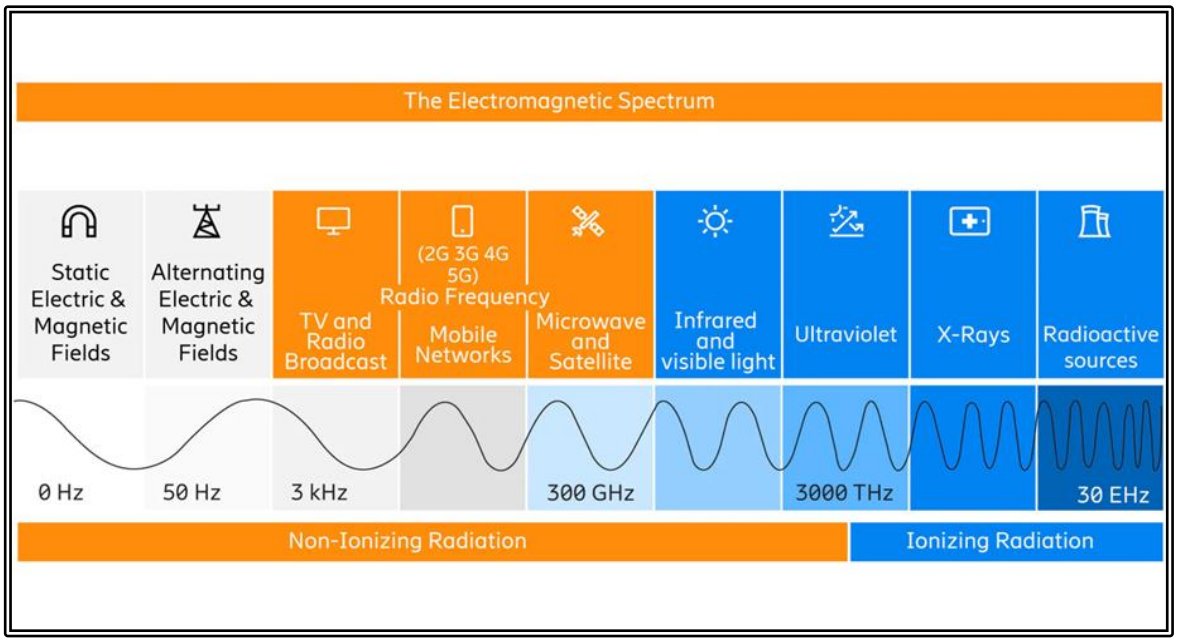


**Figure 2.5: Electromagnetic wave spectrum[51 ]**

## 2-6:Antenna

An antenna is a metallic apparatus such as a rod or wire for radiating or transmitting radio waves. It is a transport hub between a free space and a steering machine. By transmission line, is a hollow pipe transporting electromagnetic energy from the transmitting source to the receiving device [53,54]. It is supplies oscillating electric currents with appropriately localized and angled directions. The directional properties of the radio waves that emits are determined by the sizes and shapes of the conductors that make up the antenna. Electrical currents delivered by the transmission line from a source are converted by a receiving antenna. a receiving antenna transforms radio waves into electrical currents that are transmitted to a receiver through a transmission line [54,55].

A communication device requires a single antenna at the end or a mixture of different entities in order to form a single antenna unit. Also, antennas can be formed in 1D, 2D or 3D configuration and maybe in linear, planar, circular, spherical, etc. Antennas come in a variety of shapes, sizes, and structures [56-58].

## 2-7: Directivity and gain of an antenna

Directivity refers to an antenna's ability to focus energy in a certain direction while transmitting or to receive . Gain is the practical worth of directivity [59].

Gain is the difference between the radiation intensity in a given direction and the radiation intensity received if the antenna radiated all of the RF power delivered to it evenly in all directions [53, 56]. Directional properties are required for all practical radio antennas. Since all of the power delivered to it is radiated fairly well in all directions, it has a gain of unity (g = 1 or G = 0) decibels (dB) in all directions. Although the isotropic

antenna is a fundamental reference for antenna gain, the dipole is a common alternative The gain of an ideal (lossless) half-wave length dipole is used in this instance .An antenna's gain is normally measured in decibels (dB).

The antenna differential causes one power loss of directivity, which is the same as gain. In fact, some of the power is lost in the antenna due to holmic losses in the components on shape of heat, leakage through the insulators, etc. The gain and directivity (in a given direction) would be the same if an antenna was lossless (100% efficient)[55,56].

## 2-8:Classification of antenna

It is classified in several ways. The first method is by frequency band of operation ,and second involves physical structure and electrical and electromagnetic architectural design. The antennas are widely used for land mobile radio, but mobile phones and base stations make up a limited percentage of all antenna types [55].

Most plain, non-directional antennas are basic dipoles or monopole. and other more complex directional antennas use arrays of components, such as Yagi-Uda , microstrip patch array, aperture array, slotted waveguide array, Used for systems with a high gain and additional benefits such as a controllable radiation pattern [58 ].

New antenna technologies are being developed that allow an antenna to adjust its pattern quickly in response to changes in the received signal's direction of arrival. These antennas, as well as the enabling technologies, are known as adaptive or "smart" antennas, and they could be used in the future for higher frequency land mobile radio (LMR) bands [55] , Adaptive

antennas (AAs) are a group of antennas that can dynamically modify their antenna pattern in response to noise, interference, and multipath.

## 2-8-1:Wire antennas

The wire antenna is a type of antennas created by wires of arbitrary length. Wire antennas can be oriented horizontally, vertically, or irregularly in relation to the ground. It may also be fed in the middle, top, or between the lengths [59,60].The length of the wire antennas is usually a multiple of the half-wavelength, i.e. n λ/2. However, an antenna with a length greater than λ/2 is referred to as a long wire antenna [53]. Straight, spiral, helix, and other types of wires are available in a variety of sizes. Monopoles and Dipoles are often used in personal applications, vehicles, homes, ships, aircrafts, and satellites [56-58].

### 2-8-1-1: Dipole antenna

Dipole antenna is made up of two straight electric lines separated by a tiny gap in the middle, through which electricity is supplied. It is shown in Figure 2.6 [55,61]. Dipole antennas are those in which the conductor length is shorter than the signal wavelength. The wire is usually half the wavelength in length. As a result, they are referred to as half-wave dipoles [42].

The electric cables should be as thin as possible. The position of the electric cable, which may be horizontal, longitudinal, or slanting. Short, half-wavelength, monopole, V-shaped, folded, Yagi-Uda, and whip antennas are examples of dipole antennas [ 58,60]. It should be noted that this type of antenna was utilized in the current study.

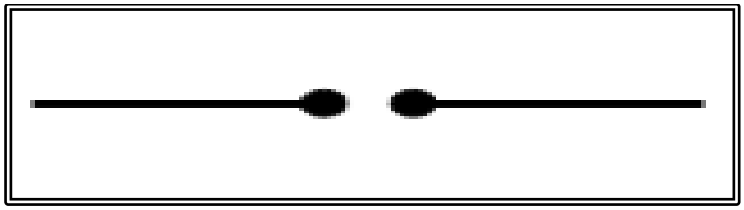

**Figure 2.6: Dipole antenna[53]**

### 2-8-1-1-1: Short dipole antenna

It is one of the most basic types of antennas, In comparison to the wavelength, the wire length is small, To be accurate < λ/10 [53]. It is made up of two thin conductors that are separated by just a limited distance. Since It is inefficient, they have fewer implementations. used in mobile communication devices , Figure 2.7 show Short dipole antenna [ 58,60].

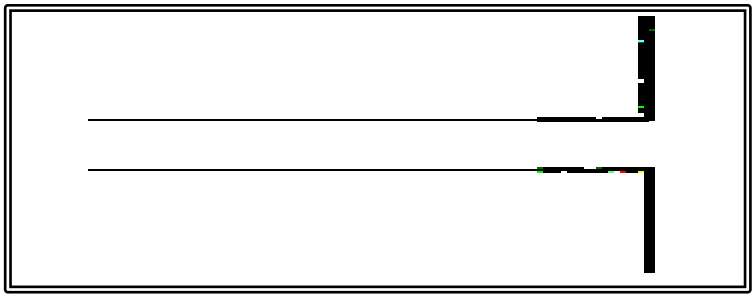

**Figure 2.7: Short dipole antenna[58]**

### 2-8-1-1-2: Half-wavelength dipole antenna

It is dipole antenna whose linear dimension from tip to tip is λ/2. Its directivity D is (1.64, or 2.1) dBi, and its Half Power Beam Width (HPBW) is 78°. A half-wavelength dipole antenna provides a good match between the radiation resistance and the impedance of the transmission line. Therefore, it is used as the reference dipole antenna to specify the directive gain of an omnidirectional antenna [55,60].

### 2-8-1-1-3: Monopole antenna

It is a kind of antenna that formed by replacing half of a dipole antenna with a perpendicular ground plane. When the ground plane is large

enough, the reflection of the EM wave makes it behave exactly the same as the missing half of the dipole, and the monopole becomes a dipole. Therefore, it is also called a half-dipole antenna. It has a half-toroidal radiation pattern, The radiation pattern is the same for monopole and half-wave dipole antennas. The field is radiated in the upper hemispheric region, resulting in half the average radiated power of a dipole antenna. These are almost all used as vehicle-mounted antennas [ 58,60,61], Figure 2.8 show Monopole antenna [61].

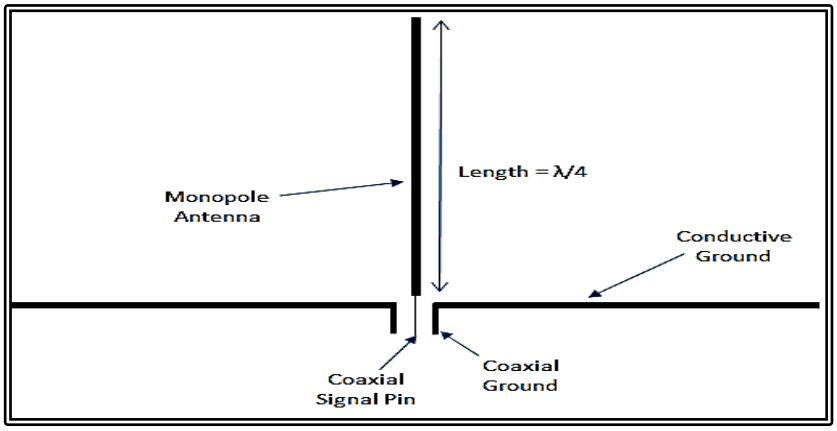


**Figure 2.8: Monopole antenna [61]**

### 2-8-1-1-4: V antenna

Rabbit ears are small V antennas that are normally hung vertically , such as those found on TV set-top boxes. To attain unidirectional properties, the V antenna's wires must be non- resonant, which can be done by reducing, if not fully removing, reflections off the wire ends. By making the slanted wires of the V relatively thick, the reflected waves can be minimized [58]. Figure 2.9 shows an inverted V antenna diagram [60].

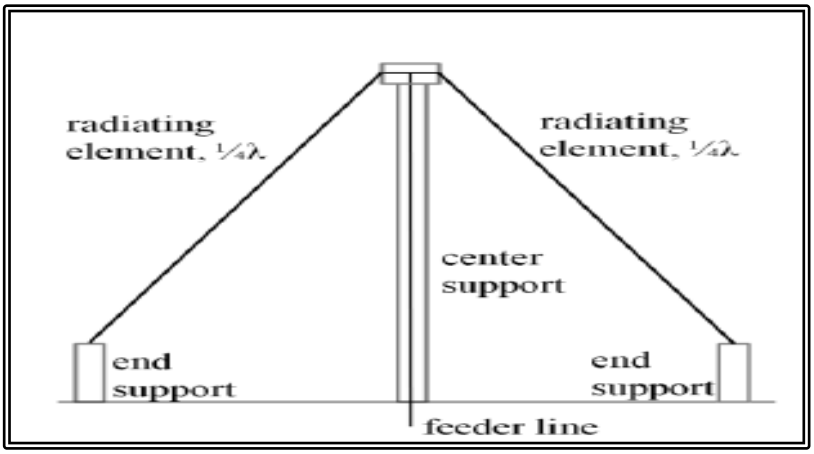


**Figure 2.9: V antenna diagram[60]**

**2-8-1-2:Loop antenna**

Another simple, inexpensive, and very versatile antenna type is the loop antenna. It is a coil with two ends that are attached to the two conductors of a transport line. The enclosed field of the loop determines the gain and loop shape (circular, rectangular, triangular, or rhombic). The use of rigid wire is needed for a circular loop. Since elastic electric cables can be used to make square and triangular loops, Because they don't need a ground plane, they're more resistant to ambient noise.

It is used for radio direction finding to filter out unwanted signals and noise. an acicular loop antenna's radiation pattern is identical to that of those radiated by an infinitesimal magnetic dipole. Loop antennas with electrically tiny circumferences or perimeters have small radiation resistances that are typically less than their loss resistances.

As a result, they are poor radiators and are rarely used for transmission in radio communication. When they are employed in such applications, they are often in the receiving mode, as in portable radios and pagers [58,59,63]. Usually, The typical circumference of a circular loop is a multiple of $\lambda/2$. The directivity E can be approximated by [60].

$$E \approx 60\pi^2 \times C\backslash\lambda \quad (2.1)$$

Where:-

C :is the circumference of the loop

Loop antenna is seen in Figure 2.10.

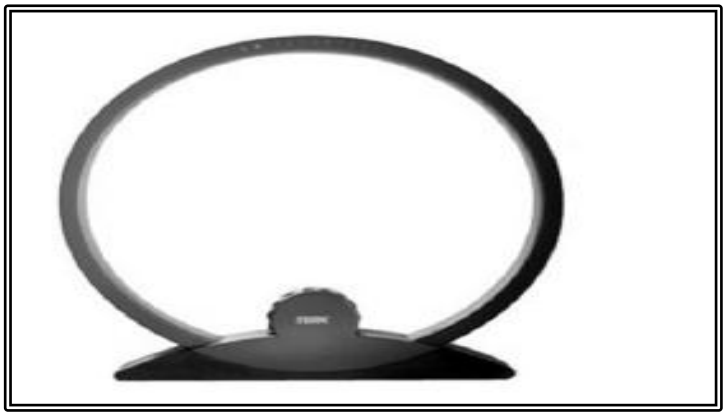

**Figure 2.10 : Loop antenna[60]**

**2-8-1-3: Helical antenna**

A normal mode cylindrical helix antenna is defined by its geometry and radiation mode. This antenna has a circumference much smaller than a wavelength (circumference < 2/3λ). As a result, its current distribution is nearly sinusoidal similar to a long straight wire antenna [59,62]. It is a terrestrial sheet placed on a helically coiled electrical cable. This is depicted in Figure 2.11 .

An axial or normal mode of operation may be used for a helical antenna. It has a single main beam that points in the direction of the helix's axis. When (πd/ λ) is in the (3/4–4/3) range, it produces circular polarized EM waves, and when (πd/ λ = 1) and (S = λ /4), it produces the best circular polarization. The polarization direction is determined by the coil's orientation. The rubber antenna used in walkie-talkies and mobile phones is an example of this antenna is use [57].

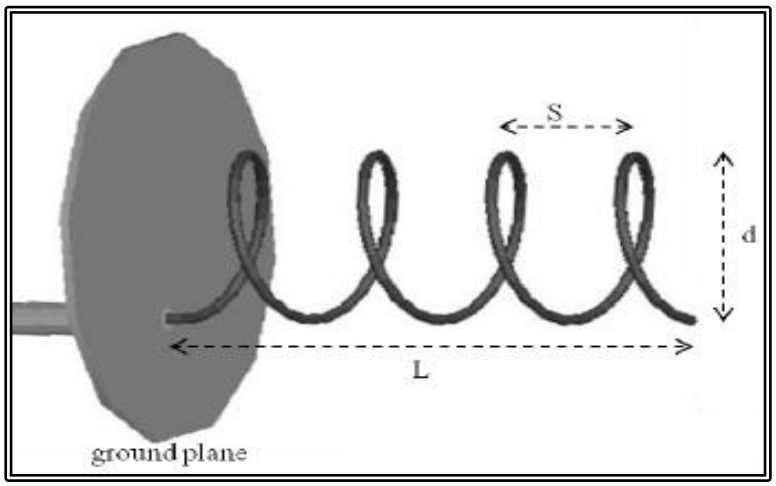


**Figure 2.11 : A helical antenna[60]**

According to equation 2.2 the helix arm length is related to height and radius. The helix has two special cases. When the pitch angle is zero, the antenna becomes a loop; when the pitch angle is 90°, the antenna becomes a linear antenna [57,62,63].

$$L = \sqrt{H^2 + (2\pi r M)^2} \qquad (2.2)$$

$$H = MS \qquad (2.3)$$

Where:-

L:length of arms , M:number of arms , H:height, r: radius and S:putch between arms.

**2-8-1-4:Yagi-Uda antenna**

The Yagi- Uda antenna consists of a series of straight components, each length roughly half of the wavelength. The powered part is the same as a half-wave dipole antenna that is center-fed. Reflectors and directors are straight rods or wires that run parallel to the powered part and are between (0.2 to 0.5) wavelengths on either side of it [53,59].

A reflector is placed behind the driven element, while a director is placed in front of the driven element. One reflector and one or two directors are present in a typical Yagi, And the antenna gain is proportional to its length. A Yagi antenna is seen in Figure 2.12 . Yagi- Uda has been widely used as a home TV antenna [56,57]. t should be noted that this type of antenna was utilized in the current study.

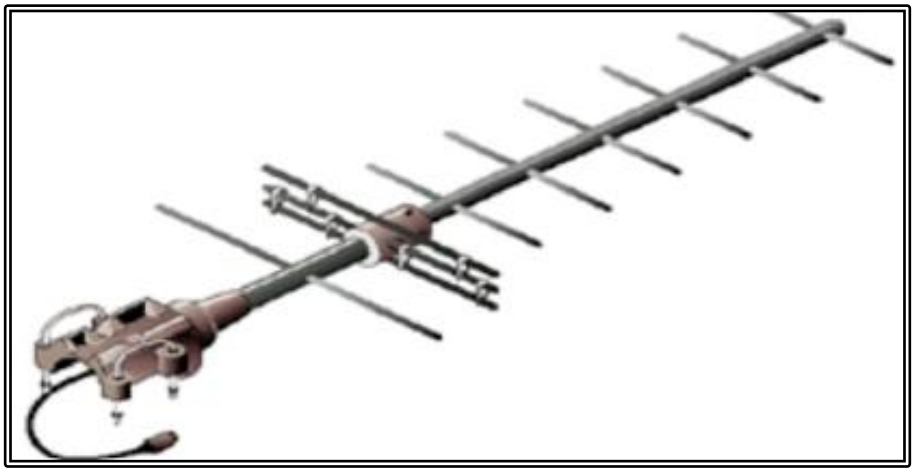

**Figure 2.12: A Yagi antenna[57].**

## 2-8-2:Aperture antenna

At microwave frequencies, aperture antennas are the most popular. An aperture antenna can be designed in a variety of geometrical forms. They can take the shape of a waveguide or a horn, with apertures that can be square, rectangular, circular, elliptical, or any other shape. Because aperture antennas may be flatly placed on the exterior of a spacecraft or aircraft, they are ideal for space applications. To protect them from environmental conditions, their aperture might be closed with a dielectric substance. The horn antenna , waveguide antenna and slot antenna are examples of aperture antennas [56,58,64].

### 2-8-2-1:The horn antenna

The horn is widely used as a feed element for large radio astronomy, satellite tracking, and communication dishes found installed throughout the world. [57].They are called feed horns when they're used as feed components in larger antennas. The overall radiation orientation corresponds to the horn antenna's axis, which may be circular, rectangular, cylindrical, or conical. Horn antennas can be fed with waveguide very easily, but they can also be fed with a coaxial cable and a proper transition. Horn antennas are usually used as active elements in a dish antenna[59,63,64].Horn antenna dimension show in Figure 2.13.The relationship between the measurements of the horn [65].

$$L = \frac{D^2}{2\lambda} \qquad (2.4)$$

Where:-

L:length and D: Diameter

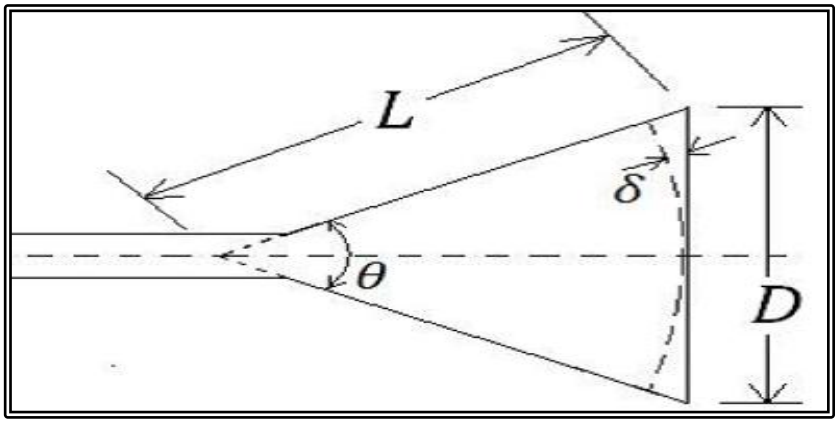


**Figure 2.13:Horn antenna dimension[64].**

## 2-8-3:Lens antennas

Lenses are generally employed to collimate incident divergent energy in order to keep it from spreading in undesirable directions. By

carefully designing the geometrical arrangement and selecting the right lens material [57].It is a convex parabolic-shaped dielectric or glass structure that allows light to converge or diverge. Since it is an optical instrument, it can emit and receive electromagnetic waves in the optical frequency spectrum.

Lens antennas are classified based on the material they are composed of as well as their geometrical form [57]. These antennas are usually used for applications requiring extremely high frequencies. Lens antennas are used as meteorological aids optical sensors, radio telescopes, and in radio astronomy , a Fresnel lens show in Figure 2.14 [57,58,60].

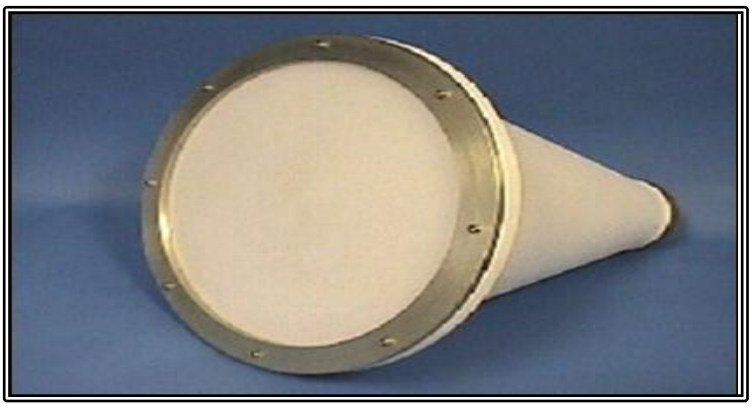

**Figure 2.14: A Fresnel lens with a conical mount [60].**

## 2-8-4:Reflector antenna

A reflector antenna has at least one reflecting surface as well as a radiator. The radiator, also known as a feeder, can be either a linear or a horn antenna. a parabolic reflector antenna or Parabolic antenna is used to send and receive signals that are utilized to communicate across long distances such as It employed in radio astronomy, microwave communications, and satellite tracking because of their high gain. Antennas of this sort has been erected with diameters as large as 305m.This kind

involve flat-plate reflector antenna, Parabolic Reflector Antenna and Corner Reflector Antenna [56,58,60]. It should be emphasized that in the current study, this form of antenna was used.

### 2-8-4-1: Parabolic reflector dish

The paraboloid reflector antenna is made up of a main antenna, such as a dipole or horn, that is located at the focal point of the paraboloid reflector. When high gain is desired, the most common kind of antenna is the parabolic reflector dish. The major benefit of the parabolic antenna is its high gain and directivity. The primary downside is the huge size of the dishes, however the main disadvantage is the big size dishes which are not easy to mount. A reflector can concentrate parallel rays on the focal point or the reflected beam from the parabola will be parallel to the axis of the parabola, As shown in the Figure 2.15 [ 60,62,66].

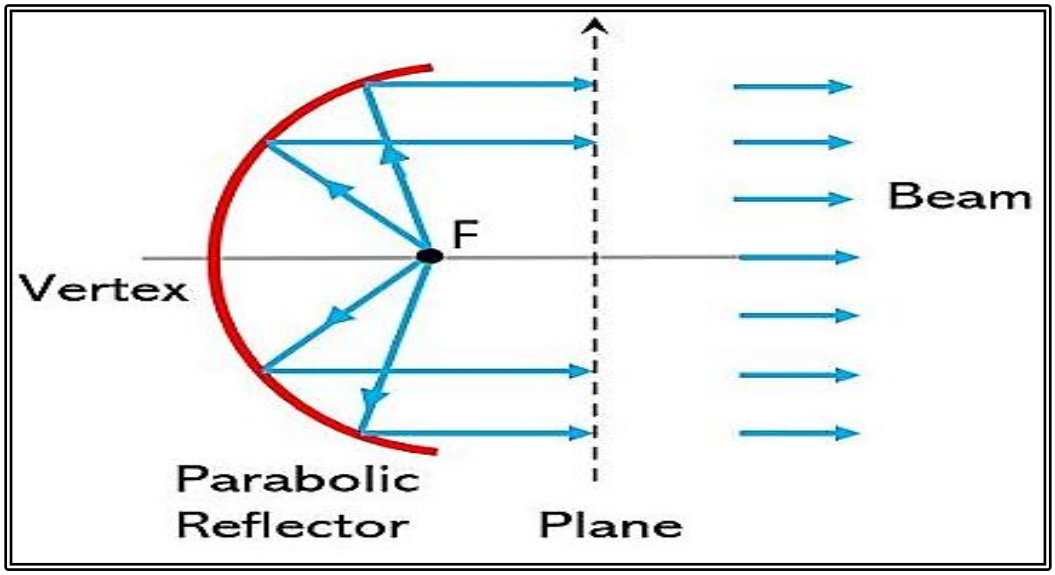


**Figure 2.15: Direction of reflected beam from a parabolic reflector antenna[66].**

The parabolic reflector antenna's beam width is proportional to its wavelength [96].

$$\theta = k\frac{\lambda}{D} \quad (2.5)$$

Where:-

$\theta$: is the beam width, D :is the diameter of the reflector.

$\lambda$ :is the wavelength and $k$ is a constant depending on the illumination from the primary feed with a value of about 60.

The location of the emphasis, or the focal length, shall be determined by

$$f = \frac{D^2}{16C} \quad (2.6)$$

C the width of the parabola, The gain is given by:

$$G = \frac{\pi D^2}{\lambda^2} \times \eta \quad (2.7)$$

Where:-

$\eta$: Efficiency

can see from equation (2.5) that the beam width of the antenna rises as the diameter of the parabolic dish decreases. Equation (2.7) indicates that the gain of the parabolic dish is proportional to the square of the diameter [62,66].

**2-8-4-2:Corner reflector antenna**

An antenna with one or more dipole elements in front of a corner reflector is known as a corner-reflector antenna. it has two flat sheets, one grid and the other a solid plate, as well as a radiator, which is normally a dipole in the corner. While this antenna has a high gain, The gain in the main beam direction is significantly greater than in the opposite direction [53,60]. It has a wide range of uses because of its ease of manufacture. For example, if the reflector is employed as a passive target for radar or

communication applications, it will return the signal in the same direction as it received it when the included angle is (90). Because of this distinguishing characteristic, military ships and vehicles are constructed with as few sharp corners as possible in order to avoid their detection by enemy radar. Corner reflectors are also commonly employed as receiving components in home television systems [58]. It is illustrated in Figure 2.16 [54].

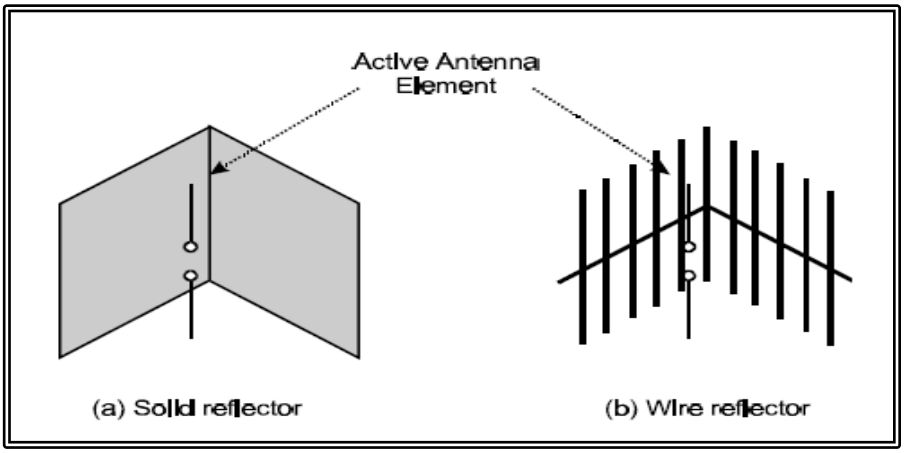


**Figure 2.16:Corner reflector antenna[54].**

### 2-8-4-3: Cassegrain antenna

It is a type of antenna that is fed from one side to the other, The main reflector has a hole at the center of the paraboloidal surface to accommodate the horn antenna's opening. A sub-reflector is positioned in front of the radiator to reflect the EM wave back to the main reflector. The Cassgrain antenna's sub-reflector is convex in relation to the main reflector, while the Gregory antenna's sub-reflector is concave in relation to the main reflector, Figure 2.17 shows the Cassgrain and Gregory Antennas diagrams [58,60,62].

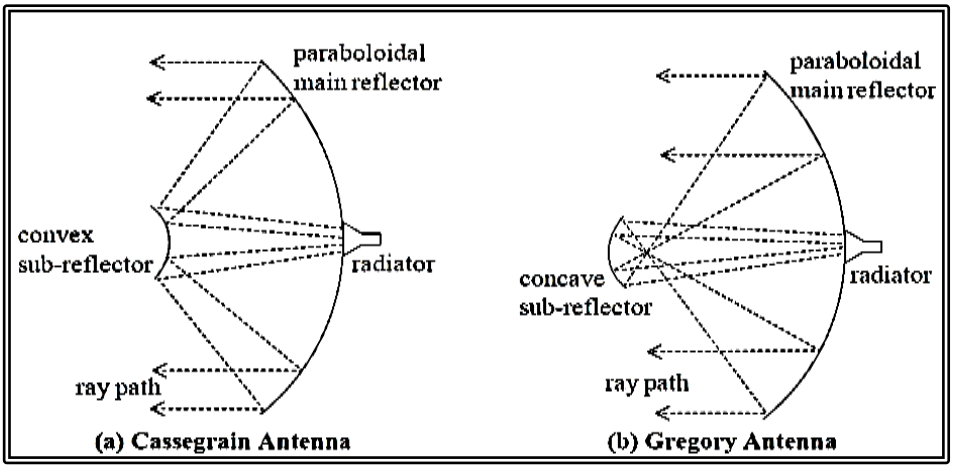


**Figure2.17 :Cassgrain and Gregory antenna diagrams[60].**

## 2-8-5: Microstrip antenna

The importance of antenna development stems from the fast expansion of contemporary wireless communication. Wireless communication necessitates the use of an antenna with an ultra-wide band, , a light weight, and a high efficiency. A microstrip patch is a type of antenna that may meet all of the requirements of contemporary wireless communication systems.

The microstrip antenna can be found in high maneuverability flights, satellites, spacecraft, missile applications, and rockets used for satellite launches and mobile phones [58]. The interesting features of the Microstrip antenna include its low profile, low cost, ease of manufacturing, compatibility with microwave semiconductor devices, and robust nature [62,65].

A microstrip antenna, also known as a patch antenna or printed antenna, consists of three layers: a metallic ground plane at the bottom, a dielectric substrate, and the metallic radiator. The radiator is fed by either a microstrip in the top layer or a coaxial line under the radiator through the ground plane and the substrate. The diagram of a microstrip antenna with the feed line in the top layer is shown in Figure 2.18 [60,66], as well as

their appealing radiation properties, rectangular and circular patches are the most common metallic patches. radiation with low cross polarization, in particular [59,60].

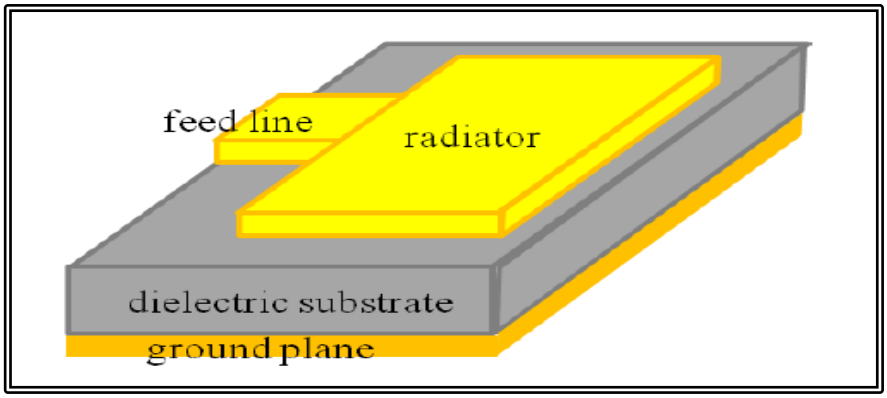


**Figure 2.18:Sketch of microstrip antenna[60]**

## 2-8-6:Array antenna

A single element patch cannot provide the required radiation characteristics for larger applications. By fabricating them as a continuous sequence of irradiative element with a valid geometrical and electrical arrangement, we can achieve the required results for various applications. An array antenna consists of a geometrical arrangement of individuals radiators that together create the desired characteristics. This array antenna can be an array of aperture antennas, microstrip antennas, or other type of antennas [64].A typical arrangement of the array is as shown in Figure 2.19.

This not only increases the characteristics but also increases additional radiation energy to radiate maximum radiation distance and direction for getting minimum in other directions [65,66]. The modern era of communication and digital equipment which are connected wirelessly one to another one needs an compact and low profile element as an interfacing device for sustained connectivity among objects that are using

either of the technologies like Wi-Fi, Bluetooth, UWB, Wi-Max, etc. [65,66].

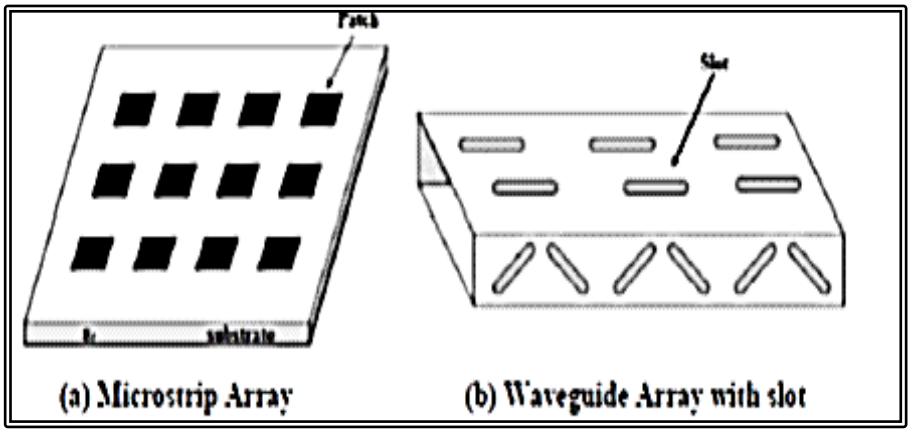


**Figure 2.19: Array antenna[65].**

Yagi-Uda antenna, microstrip patch array, aperture array, slotted waveguide array ,Used for very high gain applications with added Advantages, such as a controllable radiation pattern[57,59].This kind involve collinear array, slotted array, and log-periodic antenna.

## 2-9:Matching network

Due to design or technology constraints, the ideal impedance of the Power Amplifier (PA) and/or the optimum impedance of the Low-Noise Amplifier (LNA) are seldom at ( 50) Ohms. The construction of an impedance matching network is required for this [67].

Impedance matching is the second important component of the harvesting system. It is technique used to ensure maximum signal power transmission from the source to the receiving device while limiting signal power reflection back to the source. The received signal will reflect from the load to the source if the source and load impedances are not equivalent.

As a result, the received signal will a loss of power. The matching circuit guarantees that the load and supply impedances are matched, eliminating such a power loss [67,68].

A simple matching circuit can be designed from a combination of resistance, inductor or capacitor. The resistor is the real part of the impedance, while the inductor and the capacitor are the reactance [67].

There are numerous methods for impedance matching circuits, as well as approaches for matching the circuit to several frequencies. Impedance matching networks are often constructed with reactance (coils or capacitors). The cost of the components, mistakes in the component value, and easier production are all advantages of not utilizing lumped components. However, the advantages of using lumped components are that they are easier to calculate and can be made smaller than microstrips (which is a type of electrical transmission line which can be fabricated with any technology where a conductor is separated from a ground plane by a dielectric layer known as the substrate). Microstrip lines are used to convey microwave-frequency signals [69,70].

Numerous matching configurations are available. The choice of configuration depends on the number of elements used for the matching and the way in which they are positioned. Nonetheless, three main circuits have been proposed . At transformer, a shunt inductor and an LC network are examples of typical matching network circuits for RF harvesting circuits. A transformer is shown in Figure 2.20 . It increases the input voltage by the factor N, which is the ratio of the transformer’s secondary voltage to its primary voltage. This approach is too expensive in RFID

applications where the cost is restricted to a few cents, but it is viable for autonomous sensors [67,69].

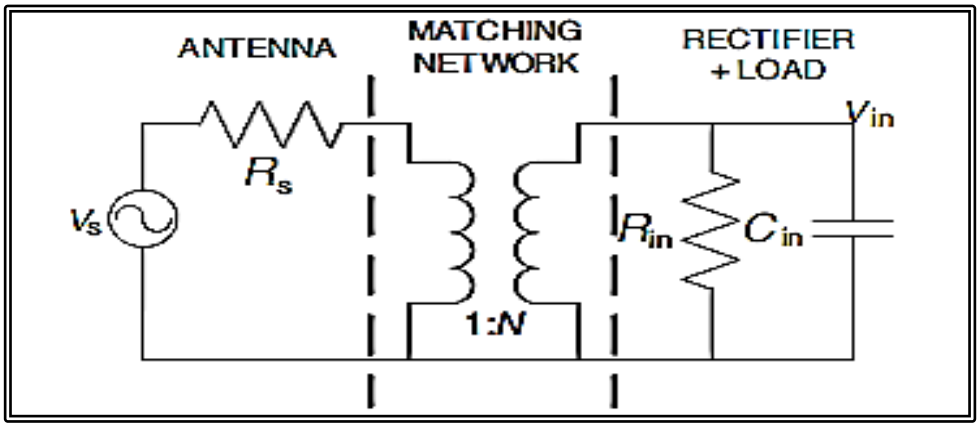


**Figure 2.20: Transformer as matching circuit[69].**

In RF transponders, the shunt inductor matching network is frequently employed as seen in Figure 2.21 [69]. $L_{shunt}$ must chime with the $C_{in}$ of the rectifier in order to match the antenna and rectifier impedances. As a result, at the operating frequency their impedances must be equivalent[67- 69].

at resonance

$$X_L = X_C \quad (2.8)$$

$$X_L = 2\pi f L \quad (2.9)$$

$$X_C = \frac{1}{2\pi f C} \quad (2.10)$$

$$w_r = 2\pi f \quad (2.11)$$

$$L_{shunt} = \frac{1}{\omega_r^2 \ C_{in}} \quad (2.12)$$

Where:-

$X_L$: reactance of inductor , $X_C$: reactance of capacitance,, $\omega_r$ :is the angular frequency at resonance and $C_{in}$: impedances of the rectifier.

So , as $C_{in}$ increases, $L_{shunt}$ must decrease. High $C_{in}$ values may need a very tiny $L_{shunt}$ value, which may be problematic. If the reactive components are well-matched, Maximum power will be transferred for $R_{in} = R_s$. The most widespread answer to the higher voltage generated on the antenna as a result of increased $R_S$ (see eq.2.13) is to increase the rectifier's input voltage ($V_{in}$) and minimize the resultant rectifier's losses. This is accomplished by using antennas with high radiation resistance (a folded dipole, for example, has a radiation resistance of around 300Ω) [67,69].

$$v_s = 2\sqrt{2R_S P_{AV}} \qquad (2.13)$$

Where:-

$v_s$ : is an AC voltage source, $R_S$ is radiation resistance, and $P_{AV}$ is the available power at the antenna.

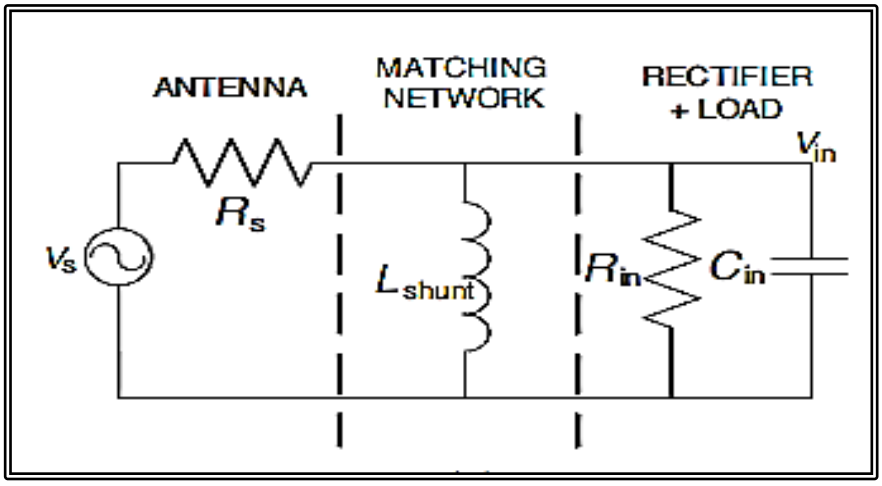


**Figure 2.21:** Shunt inductor matching network **[69].**

LC type impedance matching networks are often made up of a series capacitor and a shunt inductor, or vice versa [70,71]. The LC

matching network raises the voltage of the antenna. It is beneficial because it gives a greater peak voltage to the rectifier and has a higher efficiency, particularly when $P_{AV}$ (and therefore $v$s) is low. This circuit is also useful in antennas with low $R_S$ that also have a low $v_S$ . The impedance faced by the matching network must be the conjugate of the antenna impedance in order to produce a resonant circuit. Thus, equating the real and imaginary portions of both impedances yields two equations that allow the values of $L_m$ and $C_m$ to be calculated. Figure 2.22 show LC-impedance matching network [69,72,73].

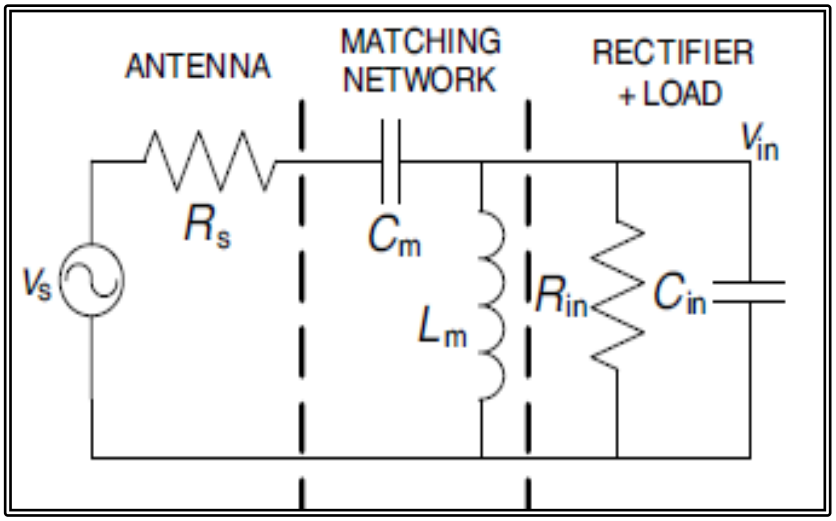


**Figure 2.22. LC- impedance matching network[69].**

The required values of the matching network are given by[73]

$$C_m = \frac{1}{w\omega_r R_s}\sqrt{\frac{R_s}{R_{in} - R_s}} \qquad (2.14)$$

$$L_m = \frac{R_{in}}{\omega_r} \cdot \frac{1}{\omega_r R_{in} C_{in} + \frac{1}{\sqrt{\frac{R_s}{R_s - R_{in}}}}} \qquad (2.15)$$

Equations (2.14) and ( 2.15) show that $L_m$ is affected by the value of $C_{in}$, but $C_m$ is not: it is solely affected by $R_S$, $R_{in}$, and $\omega_r$. $L_m$ drops as $C_{in}$ rises, just as it does in the shunt inductor matching network. As a result, $C_{in}$ must be maintained low enough [67,69].

$$G = \frac{v_{in}}{v_s} = \frac{1}{2} \cdot \sqrt{\frac{R_{in}}{R_s}} \qquad (2.16)$$

Where :

G:denoted the voltage gain.

As a result, if $R_{in} > R_s$, the voltage will be increased. Because the circuit Q is provided by equation(2.17),The circuit becomes more selective. The boosting factor (Q ) is depicted in the equation below[69].

$$Q = \sqrt{\frac{R_{in}}{R_s} - 1} \qquad (2.17)$$

## 2-10: Rectifier theory

A rectifier is a circuit that transforms an AC voltage into a DC voltage collected by an antenna . The generation of a battery-like voltage from extremely little input RF power is a major challenge for the rectifier design. Generally, there are three main options for a rectifier, A diode , a bridge of diodes and a voltage rectifier multiplier. There are lots of different types of rectifier design and this section will focus on those commonly used in RF harvesting application [67,74,75].

## 2-10-1:Villard circuit(half-wave rectifier)

The most fundamental topology of the rectifier is the half-wave rectifier that comprises. This consists a single diode $D_1$ and a capacitor. The circuit is shown in Figure 2.23. Since a silicon diode will pass current in only one direction, it is ideally suited for converting alternating current AC to direct current DC When AC voltage is applied to a diode, the diode conducts only on the positive alternation; that is, when the anode of the diode is positive with respect to the cathode. When positive voltage is applied from the source current will go through the diode $D_1$ and charge capacitor $C_1$.When the waveform becomes negative, charge will be released from the capacitor and can be seen as a DC-voltage at the output, Capacitor smooths the rectified voltage. Moreover, the output. $V_{out}$ is discontinuous since the negative cycle is cutoff. As seen in Figure 2.24, the first diagram is the original sine wave, the middle one shows the use of a diode, and the bottom one shows the combination of a diode and a capacitor [37,48].

Despite its simplicity, a half-wave rectifier is usually inadequate for common applications for ambient RF energy harvesting since the incident power density is relatively low which does not satisfy the biasing requirement of the circuit. Also, the breakdown voltage of the single diode rectifier is limited which could affect the power handling capability of the circuit [72, ,77 ].

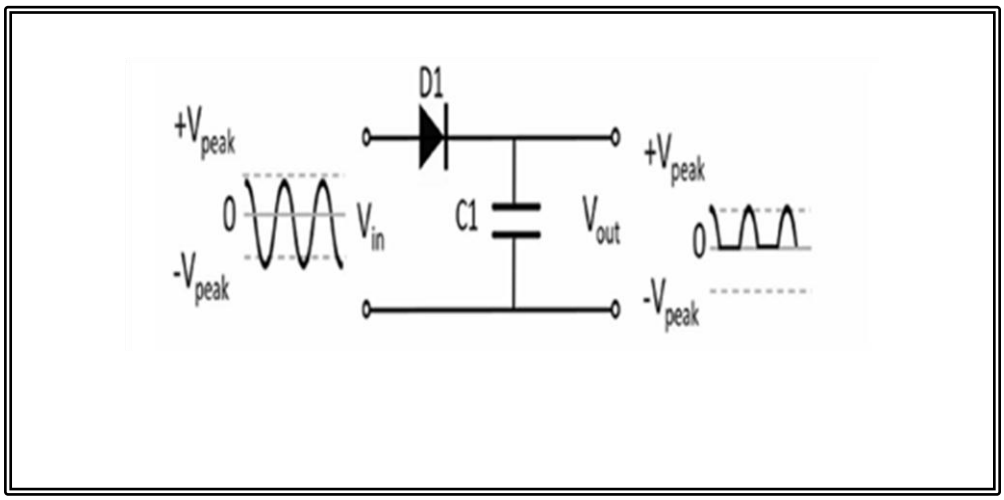


**Figure 2.23:Diode rectifier( A half-wave rectifier) circuit [77].**

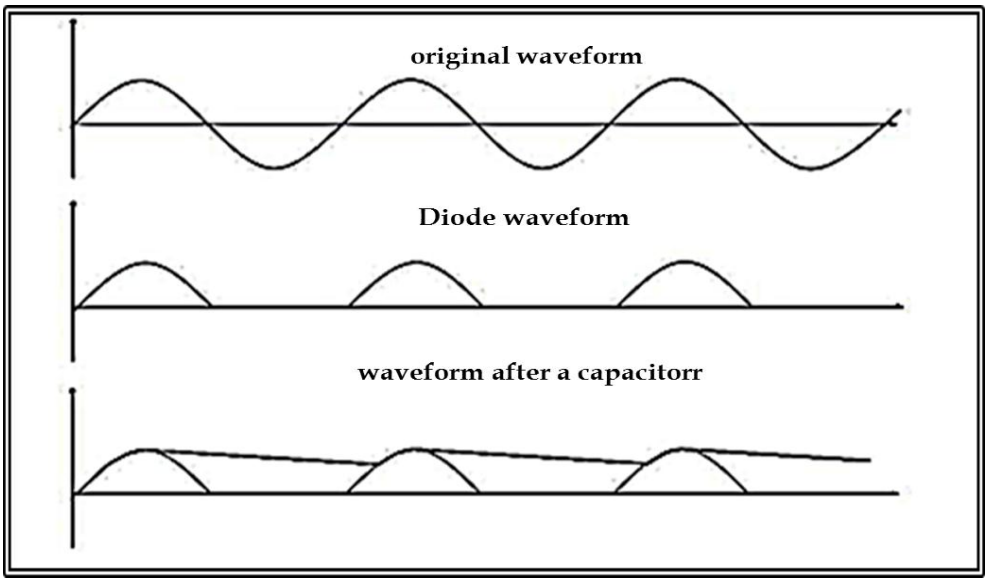


**Figure 2.24: Diagram of output wave of diode rectifier [37].**

A half-wave rectifier produces a large alternating component and discards half of the cycle. In order to use the whole cycle, you need to rectify the other half as well, flipping it to the positive side. This can be done in several ways, one of the most commonly used is the Graetz diode bridge rectifier [72,77].

## 2-10-2:Graetz diode bridge rectifier

A half-wave rectifier generates a significant alternating component while discarding half of the cycle. To use the entire cycle, must correct the other half as well, turning it to the positive side. This may be accomplished in a variety of methods, one of which is the Graetz diode bridge rectifier, which is named after its inventor. a bridge rectifier that rectifies both positive and negative cycles of the AC input but retains $V_{out} = V_{peak}$ by alternatively blocking pairs of diodes $D_1$, $D_4$ and $D_2$, $D_3$ Figure 2.25 [75,76].

Figure 2.26 depicts the implementation of a Graetz diode bridge rectifier. The top figure depicts the original waveform, the middle one depicts the rectified waveform, and the bottom one depicts the usage of a capacitor in conjunction with the diode bridge. [37, 76,77].

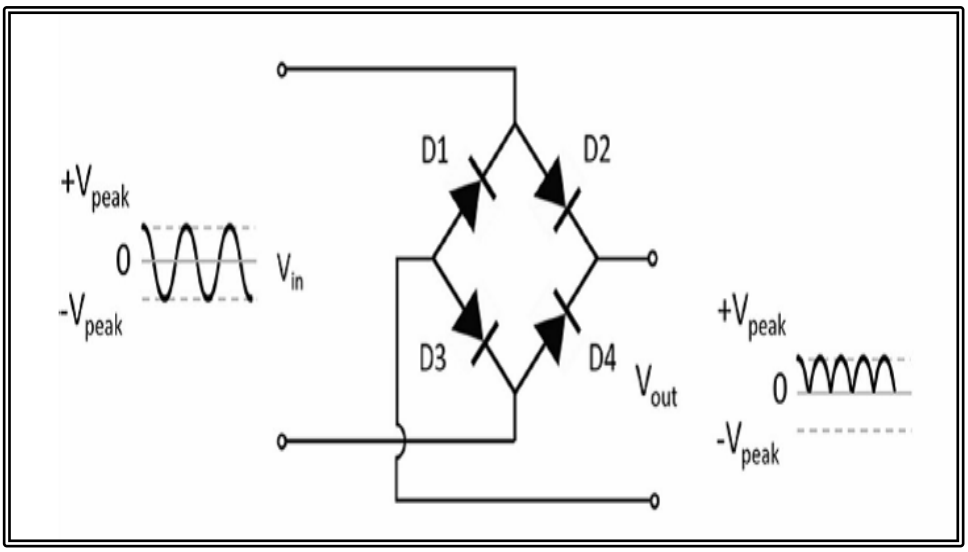


**Figure 2.25: Diode bridge rectifier circuit [77].**

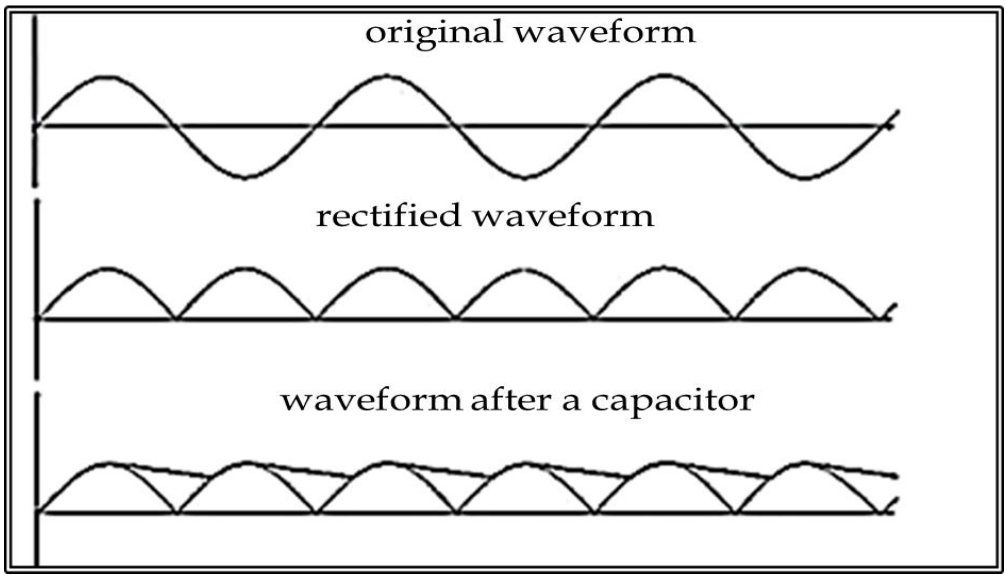


**Figure 2.26: Diagram of output wave of diode bridge rectifier[37].**

The diode in Figure 2.23 and the diode bridge in Figure 2.25 .provide an output DC voltage to the load ($V_{OUT}$) whose amplitude is lower than that of the incoming signal. So full-wave rectifier is preferable [75,77].

## 2-10-3:Greinacher circuit

An additional advantage of rectifiers is that they can , depending on construction, multiply the voltage they deliver. the method for increasing voltages is known as voltage multiplication. Voltage multipliers are used primarily to develop high voltages where low current is required. When voltage is stepped up, the output current decreases. This is also true of voltage multipliers. Although the measured output voltage of a voltage multiplier may be several times greater than the input voltage, once a load is connected the value of the output voltage decreases [78,79]. Also any small fluctuation of load impedance causes a large fluctuation in the output voltage of the multiplier. For this reason, voltage multipliers are used only in special applications where the load is constant and has a high impedance or where input voltage stability is not critical. Voltage multipliers may be

classified as voltage doublers, triplers, or quadruplers. The classification depends on the ratio of the output voltage to the input Voltage [72,80].

The Greinacher rectifier is a more sophisticated rectifier compared to the Villard circuit and is shown in Figure 2.27. The primary advantage is that the output voltage has significantly less ripple. Assume ideal diodes with a threshold voltage of (0) V, no reverse current, and zero conduction resistance and that vin is a sinusoidal wave. When the input is in its negative period of the sinusoidal waveform, current will flow through $D_1$ and charge $C_1$ to the input voltage $V_p$. During the positive period of the input, $C_1$ will be discharged through $D_2$ and charge $C_2$ up to $2V_p$ [51,70].

If all the elements are ideal, the voltage at this point is $V_{in} + V_{in}$ ($V_1$ in Figure 2.28). $D_2$ rectifies the signal at point A and capacitor $C_2$ holds the output voltage ($V_{OUT}$) at the peak value of $V_1$. Thus, the OCV (open circuit voltage) of the rectifier is a DC voltage with a value $2V_{in}$. In steady-state operation, $I_{OUT}$ is drained from $C_2$, and this capacitor is recharged when $V_1$ is higher than $V_{OUT}$ dashed line in Figure 2.28 [51,67,82].

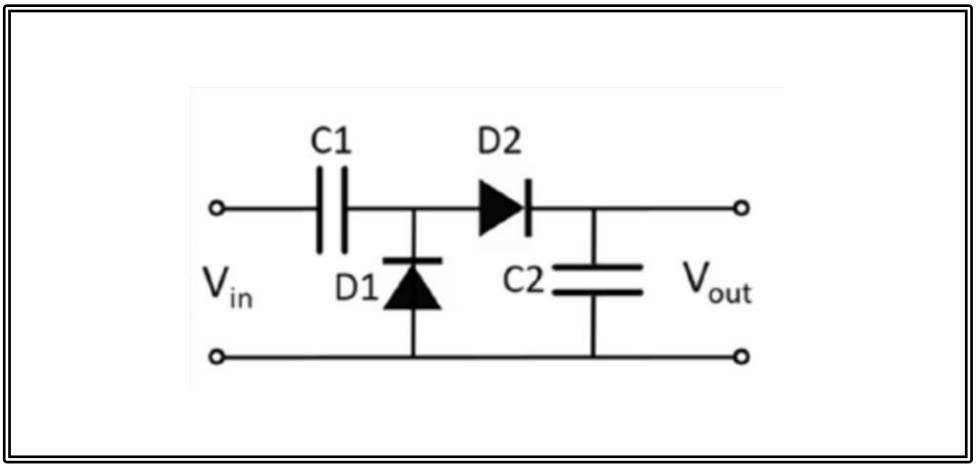


**Figure 2.27: Grenaches circuit [70].**

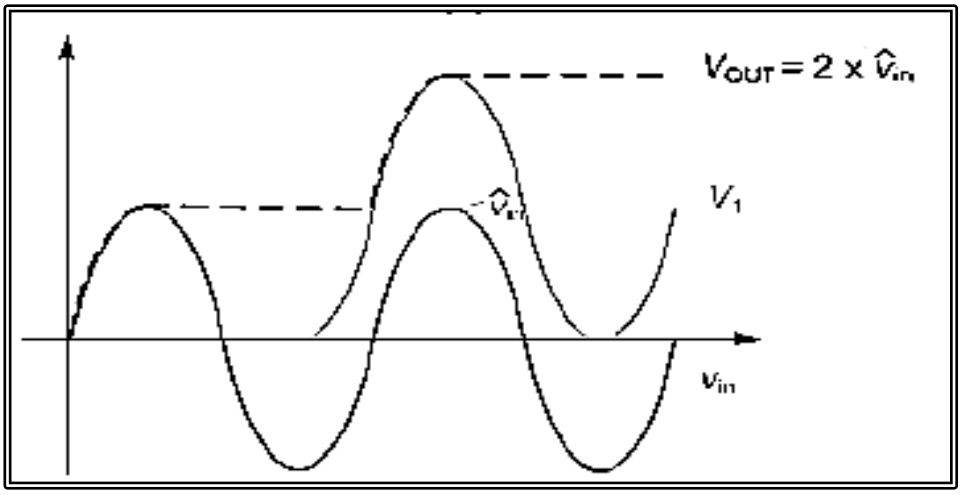


**Figure 2.28:Transient wave forms [67].**

$V_{in}$ can be in the millivolt level, so in order to obtain higher output voltages, the circuit can be cascaded by using n stages Figure 2.29 shows a two stage rectifier multiplier [67,76,79].

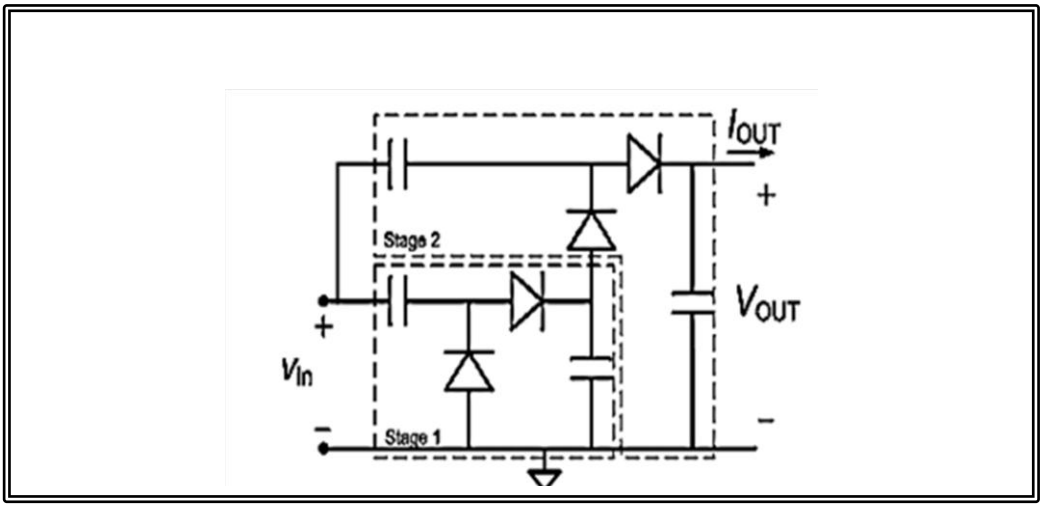


**Figure2.29: Two-stage voltage multiplier rectifier circuit [67].**

In the case of an n-stage rectifier , $V_{out}$ in open circuit is[67].

$$V_{out} = 2nV_{in} \qquad (2.18)$$

The input power ($P_{in}$) equals the output power ($P_{OUT}$) in a lossless rectifier, and Rin may be computed from the resistance connected at the output ($R_{Load}$) as[97]:

$$R_{in} = \frac{{V_{in}}^2}{2P_{in}} = \frac{{V_{out}}^2}{P_{out}}\frac{1}{8n^2} = \frac{R_{Load}}{8n^2} \quad (2.19)$$

As n rises, Rin drops for a given $R_{Load}$. Otherwise, the ideal value of $R_{Load}$ grows as n increases given a matched value of $R_{in} = R_{ant}$. When considering the diode's threshold voltage ($V_T$), the OCV is[67]:

$$\mathrm{V_{out}} = 2\mathrm{n}(\mathrm{V}_{in} - V_T) \quad (2.20)$$

The output D.C. power in dBm can be calculated by[77 ].

$$\mathrm{P_{DC}(dBm)} = 10 \times \log_{10}(\frac{V_{out}^2}{R_{Load}} \times 10^{-3}) \quad (2.21)$$

Where:-

$V_{DC}$ is the measured output voltage and $R_{Load}$ is the optimal load.

Rectifier efficiency can be calculated by [76].

$$\eta = \frac{P_{out}}{P_{in}} \quad (2.22)$$

$$P_{out} = \frac{V_{out}^2}{R_{load}} \quad (2.23)$$

$$\eta = \frac{{V^2}_{out}}{P_{in}R_{Load}} = \frac{{V^2}_{DC}}{P_{in}R_{Load}} \quad (2.24)$$

Where:-

$V_{DC}$ is the output DC voltage through the resistive load $R_{Load}$ and $P_{in}$ is the input power of the rectifying circuit.

It should be emphasized that in the current study, this form of rectifier was used.

## 2-10-4:Full wave series multiplier (Delon Circuit)

Figure 2.30 shows a circuit called Delon circuit. The function is similar to the Greinacher circuit and the output voltage is double the input voltage. The two capacitors are each charged during the positive respectively the negative part of the input sinusoidal [70,72].

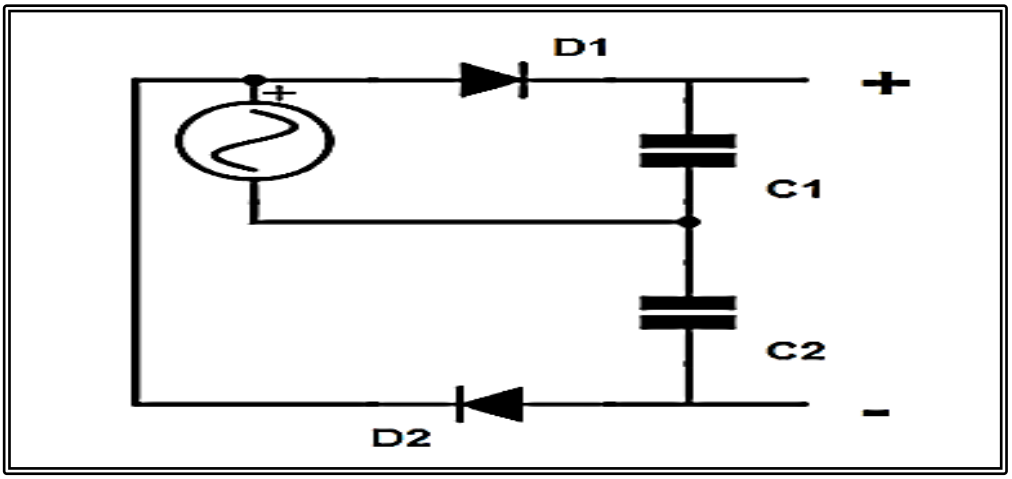


**Figure 2.30: Full wave series multiplier circuit [72].**

## 2-10-5:Full wave Greinacher voltage quadruple circuit

A rectifier based on the Greinacher circuit but extended into a voltage quadrupler. It is equivalent to a two-stage voltage doubler circuit formed in a bridge type and the topology is given in Figure 2.31. There are two branches with two diodes in each branch. The biasing voltage of each diode can be partially produced by the output of the previous diode. The total RF power consumption is reduced by using the new configuration . Resulting

in a higher output voltage compared to the original Greinacher rectifier. The benefit is obviously a higher output voltage, however it creates a more complex circuit and the total power output will not be higher since the energy will be divided into two sub circuits [76,78,82].

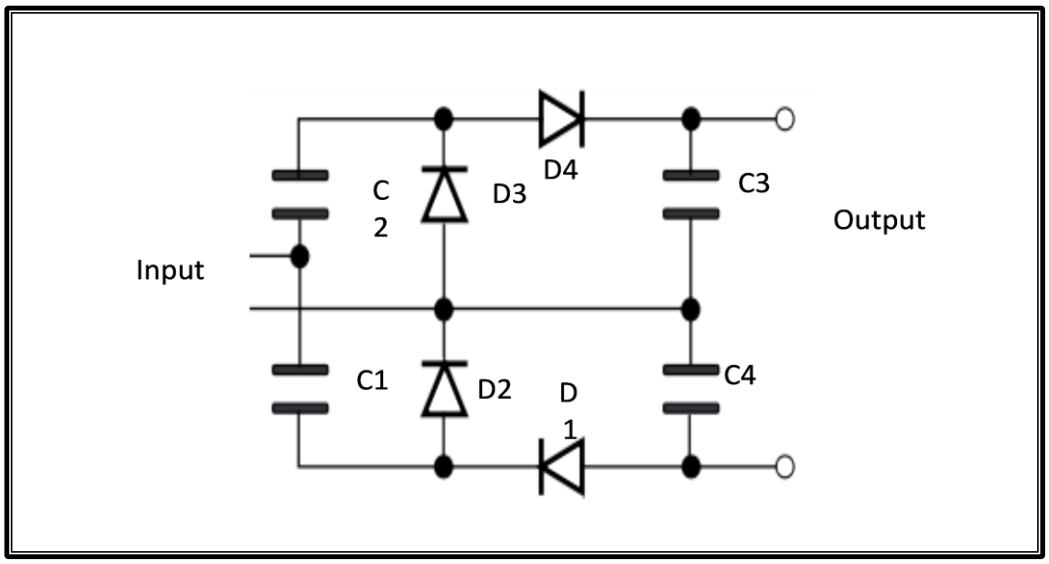


**Figure 2.31: Full wave Greinacher voltage quadruple circuit[78].**

## 2-11:Filter Circuit

When AC is converted to DC using rectifiers, the DC output contains unwanted alternating current components known as ripple. Ripple components are high frequency AC Signals in the DC output of the rectifier. These are not desirable, so they must be filtered. If the ripple surpasses the prescribed value, the system experiences a variety of undesirable impacts such as include stray overheating, audible noise, and so on. Ripple can be mitigated using an output filter [83,84,85] .

The filter is a device that allows passing the DC component of the load and blocks the ac component of the rectifier output. Thus the output of the filter circuit will be a steady DC voltage. The filter circuit can be

constructed by the combination of components like capacitors, resistors, and inductors. Inductor is used for its property that it allows only DC components to pass and blocks AC signals. Capacitor is used so as to block the dc and allows AC to pass. Depending upon the passive element used, the filters can be classified as [86,87]

### 2-11-1: Shunt capacitor filter

This sort of filter is made out of a big capacitor linked across the load resistor RL. This capacitor has a low reactance to the alternating current components and a very high impedance to direct current. As a result, the alternating current components in the rectifier output find a low reactance path through the capacitor and only a small part flows through RL, producing small ripple at the output as shown in Figure 2.32 [83].

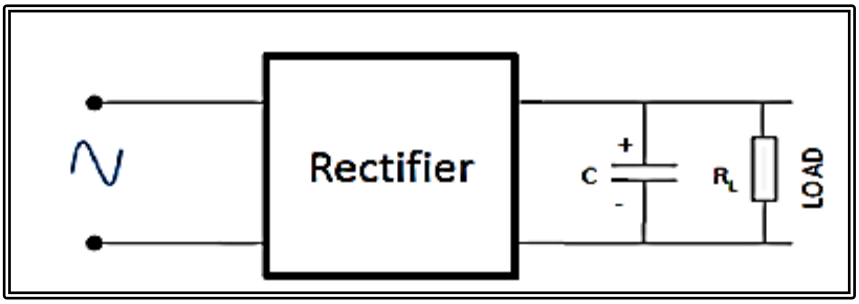


**Figure 2.32:Rectifier with shunt capacitor[83].**

$$X_c = \frac{1}{2\pi f c} \qquad (2.25\ )$$

In this case, $X_c$ shown in equation (2.25 ) should be smaller than $R_L$. Because current must flow through C, and C must be charged. If C is very tiny, $X_c$ is high, and current runs through $R_L$ alone, with no filtering action taking place. When the diode (in the rectifier) is conducting, the capacitor C is charged, and when the diode is not conducting, the capacitor C is

drained through $R_L$. When the input voltage ( $v = V_m \sin\omega t$ ) Exceeds the capacitor voltage, C is charged. When the input voltage is less than the capacitor voltage, C discharges via RL. The capacitor's stored energy keeps the load voltage high for an extended length of time. The diode only conducts for a brief period of high current [70,87].Figure 2.33 depicts the waveforms [83].

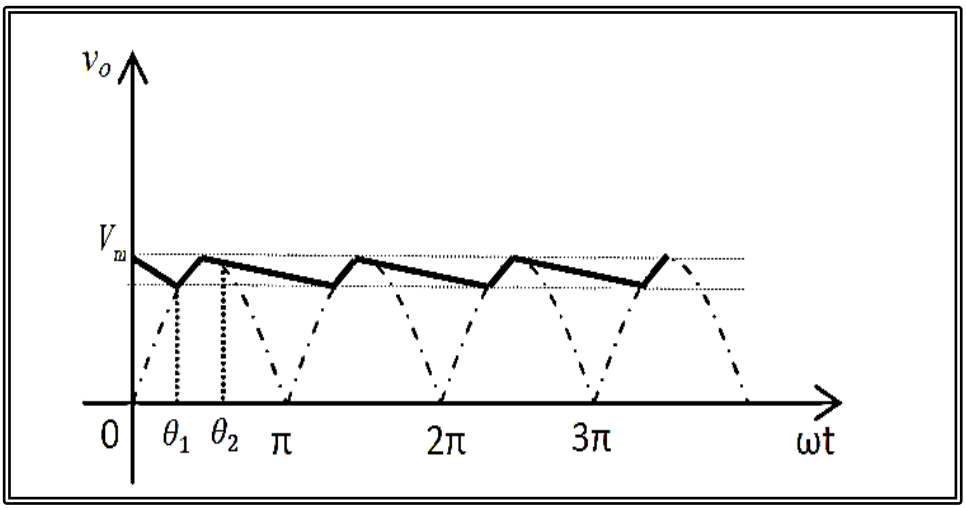


**Figure 2.33:The waveforms of rectifier with shunt capacitor[83].**

A capacitor resists rapid voltage changes across it. As a result, the ripple voltage is reduced. The capacitor's discharge is determined by the time constant $\tau = C.R_L$. As a result, the smoothness and amplitude of the output voltage are determined by the values of capacitors C and $R_L$. The smoothness of the output rises as the value of C increases [83].

However, the maximum value of the capacitor is restricted by the diode's current rating. A reduction in the value of RL also raises the load current and decreases the time constant. These filters are employed in circuits with low load current, such as transistor radio receivers, calculators, and so on [83,87]. Advantage shunt capacitor low cost, small

size and weight ,can be connect with for Half Wave ( HW) and Full Wave (FW) rectifier, good characteristics and improved D.C output.

It should be noted that this form of filter was utilized in the current study.

**2-11-2: Series inductor filter**

The Inductor L is linked in series between the rectifier circuit and the load, as the filter circuit's name indicates. The inductor has the property of resisting current changes that pass through it. In other words, the inductor provides high resistance to the ripples while providing no impedance to the required DC components. As a result, the ripple components will be removed. When the rectifier output current exceeds a specific threshold, energy is stored in the form of a magnetic field, which is released when the output current falls below the average value [84]. Because the current in all sections of the series circuit is the same, an inductor L is connected in series with the load, as illustrated in Figure 2.34 [86,87 ].

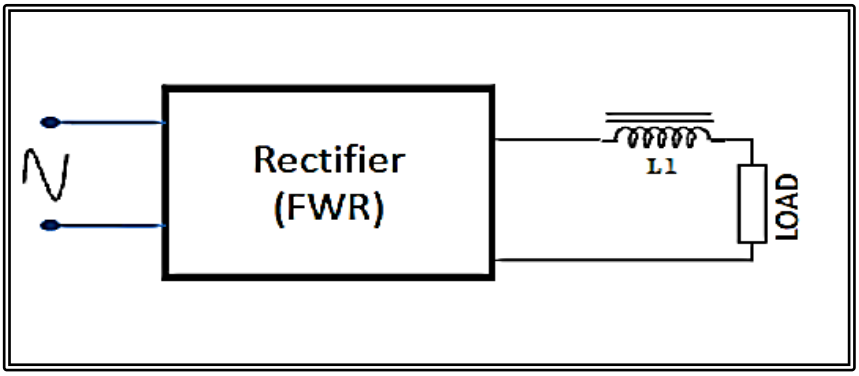


**Figure 2.34:Rectifier with series inductor[83].**

The use of an inductor prevents the current from rapidly increasing or decreasing. When the inductor is sufficiently big, the current becomes continuous and almost constant. The inductor stops the current from ever reaching its maximum value, which would otherwise be achieved in the

absence of a filter inductor. As a result, the output voltage is never equal to the peak value of the applied sine wave. As a result, a rectifier whose output is filtered by an inductor cannot produce as high a voltage as a rectifier whose output is filtered by a capacitor. However, this disadvantage is partially offset by the inductor filter, which allows for a higher current without causing a significant change in output voltage. This is why an inductor filter is appropriate for high power applications [83,87].

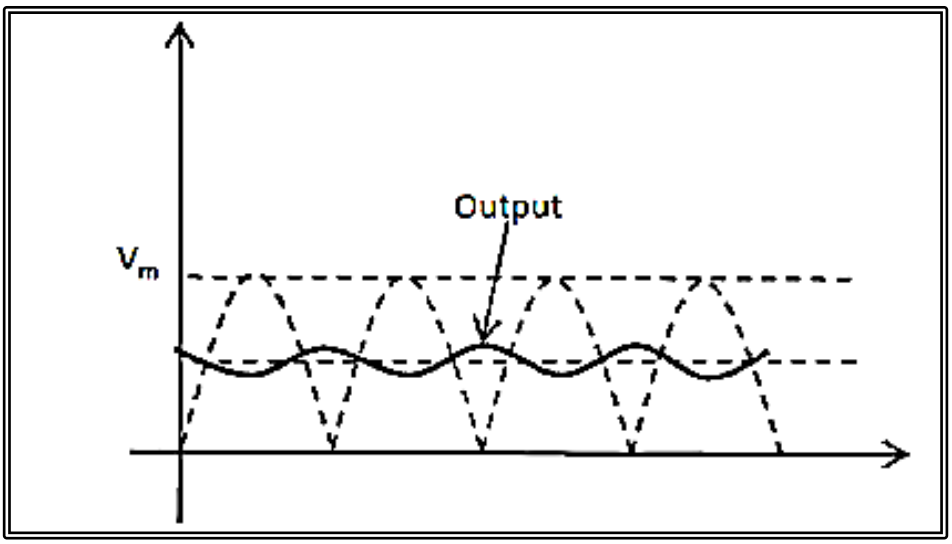


**Figure 2.35:The waveforms of rectifier series inductor filter [87].**

Advantages series inductor filter are sudden changes in current out and Improved filter action at high load currents. Disadvantages are reduced output voltage due to the drop across the inductor , bulky and large size, Not suited for HW.

### 2-11-3: LC filter

To increase the filtering effect of rectified voltage and current, a capacitor-inductor filter is employed. As observed in previous sections, the capacitor or inductor alone cannot perform the filter action properly since

the former is appropriate for low-power applications and the latter is suitable for high-power applications[84].

When the capacitor and inductor are coupled, however, they create high quality DC voltage and current. The capacitor's role is to smooth out changes in voltage, whereas the inductor's function is to smooth out variations in current. The capacitor-inductor filter is extensively utilized in high-power applications due to the uniform flow of current [84,87].

L-C filters can be of two types: Choke Input L-section Filter and Π – Filter or Capacitance Input Filter.

**2-11-3-1: Choke Input L-section Filter**

The ripple factor of an inductor filter grows as the load current $R_{load}$ increases. The ripple factor of a capacitor filter is inversely proportional to the load resistance. In terms of cost, both inductor filters and capacitor filters are unsuitable for sensor applications [84,87].

L-C inductor input, also known as an L-section filter, is made up of an inductor (L) connected in series with a half or full wave rectifier and a capacitor (C ) the load. Because its form resembles an inverted L-shape, this configuration is also known as a choke input filter or L-section filter. A single L-C circuit will not suffice to improve the smoothing action of the filter circuit. A smooth filtered output will be obtained by arranging many L-section filters. The circuit design and smoothed waveform of a full wave rectifier output are shown in Figures 2.36 and 2.37 [84,87].

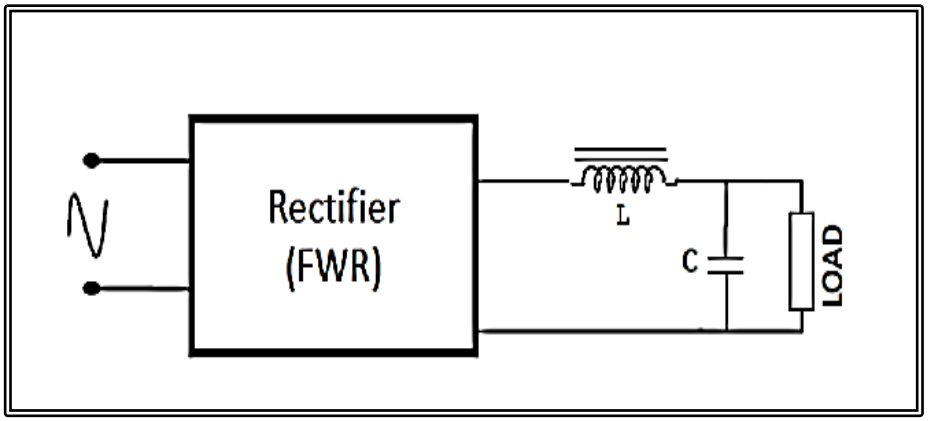


**Figure 2.36: Circuit diagram of L-section filter[87].**

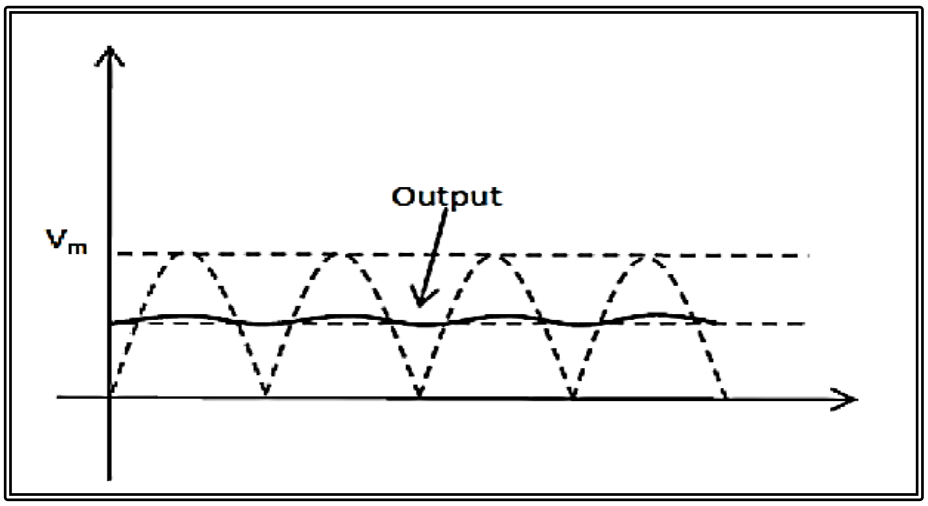


**Figure 2.37 : Waveform of a full wave rectifier output with LC filter[87 ]**

### 2-11-3-2: Π – Filter or Capacitance Input Filter

Π shape with two shunt capacitances ($C_1$ and $C_2$) and an inductance filter ( L ). As the rectifier output is provided directly into the capacitor it also called a capacitor input filter. The output from the rectifier is first given to the shunt capacitor C. The rectifier used can be half or full wave and the capacitors are usually electrolytic even though they large in size. In practical applications, the two capacitances are enclosed in a metal container which acts as a common ground for the two capacitors. Circuit

diagram and the waveform are given below in Figures 2.38 and 2.39 respectively [87].

When compared to other type of filters, the Π – Filter has some advantages like higher DC voltage and smaller ripple factor. But it also has some disadvantages like poor voltage regulation, high peak diode current, and high peak inverse voltage. This filter is divided into two – a capacitor filter and a L-section filter. Here the first capacitor $C_1$ offers a low reactance to AC component of rectifier output but provide more reactance to DC components. Therefore most of the AC components will bypass through $C_1$ and the DC component flows through chock L. The chock offers very high reactance to the AC component. Thus it blocks AC components while pass the DC [84,87].

The capacitor $C_2$ by passes any other AC component appears across the load and get steady DC. The voltage regulation is poor for this circuit as the output voltage falls off rapidly with the increase in load current. Advantages circuit more output voltage, ripple less output and suitable to be used with both HWR and FWR .Disadvantages are large in size and weight and high cost [84, 87].

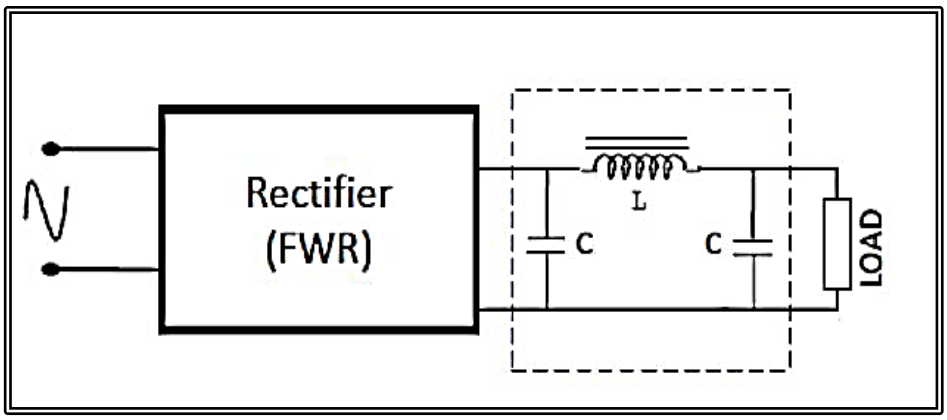


**Figure 2.38 : Circuit diagram of capacitance input filter[87].**

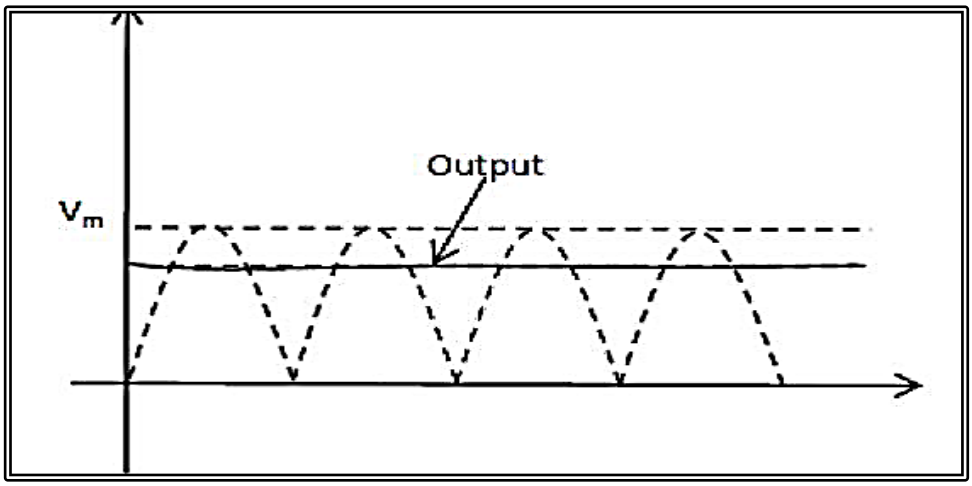


**Figure 2.39 : Waveform of a full wave rectifier output with capacitance input filter [ 87 ]**

## 2-12:ADS software

ADS software it has superior characteristics such as freedom in schematics and layout modification, as well as time-efficient simulation. The ADS platform includes solutions for design entry, synthesis, system, circuit, 3D EM simulation, analysis/post processing, and a complete manufacturing cycle. The modeling and analysis can be done through simulations to create an approximation of the results that will be obtained. The software comes with a significant number of predefined libraries and components that can be used. There are several different simulations that ADS can perform [88].

It is commonly used for simulating analog RF and microwave circuits. Harmonic balance simulation is ideal for high-frequency circuit and system simulation and has several advantages over traditional time-domain transient analysis. The frequency-domain voltages and currents are obtained through harmonic balance simulation. Calculating the steady-state

content of voltages or currents in a circuit directly. ADS Main Window show in Figure 2.40.It is the first interface to start using the ADS. It helps to access all the features supported by ADS. It allows to:

1-Create and manage a workspace .

2-Organize design data in virtual folders.

3-Open design view (s) and data display window.

4-Perform design flow settings.

5- Set program preferences.

6-ADS allows you to open only one workspace for a given instance.

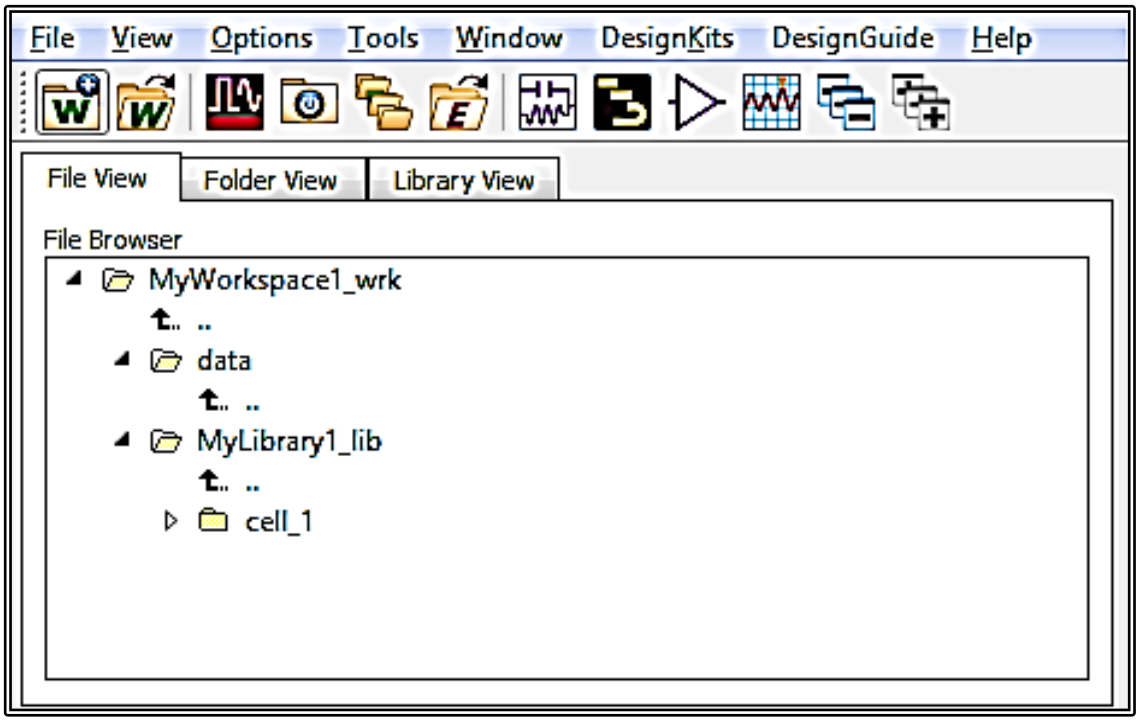


**Figure 2.40: The ADS software main window.**

The Drawing area is where you create your designs. The Component Palette contains buttons for placing components. The Prompt panel

provides messages to assist you during the execution of most commands, as well as various pieces of information to assist you in creating a design. The following Figure 2.41 displays the parts of a schematics view.

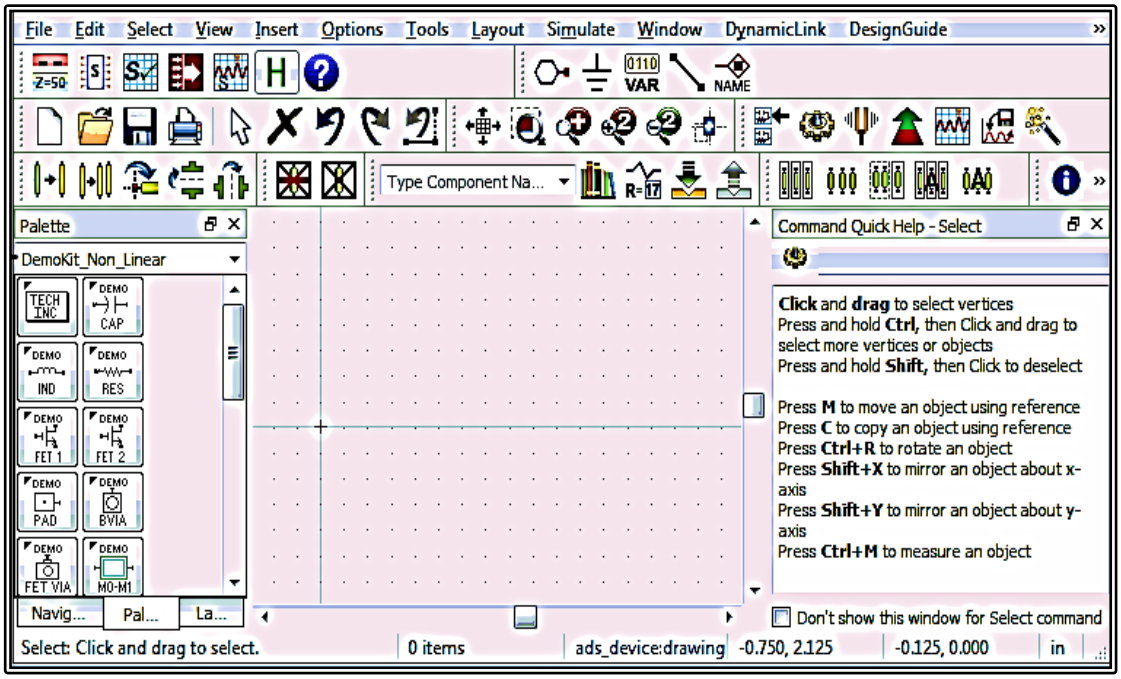


**Figure 2.41: Front view window of ADS software.**

# Chapter Three

# Simulation Work

## 3-1: Simulations Work setup

To identify the suitable frequency bands field A field investigation was done in Babylon to determine the availability of cell phone towers and the Internet. To perform a suitable and neat circuit design a finest diodes, and capacitance values have been chosen. After performing a study on rectifier circuits that were typically used in radio frequency harvesting applications, the optimal rectifier circuit and voltage doubling circuit were determined. The voltage doubling circuit was simulated using the software ADS ( 2020 64-bit Simulations). the circuit stage is an HSMS-7630 modified voltage multiplier, arranged in series .The voltage output ,and efficiency of each phase was measured. To maximize the amplification circuits efficiency, a model of an energy harvesting system has been suggested as a parallel phases (two , three , four, five, six, seven, and eight) phases for a voltage doubling circuit with three phases. Practical measurements of series and parallel circuits were also taken, and these were compared.

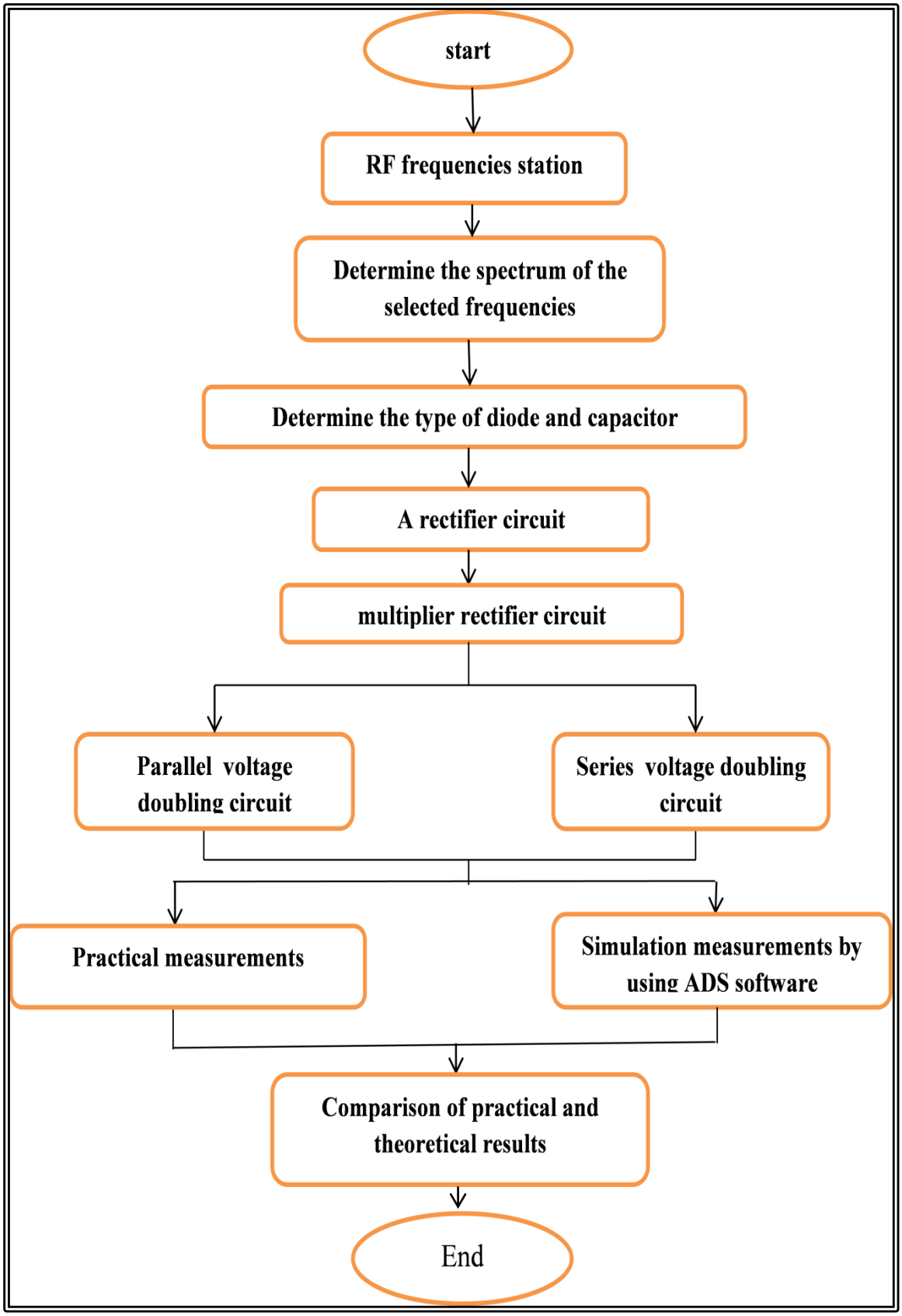


**Figure3. 1: Simulation Schematic**

## 3-2:Simulation measurements

The number of rectifier stages has a significant impact on the energy harvesting circuit's output voltage. Each stage works as a voltage multiplier which has been connected in series. The number of stages in the energy harvesting circuit is directly proportional to the output voltage. However, practical constraints impose a limit on the number of stages that can be used and as well as on a result of the output voltage . Due to the parasitic effect of the constituent capacitors of each stage, the voltage gain decreases as the number of stages increases. The voltage doubling circuit was simulated using the software ADS ( 2020 64-bit) Simulations. The voltage doubling circuit was designed with values ranging from (20 to -20) dBm for the input RF power and circuit stages ranging from (1 to 12) . In the simulation, the circuit stage is an HSMS-7630 modified voltage multiplier, arranged in series. After that, the voltage output of each phase was measured. The output power was calculated using Equation (2.20) .The capacitance values (8) pF were used to have the same value for all the stages at the frequency range (400-680) MHz, and (7.5) pF at the frequency range (700-900) MHz and (7) pF at the frequency range (2.5) GHz.

### 3-2-1: Three-stages voltage multiplier circuit

The design of a three- stage voltage multiplier circuit has been implemented as shown in Figure 3.2, with the filter capacitor across the load resistor. The range values of the input voltages within (2.23-0.22 )Volt and the output voltages of the three-phases voltage multiplier circuit have been presented in Table 3.1 under different frequencies of the waveforms (400-680) MHz, (700-900) MHz, and (2.5) GHz.

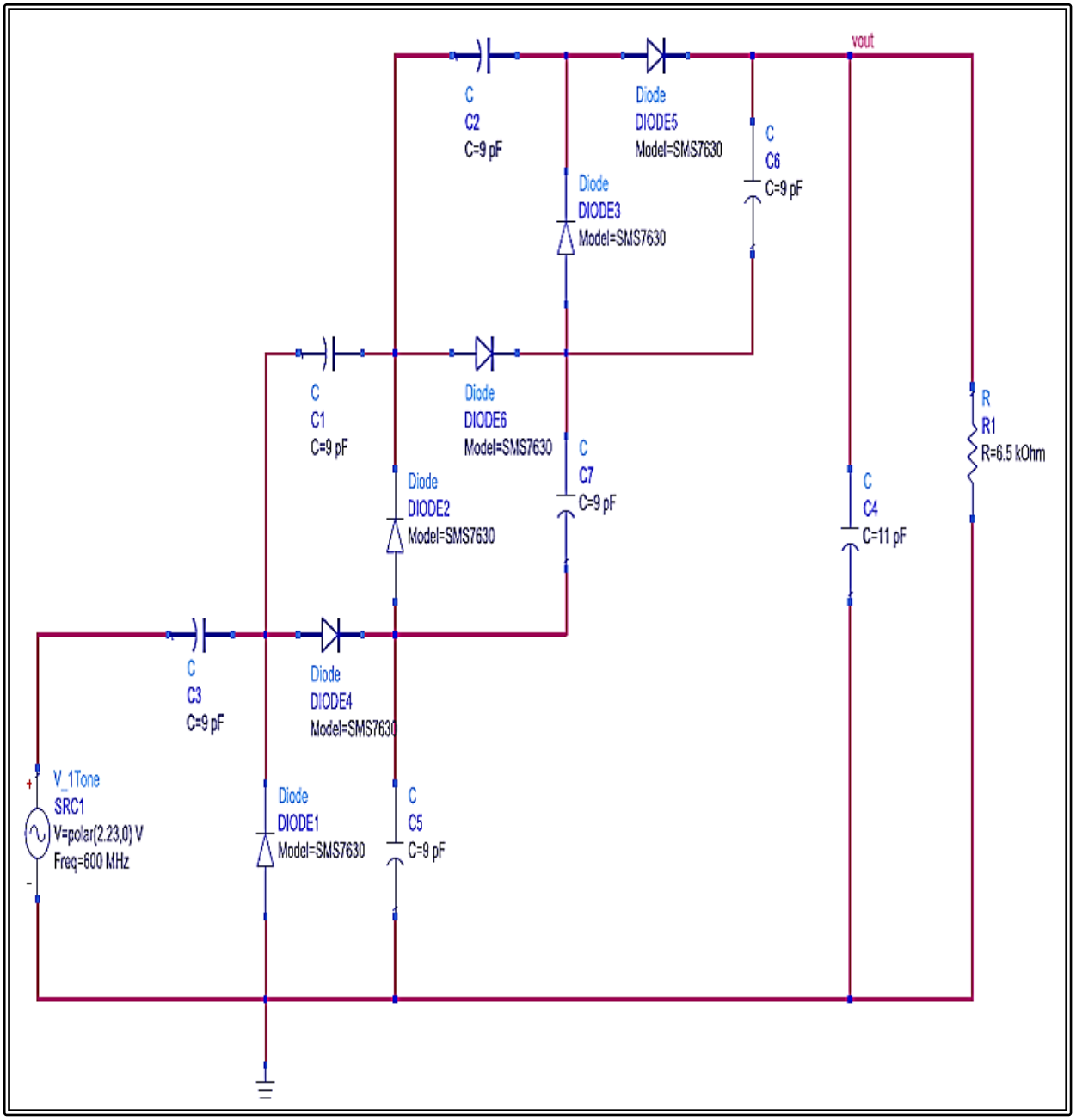


**Figure 3. 2: The voltage doubling circuits for three stages**

**Table 3. 1:$V_{out}$ of three- stage at (400-680) MHz,(700-900) MHz and (2.5) GHz**

| $V_{in}$(Volt) | Three-stage | | |
|---|---|---|---|
| | (400-680) MHz | (700-900) MHz | (2.5) GHz |
| | $V_{out}$ (Volt) | $V_{out}$ (Volt) | $V_{out}$ (Volt) |
| 2.23 | 5.600 | 5.700 | 5.600 |
| 1.77 | 5.500 | 5.490 | 5.490 |
| 1.41 | 4.960 | 4.900 | 4.950 |
| 1.12 | 3.970 | 3.850 | 3.820 |
| 0.89 | 3.100 | 2.850 | 2.850 |
| 0.70 | 2.190 | 2.100 | 2.110 |
| 0.56 | 1.600 | 1.540 | 1.540 |
| 0.44 | 1.180 | 1.100 | 1.070 |
| 0.35 | 0.850 | 0.780 | 0.740 |
| 0.28 | 0.580 | 0.550 | 0.500 |
| 0.22 | 0.400 | 0.370 | 0.320 |
| 0.17 | 0.260 | 0.235 | 0.180 |
| 0.14 | 0.160 | 0.145 | 0.117 |
| 0.11 | 0.100 | 0.090 | 0.070 |
| 0.08 | 0.065 | 0.058 | 0.047 |
| 0.07 | 0.038 | 0.036 | 0.028 |
| 0.05 | 0.024 | 0.023 | 0.018 |
| 0.04 | 0.015 | 0.014 | 0.011 |
| 0.03 | 0.010 | 0.009 | 0.007 |
| 0.025 | 0.006 | 0.005 | 0.004 |
| 0.022 | 0.004 | 0.003 | 0.003 |

The $V_{out}$ of the doubling circuits for three stages is illustrated in Figures 3. 3, 3. 4, and 3. 5 at $V_{in}$ equal to (2.23) Volt and under frequency waveforms of (400-680) MHz, (700-900) MHz and (2.5) GHz, respectively.

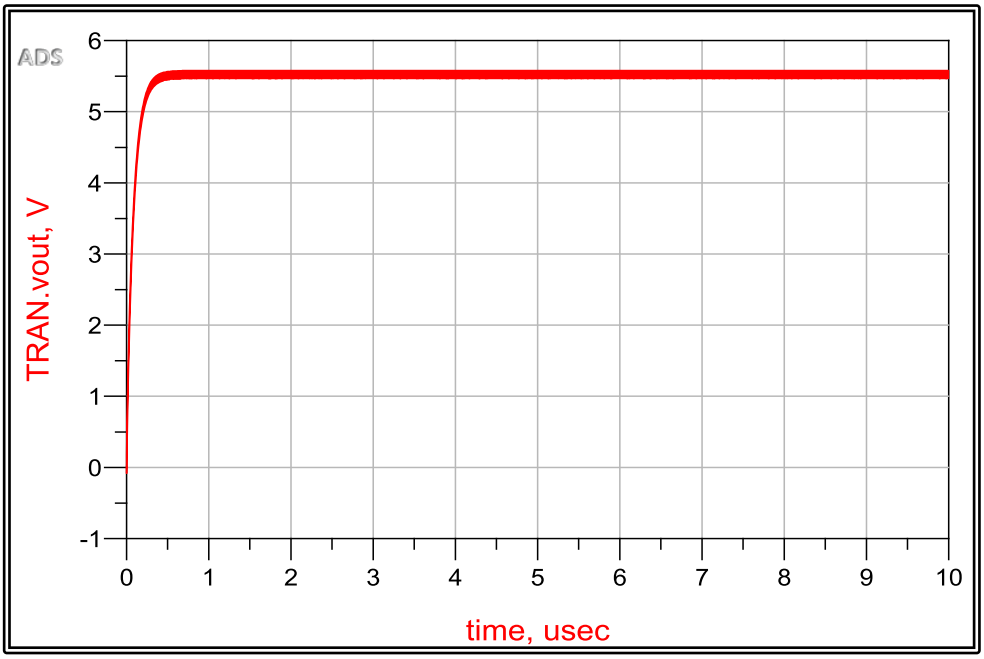


**Figure 3. 3: $V_{out}$ with time at (400-680) MHz**

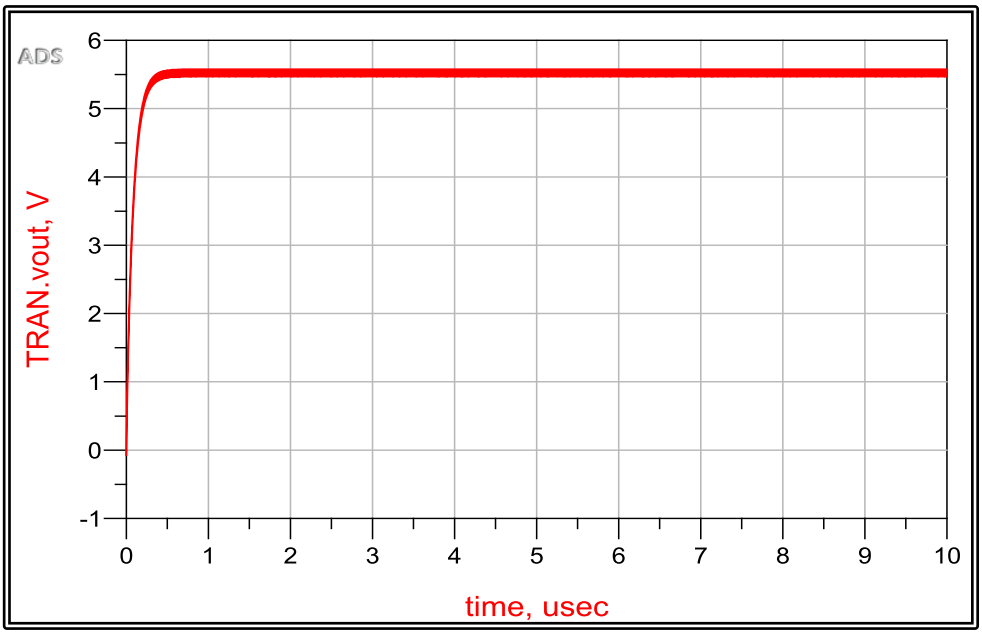


**Figure 3. 4:$V_{out}$ with time at (700-900) MHz**

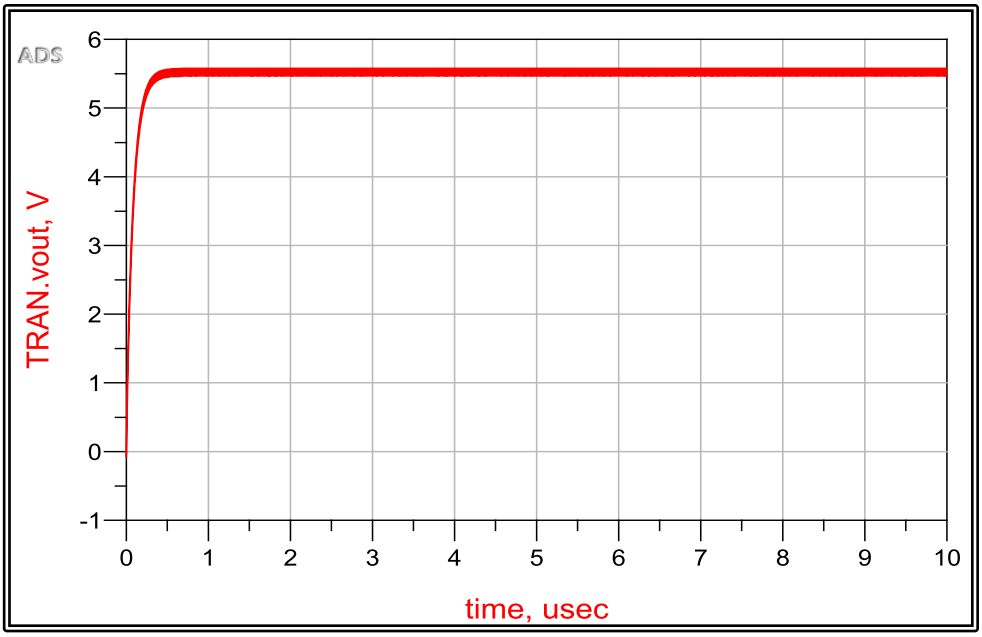


**Figure 3. 5 :$V_{out}$ with time at (2.5) GHz**

### 3-2-2: Five-stage voltage multiplier circuit

The design of the five- stage voltage multiplier circuit is presented in Figure 3. 6 . A filter capacitor is connected across the load resistor.

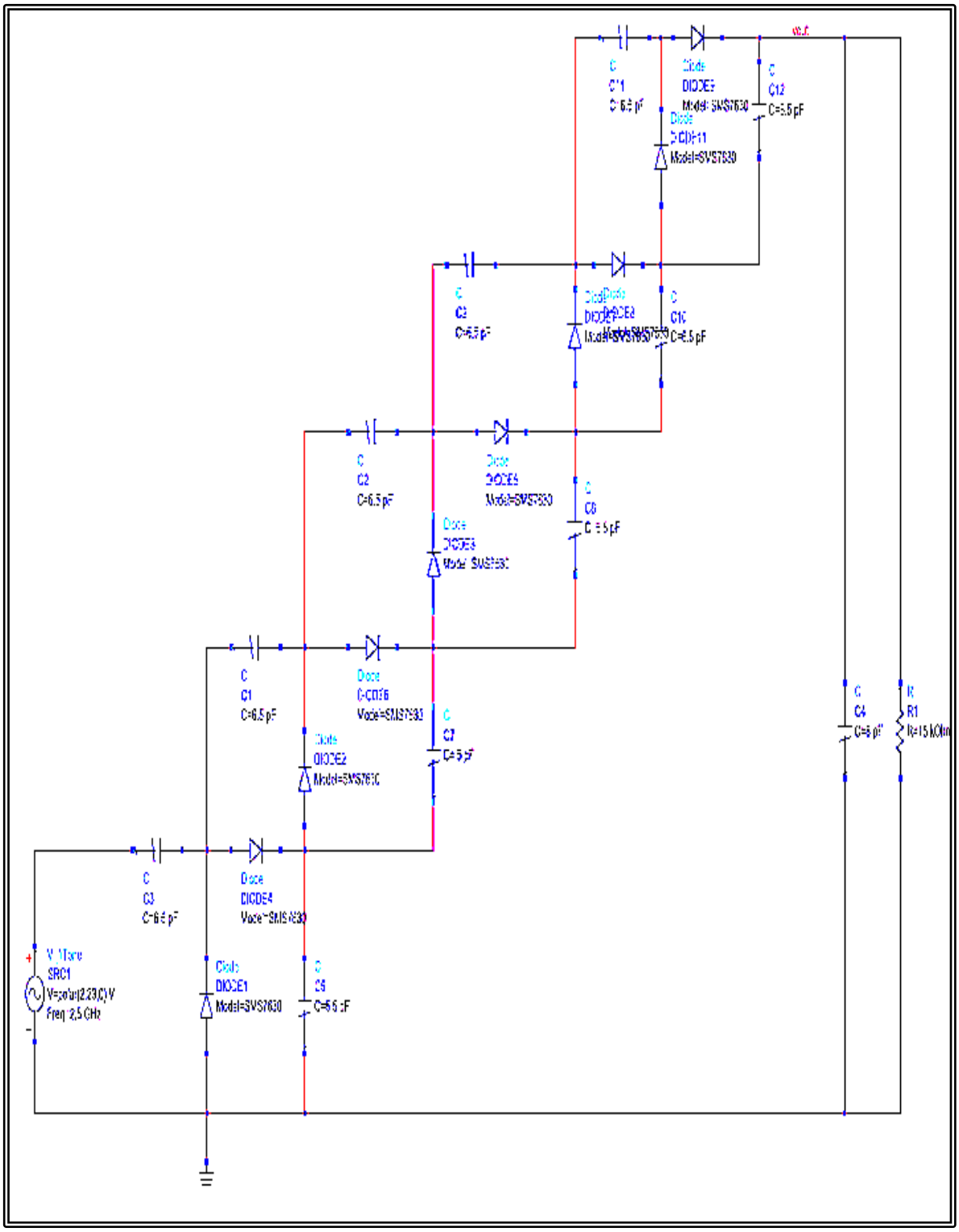


**Figure3. 6: The voltage doubling circuits for five stages**

Table 3.2 shows the values of the input voltages in the range of (2.23-0.22 ) Volt and the output voltages of the five -phase voltage

multiplier circuit . At (400-680) MHz, (700-900) MHz, and (2.5) GHz frequencies.

**Table 3.2:$V_{out}$ for five stages at (400-680)MHz,(700-900)MHz and (2.5)GHz**

| $V_{in}$(Volt) | Five -stage | | |
|---|---|---|---|
| | (400-680) MHz | (700-900) MHz | (2.5) GHz |
| | $V_{out}$ (Volt) | $V_{out}$ (Volt) | $V_{out}$ (Volt) |
| 2.23 | 8.800 | 8.800 | 9.000 |
| 1.77 | 8.200 | 8.200 | 8.300 |
| 1.41 | 7.200 | 7.100 | 6.850 |
| 1.12 | 5.600 | 5.500 | 5.200 |
| 0.89 | 4.200 | 3.600 | 3.810 |
| 0.70 | 3.130 | 2.300 | 2.750 |
| 0.56 | 2.330 | 1.600 | 1.950 |
| 0.44 | 1.700 | 1.050 | 1.360 |
| 0.35 | 1.210 | 0.700 | 0.920 |
| 0.28 | 0.840 | 0.440 | 0.600 |
| 0.22 | 0.560 | 0.260 | 0.400 |
| 0.17 | 0.380 | 0.150 | 0.260 |
| 0.14 | 0.250 | 0.093 | 0.165 |
| 0.11 | 0.160 | 0.055 | 0.099 |
| 0.08 | 0.105 | 0.034 | 0.065 |
| 0.07 | 0.065 | 0.021 | 0.040 |
| 0.05 | 0.043 | 0.013 | 0.026 |
| 0.04 | 0.025 | 0.008 | 0.016 |
| 0.03 | 0.017 | 0.005 | 0.010 |
| 0.025 | 0.011 | 0.003 | 0.007 |
| 0.022 | 0.007 | 0.002 | 0.005 |

Figures 3. 7, 3. 8 and 3. 9 show the $V_{out}$ for voltage doubling circuits with five stages . At a Vin of (2.23) Volt and frequencies of (400-680) MHz, (700-900) MHz, and (2.5) GHz.

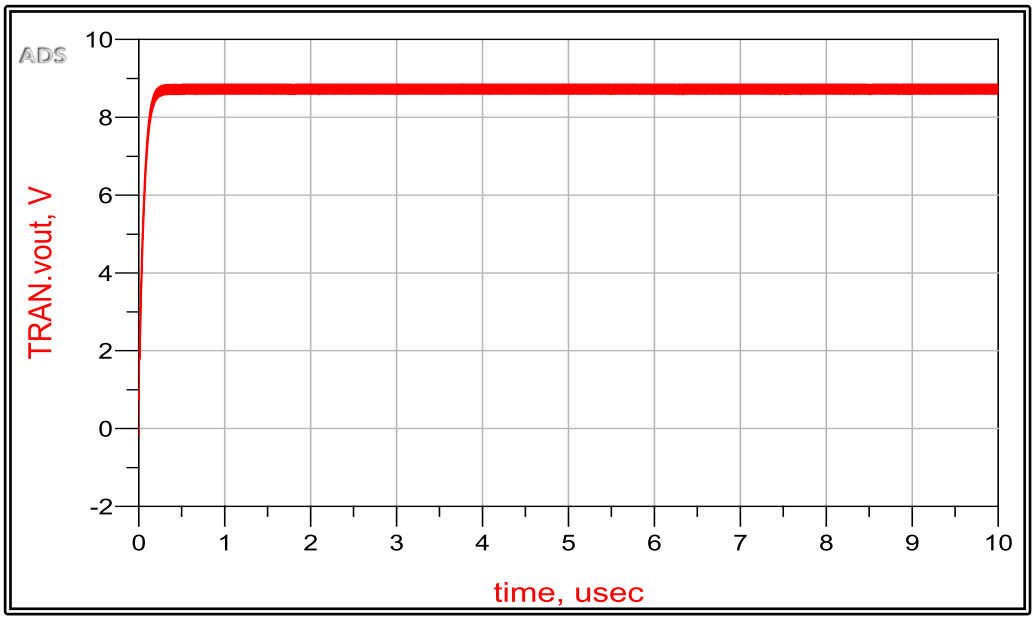


**Figure 3. 7: $V_{out}$ with time at (400-680) MHz**

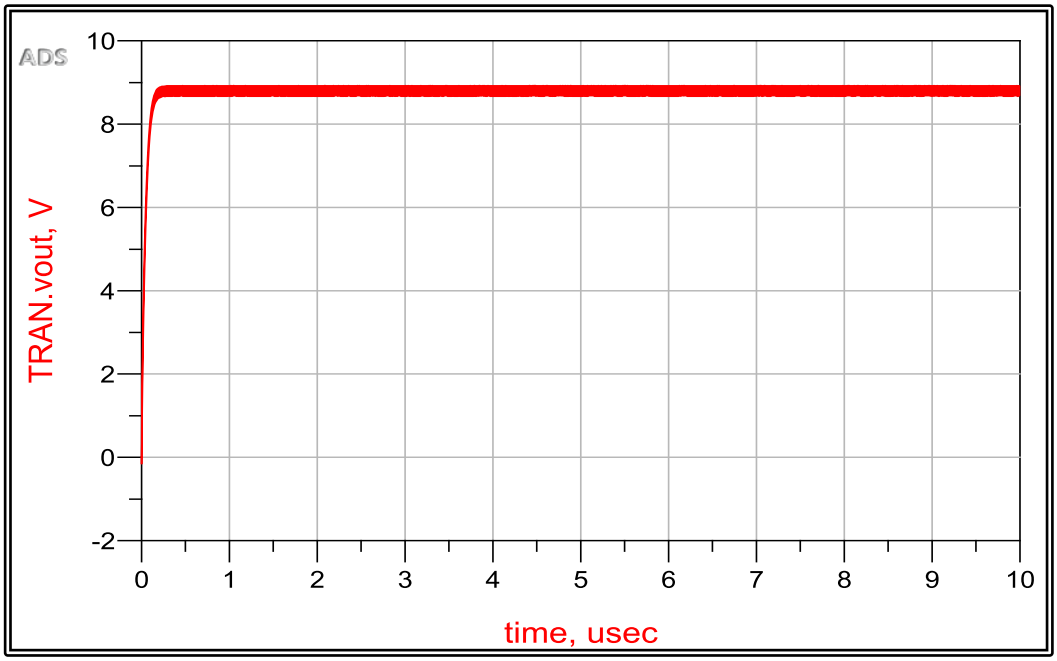


**Figure 3. 8:Vout with time at (700-900) MHz**

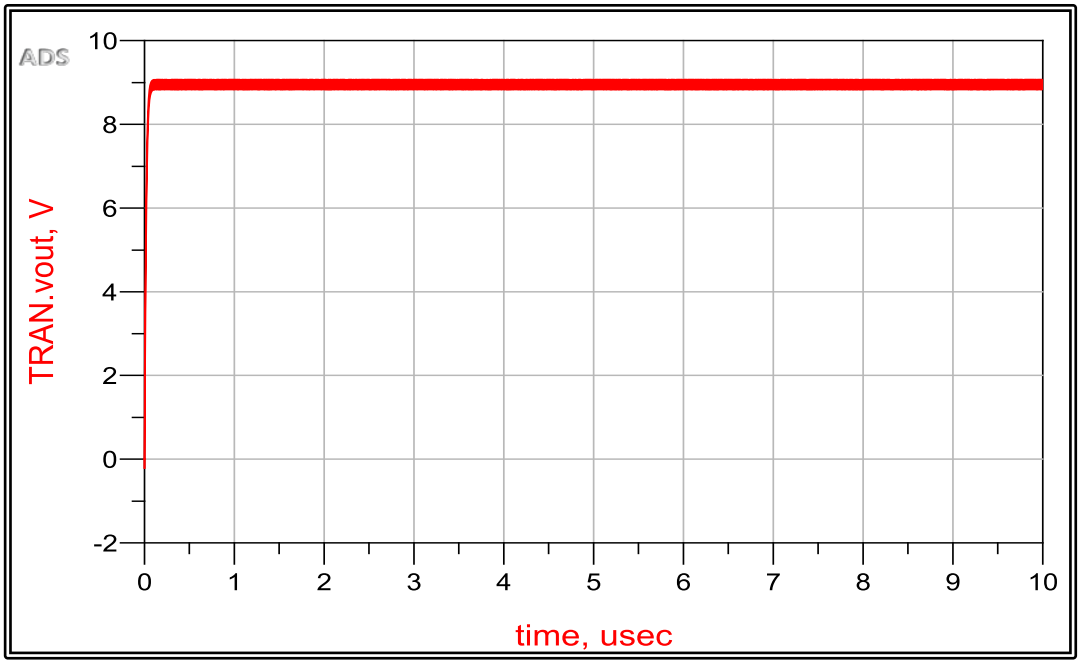


**Figure 3. 9:Vout with time at (2.5) GHz**

### 3-2-3: Seven-stage voltage multiplier circuit

The seven-stage voltage multiplier circuit design that was implemented is depicted in Figure 3.10. Across the load resistor is connected filter capacitor.

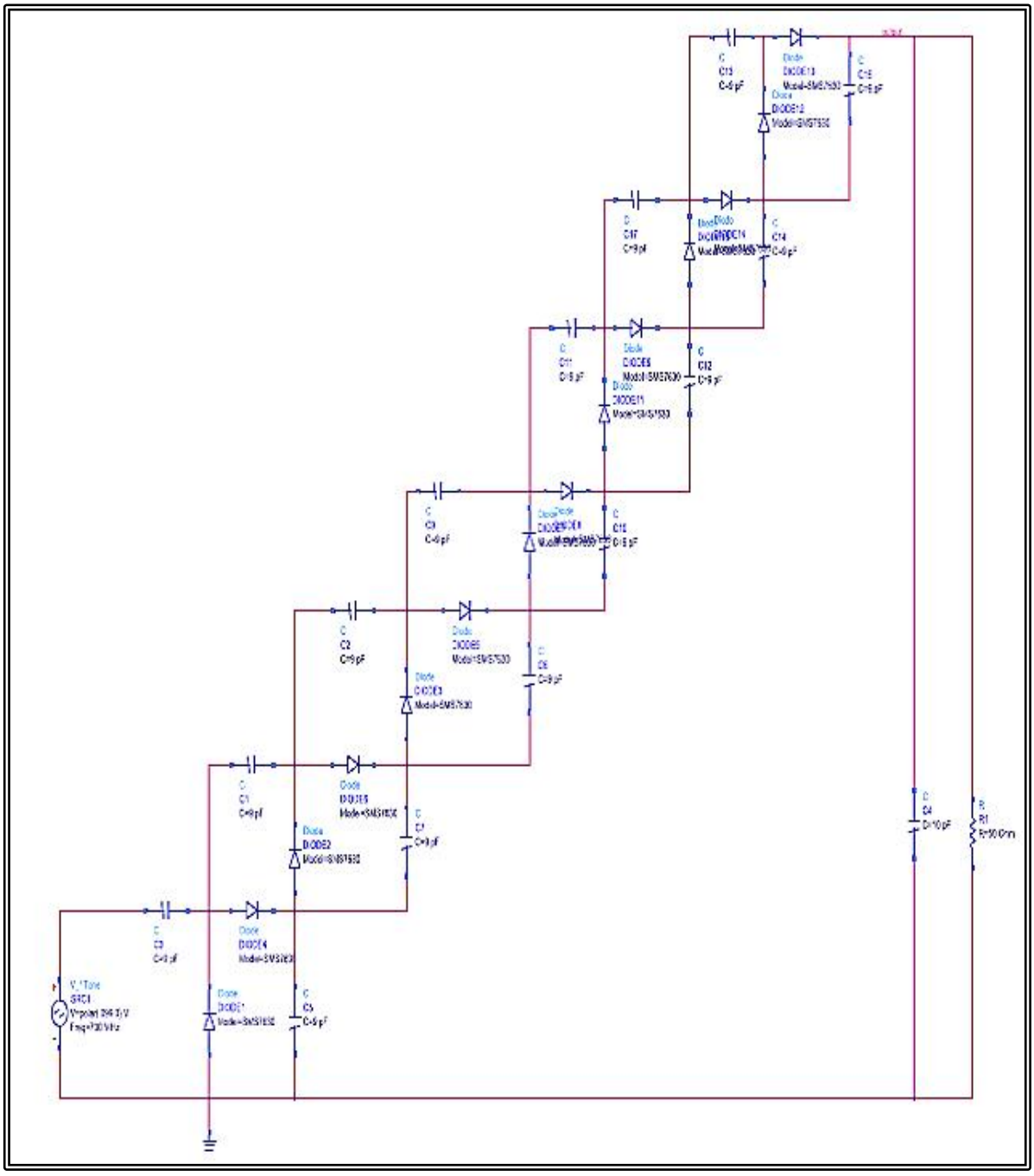

**Figure 3.10: The voltage doubling circuits for seven stages**

Table 3.3 shows the values of the input voltages in the range of (2.23-0.22 )Volt and the output voltages of the seven -phase voltage multiplier circuit . At (400-680) MHz, (700-900) MHz, and (2.5) GHz frequencies.

**Table 3.3:$V_{out}$ for seven stages at(400-680)MHz,(700-900)MHz and (2.5)GHz**

| $V_{in}$(Volt) | Seven-stage | | |
|---|---|---|---|
| | (400-680) MHz | (700-900) MHz | (2.5) GHz |
| | $V_{out}$ (Volt) | $V_{out}$ (Volt) | $V_{out}$ (Volt) |
| 2.23 | 11.00 | 10.50 | 11.00 |
| 1.77 | 10.00 | 9.300 | 9.35 |
| 1.41 | 8.500 | 7.840 | 7.60 |
| 1.12 | 6.700 | 6.100 | 5.80 |
| 0.89 | 4.990 | 4.550 | 4.20 |
| 0.70 | 3.700 | 3.300 | 2.99 |
| 0.56 | 2.650 | 2.360 | 2.15 |
| 0.44 | 1.700 | 1.700 | 1.49 |
| 0.35 | 1.210 | 1.190 | 0.99 |
| 0.28 | 0.840 | 0.800 | 0.65 |
| 0.22 | 0.560 | 0.530 | 0.401 |
| 0.17 | 0.380 | 0.350 | 0.260 |
| 0.14 | 0.250 | 0.231 | 0.165 |
| 0.11 | 0.160 | 0.148 | 0.105 |
| 0.08 | 0.105 | 0.099 | 0.063 |
| 0.07 | 0.065 | 0.062 | 0.043 |
| 0.05 | 0.043 | 0.040 | 0.028 |
| 0.04 | 0.025 | 0.025 | 0.018 |
| 0.03 | 0.017 | 0.017 | 0.012 |
| 0.025 | 0.011 | 0.010 | 0.007 |
| 0.022 | 0.007 | 0.007 | 0.005 |

Figures 3.11, 3.12 and 3.13 depict the $V_{out}$ for seven-stage voltage doubling circuits. at (2.23) Volt and frequencies of (400-680) MHz, (700-900) MHz, and (2.5) GHz.

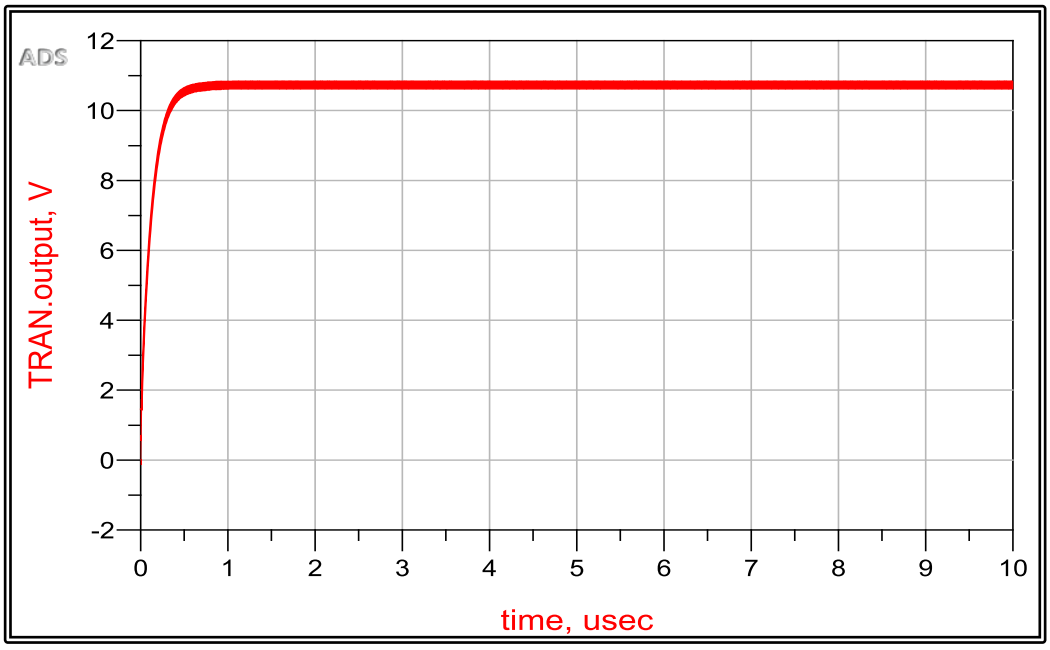


**Figure 3.11:$V_{out}$ with time at (400-680) MHz**

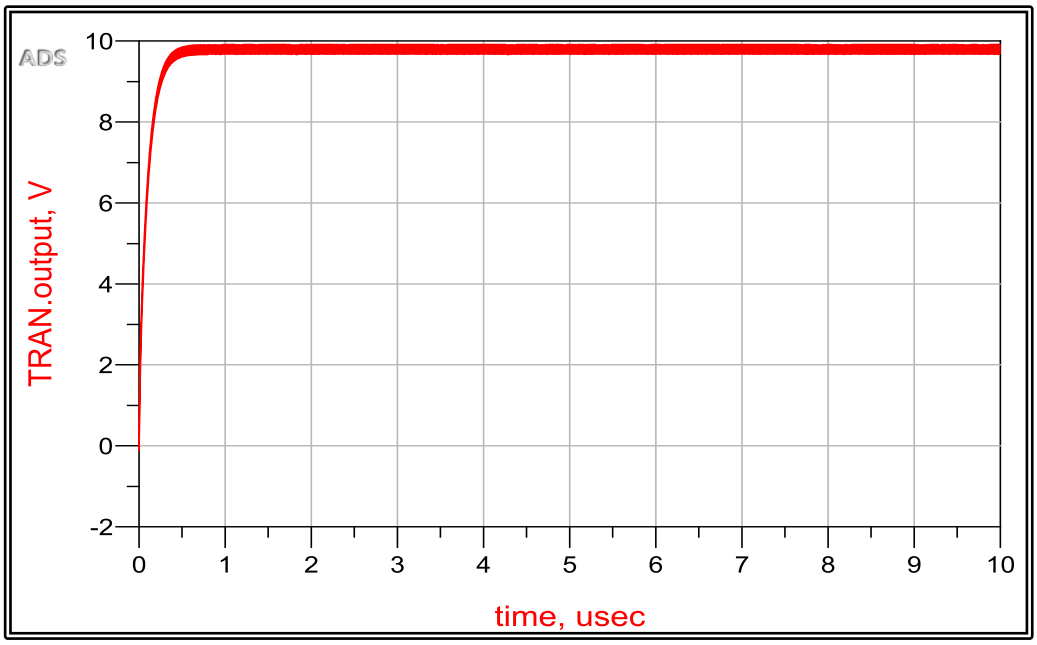


**Figure 3.12:$V_{out}$ with time at (700-900) MHz**

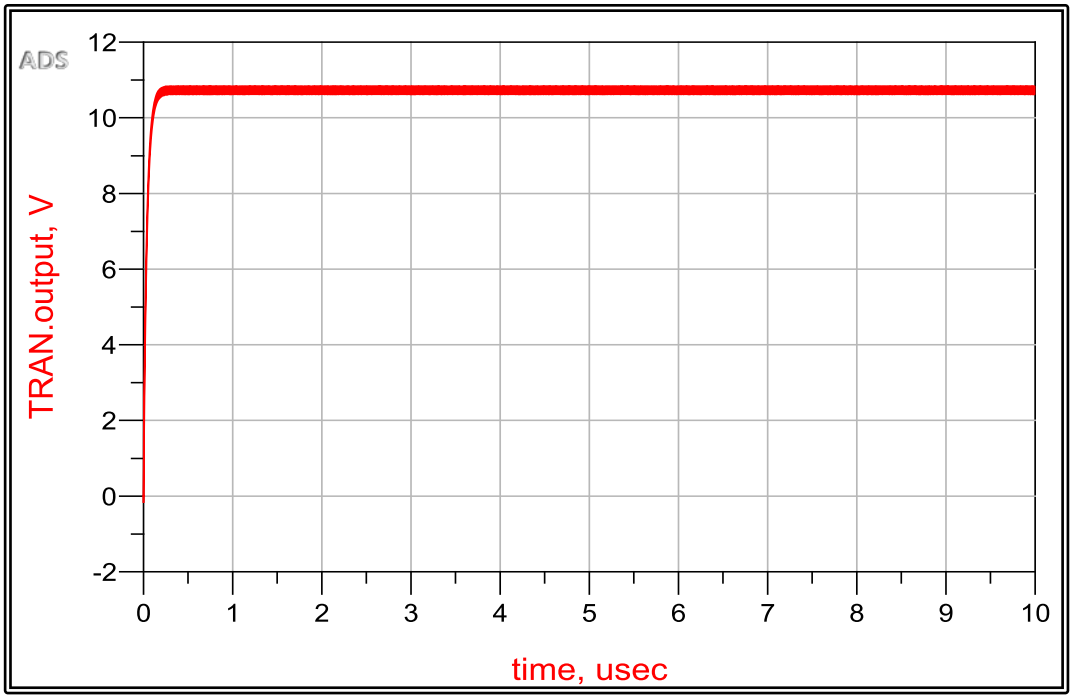


**Figure 3.13:$V_{out}$ with time at (2.5) GHz**

### 3-2-4: Ten-stage voltage multiplier circuit

Figure 3.14 depicts the ten-stage voltage multiplier circuit design that was implemented . A filter capacitor is connected across the load resistor.

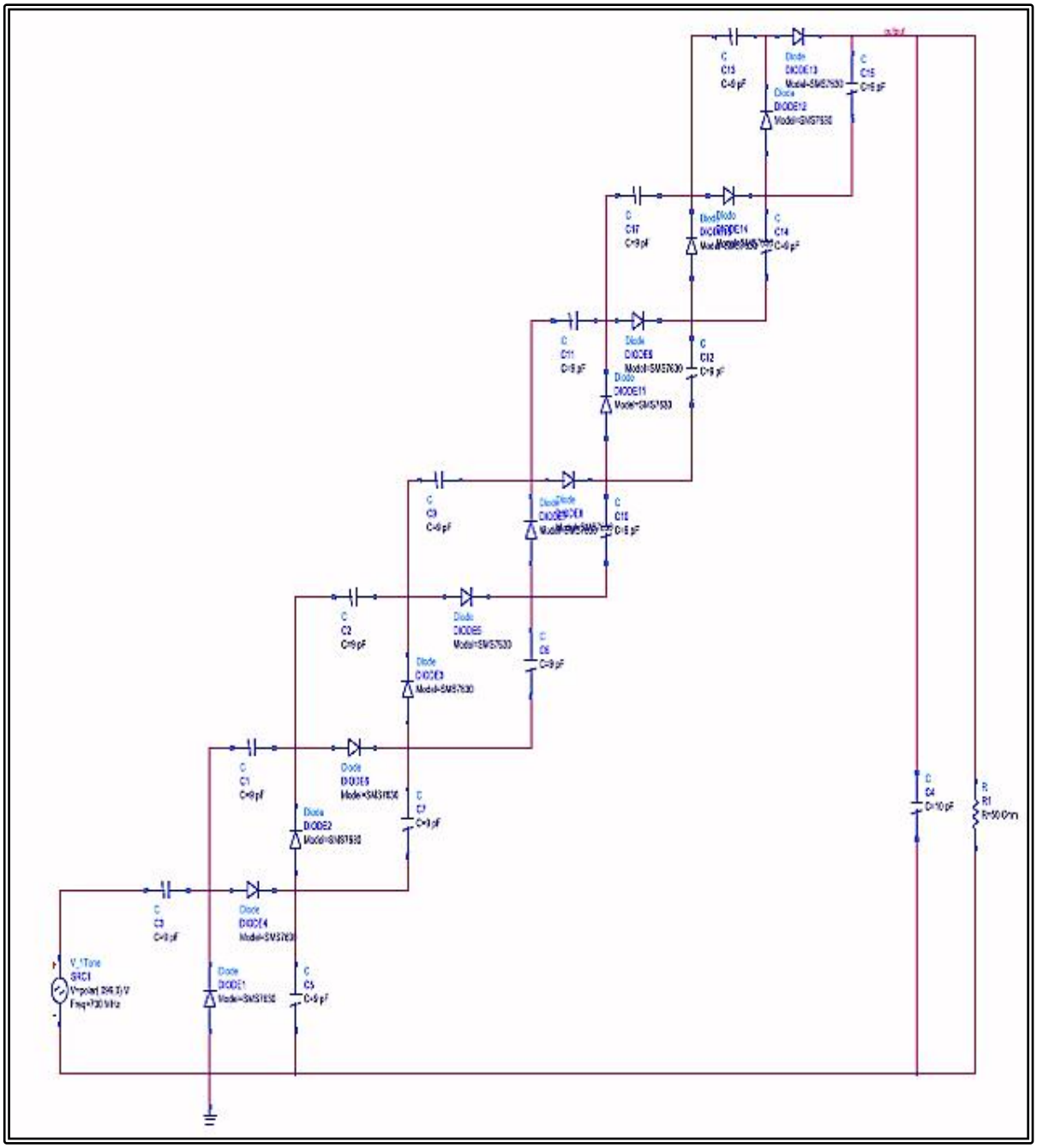

**Figure 3.14: Ten-stage voltage doubling circuits**

The values of the input voltages in the range of (2.23-0.22 ) Volt and the output voltages of the ten-phase voltage multiplier circuit are shown in Table 3.4 at frequencies of (400-680) MHz, (700-900) MHz, and (2.5) GHz.

**Table 3.4:$V_{out}$ for ten stage at(400-680) MHz,(700-900) MHz and (2.5) GHz**

| $V_{in}$ (Volt) | Ten-stage | | |
|---|---|---|---|
| | (400-680) MHz | (700-900) MHz | (2.5) GHz |
| | $V_{out}$ (Volt) | $V_{out}$ (Volt) | $V_{out}$ (Volt) |
| 2.23 | 13.50 | 13.00 | 12.800 |
| 1.77 | 12.20 | 11.90 | 10.95 |
| 1.41 | 10.80 | 10.00 | 8.700 |
| 1.12 | 8.200 | 7.800 | 6.500 |
| 0.89 | 6.100 | 5.700 | 4.700 |
| 0.70 | 4.450 | 4.100 | 3.400 |
| 0.56 | 3.300 | 3.000 | 2.430 |
| 0.44 | 2.390 | 2.150 | 1.700 |
| 0.35 | 1.850 | 1.560 | 1.200 |
| 0.28 | 1.320 | 1.130 | 0.831 |
| 0.22 | 0.940 | 0.780 | 0.595 |
| 0.17 | 0.530 | 0. 550 | 0.410 |
| 0.14 | 0.380 | 0. 370 | 0.275 |
| 0.11 | 0.275 | 0. 250 | 0.180 |
| 0.08 | 0.190 | 0. 170 | 0.081 |
| 0.07 | 0.125 | 0.113 | 0.054 |
| 0.05 | 0.085 | 0.072 | 0.034 |
| 0.04 | 0.054 | 0.049 | 0.023 |
| 0.03 | 0.035 | 0.031 | 0.010 |
| 0.025 | 0.023 | 0.021 | 0.015 |
| 0.022 | 0.014 | 0.013 | 0.019 |

The $V_{out}$ for ten-stage voltage doubling circuits is depicted in Figures 3.15, 3.16, and 3.17 at a voltage of (2.23) Volts and frequencies of (400-680) MHz, (700-900) MHz, and (2.5) GHz.

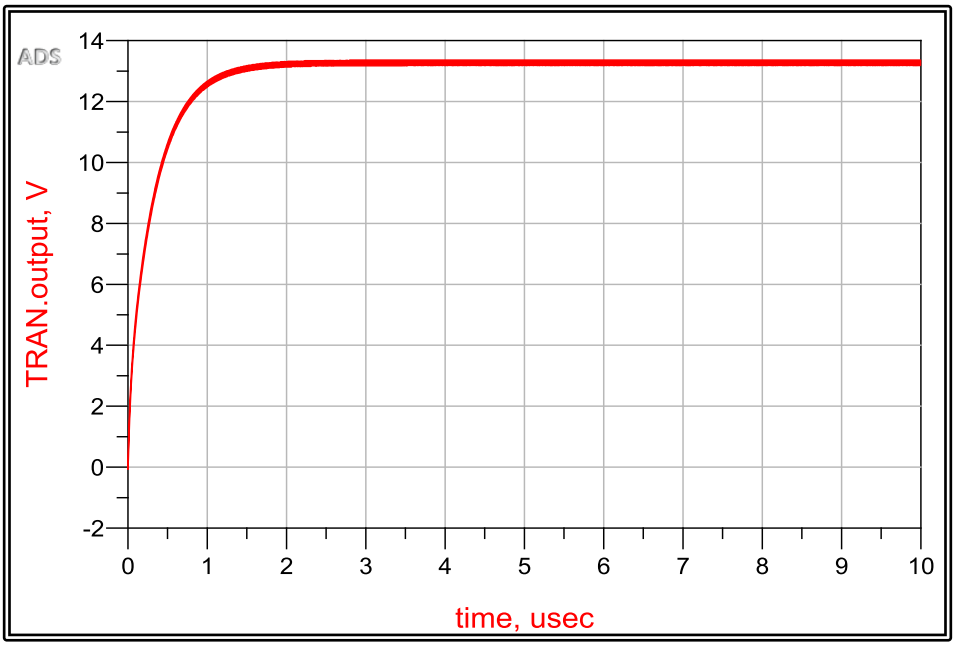


**Figure 3.15: $V_{out}$ with time at(400-680) MHz**

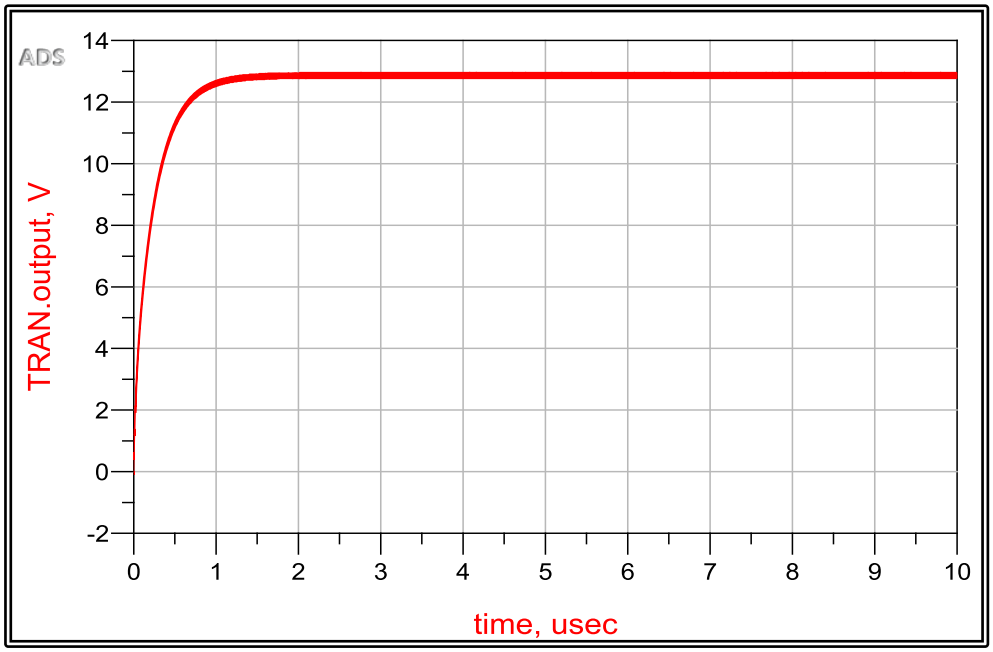


**Figure 3.16: Vout with time at(700-900) MHz**

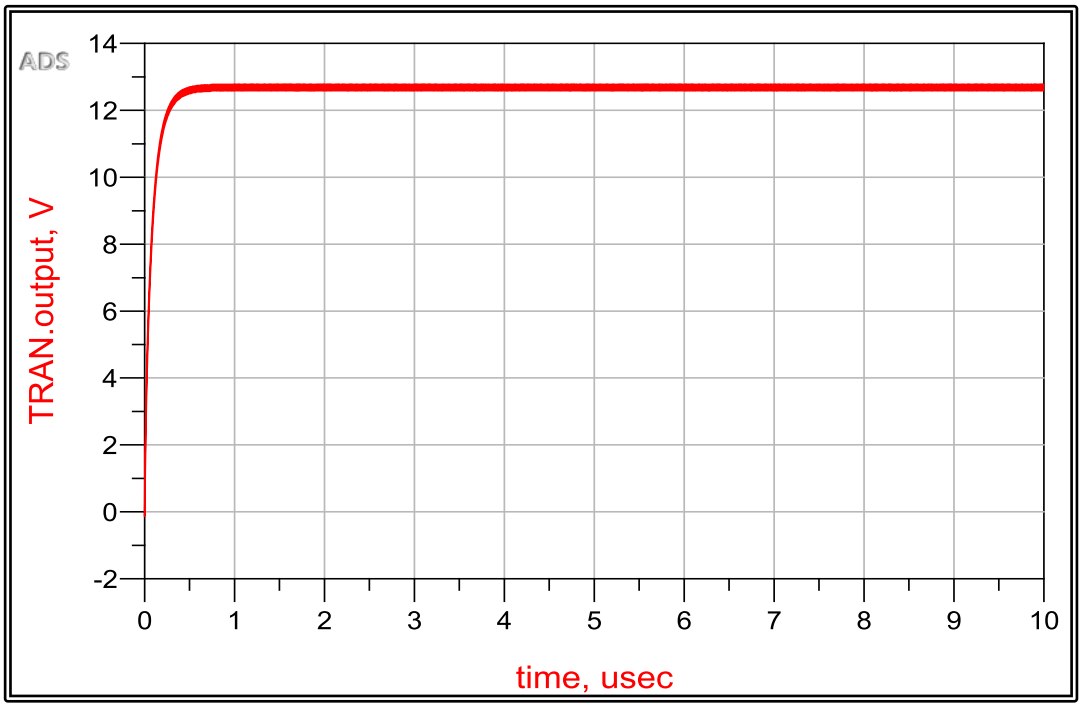


**Figure 3.17: $V_{out}$ with time at (2.5) GHz**

### 3-2-5: Twelve-stage voltage multiplier circuit

The twelve-stage voltage multiplier circuit design that was implemented is depicted in Figure 3.18. A filter capacitor is connected across the load resistor.

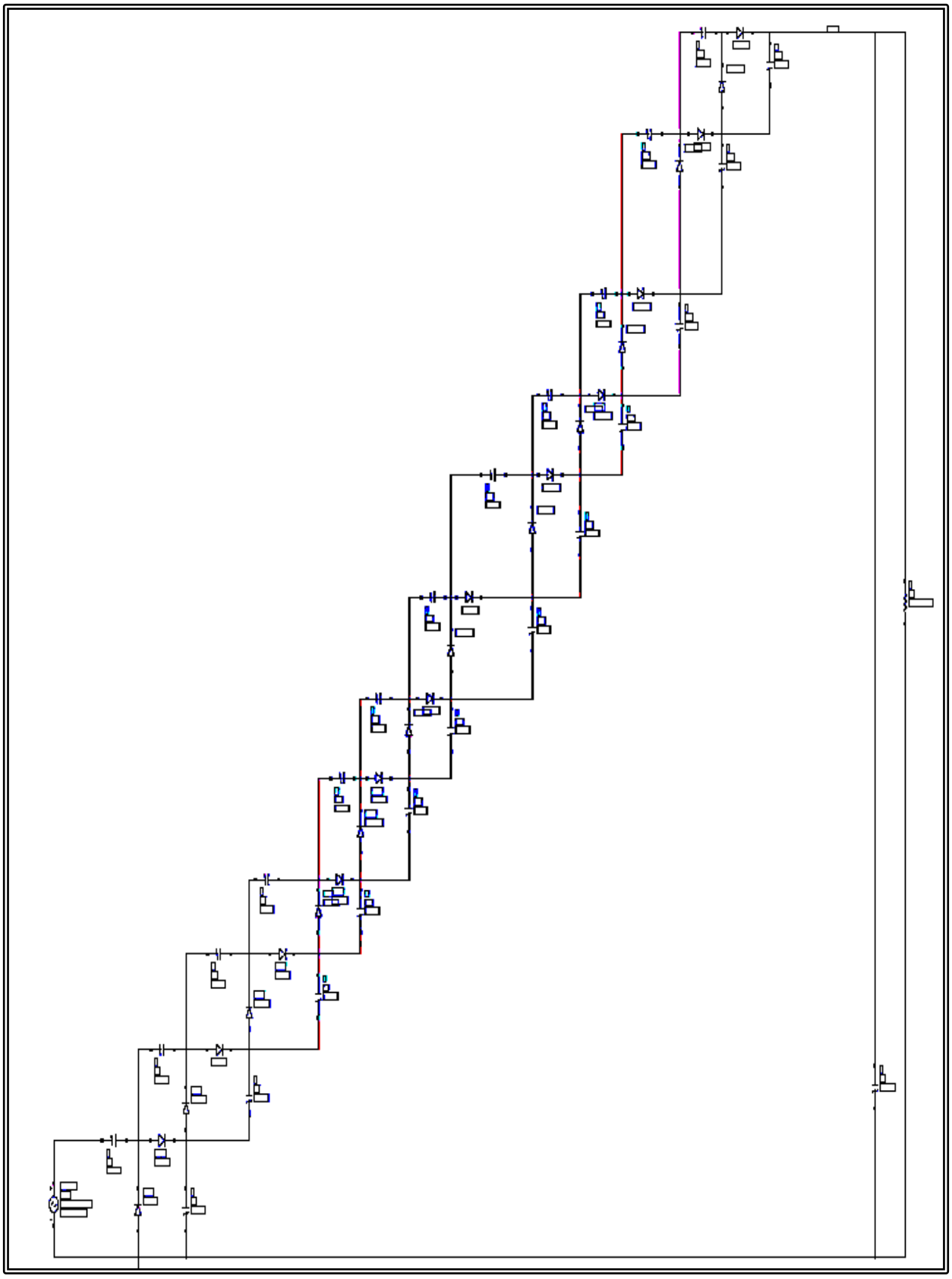

**Figure 3.18: The voltage doubling circuits for twelve- stage**

The values of the input voltages within the range of (2.23-0.22 ) Volt and the output voltages of the twelve -phase voltage multiplier circuit are shown in Table 3.5 at frequencies of (400-680) MHz, (700-900) MHz, and (2.5) GHz.

**Table 3.5:$V_{out}$ for twelve stages at(400-680) MHz,(700-900) MHz and (2.5) GHz**

| $V_{in}$(Volt) | Twelve-stage | | |
|---|---|---|---|
| | (400-680) MHz | (700-900) MHz | (2.5) GHz |
| | $V_{out}$ (Volt) | $V_{out}$ (Volt) | $V_{out}$ (Volt) |
| 2.23 | 12.70 | 12.50 | 12.80 |
| 1.77 | 11.80 | 11.50 | 10.80 |
| 1.41 | 10.10 | 9.550 | 8.720 |
| 1.12 | 7.900 | 7.500 | 6.450 |
| 0.89 | 6.000 | 5.600 | 4.700 |
| 0.70 | 4.500 | 3.900 | 3.400 |
| 0.56 | 3.300 | 2.800 | 2.400 |
| 0.44 | 2.350 | 2.000 | 1.700 |
| 0.35 | 1.700 | 1.400 | 1.200 |
| 0.28 | 1.160 | 1.000 | 0.841 |
| 0.22 | 0.790 | 0.680 | 0.595 |
| 0.17 | 0.550 | 0.480 | 0.415 |
| 0.14 | 0.380 | 0. 340 | 0.280 |
| 0.11 | 0.250 | 0. 220 | 0.185 |
| 0.08 | 0.170 | 0. 154 | 0.130 |
| 0.07 | 0.110 | 0. 100 | 0.084 |
| 0.05 | 0.075 | 0.065 | 0.056 |
| 0.04 | 0.049 | 0.042 | 0.035 |
| 0.03 | 0.030 | 0.027 | 0.023 |
| 0.025 | 0.020 | 0.018 | 0.015 |
| 0.022 | 0.012 | 0.011 | 0.011 |

The $V_{out}$ for voltage doubling circuits for twelve- stage is depicted in figure 3.19 , 3.20 , and 3.21 at $V_{in}$ equal to (2.23) Volt and frequencies of (400-680) MHz,(700-900) MHz and (2.5) GHz.

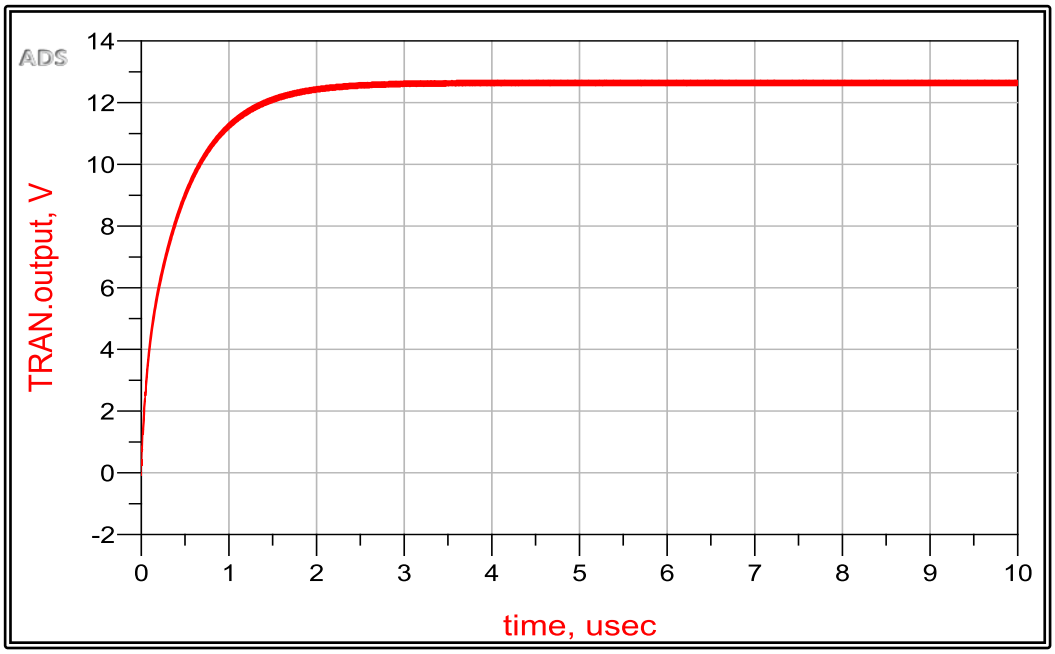


**Figure 3.19: $V_{out}$ with time at(400-680)MHz**

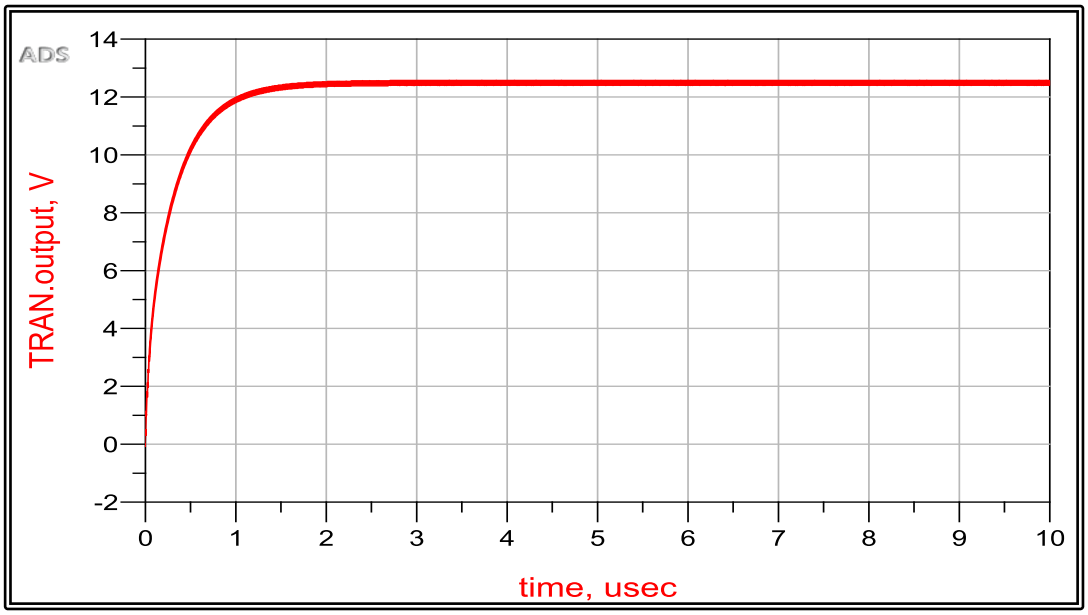


**Figure 3.20: Vout with time at (700-900) MHz**

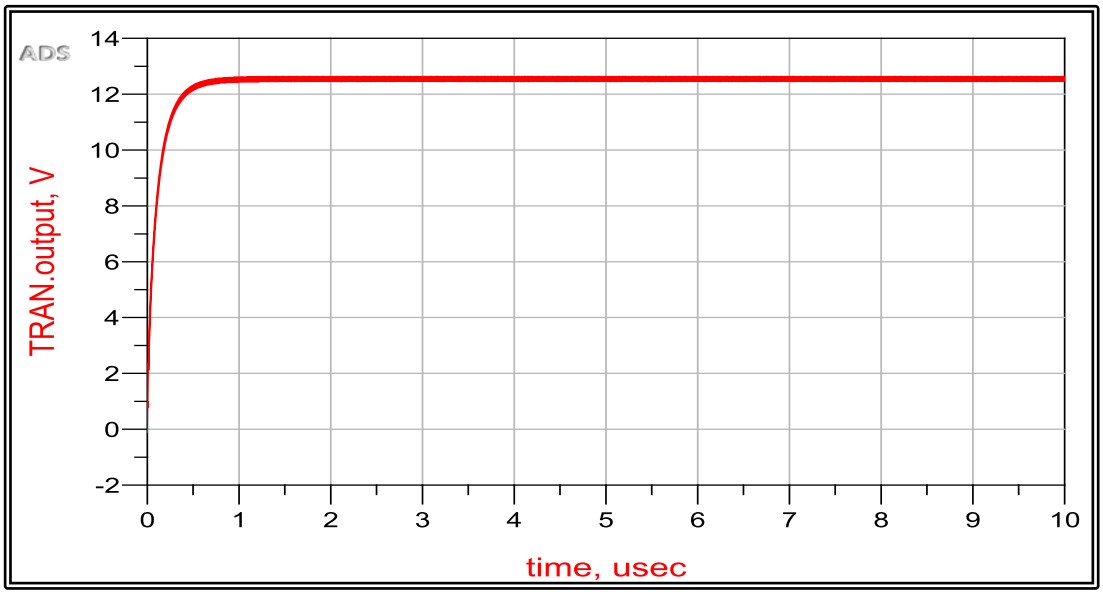


**Figure 3.21:Vout with time at (2.5) GHz**

Parametric research is carried out prior to the manufacturing of the final structure to pre-determine the best performance of the proposed rectifier. The following parameters were investigated: (1) the number of stages; and (2) capacitance variation in stages. All of the experiments were carried out utilizing the (ADS) software for simulation. The first parameter studied is the number of stages of the suggested rectifier for optimum rectified output voltage is. an analysis on the optimum number of stage was carried out for the proposed rectifier for input power from 20 dBm to -20dBm. The proposed rectifier is designed to operate at 400-680 MHz ,700-900 MHz and (2.5) GHz frequencies for energy harvesting.

Figures 3. 3, 3. 4, and 3. 5 show that the output is equivalent to (5.6)Volt for input voltage (2.23)Volt, showing a voltage doubling that is nearly three times input voltage of a three-phase circuit. Figures 3. 7, 3. 8, and 3. 9 indicate that when the input voltage is (2.23) Volt, it doubles to 9 volts, which is approximately equal to five times the input voltage.

Figures 3.11, 3.12, and 3.13 demonstrate that the input voltage is increased to (11) Volt, which is which is approximately equal to seven times the input voltage. Figures 3.15, 3.16, and 3.17 demonstrate that the input voltage is increased to (13) Volt. Figures 3.19, 3.20, and 3.21 demonstrate that the input voltage is increased to (12.8) Volt. See that the output voltage of the phases (3 ,5, 7) is good, but there is a steep slope of the output voltage of the phases (10 and 11), which is due to the parasitic impact of the constituent capacitors of each stage, and the voltage gain diminishes as the number of stages grows, In addition to increasing the circuit's impedance. The circuit has been implemented for all frequency bands.

The table below compares the theoretical results of reference[9] with the present study results at frequency of 900 MHz.

**Table 4.6:Voltage at 4 $^{th}$- 6$^{th}$ stages of rectifier voltage doubler reference [9 ]and Voltage at 3 th,5th and 7th stages of rectifier voltage doubler [current work].**

| Power(dB)[9] | 6$^{th}$ stage voltage(V) | 5th stage voltage(V) | 4$^{th}$ stage voltage(V) | Frequncy | Load |
|---|---|---|---|---|---|
| 15 | 4.83 | 3.89 | 3.92 | 900MHz | 2KΩ |
| 10 | 2.32 | 2.08 | 2.1 | | |
| 5 | 0.95 | 0.95 | 0.95 | | |
| 0 | 0.3 | 0.31 | 0.31 | | |
| Power(dB)[ current work] | 7$^{th}$ stage voltage(V) | 5th stage voltage(V) | 3th stage voltage(V) | Frequncy | Load |
| 15 | 8 | 6.3 | 4.41 | 900MHz | 4KΩ |
| 10 | 4.6 | 2.75 | 2.1 | | |
| 5 | 1.9 | 1.12 | 0.93 | | |
| 0 | 0.78 | 0.36 | 0.37 | | |

From Table 4.6 see that the results obtained from the voltage doubling circuits are superior to those obtained from the reference [9].

The effect of various combinations of capacitance in circuits on the rectified output voltage has been examined. The rectified output voltage does change substantially for different combinations of stage capacitance, as seen in Tables 3. 1, 3.2, 3.3, 3.4 and 3.5.

The relationship between the output voltage and the input power has been set at phases (3, 5, 7, 10, and 12 ) at (400-680) MHz as shown in the diagram 3.22.

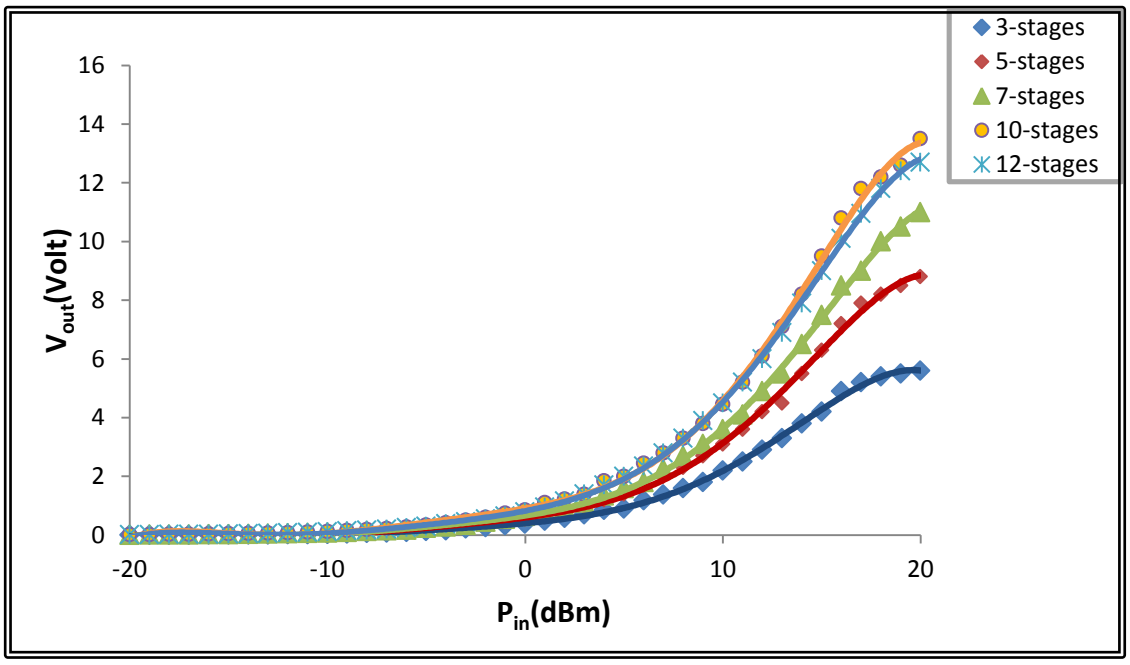


**Figure 3.22: $P_{in}$ with $V_{out}$ at (400-680) MHz for 3,5,7,10 and 12 stage**

At (700-900) MHz, the relationship between the output voltage and the input power has been drawn for phases 3, 5, 7, 10, and 12. As shown in the diagram 3.23.

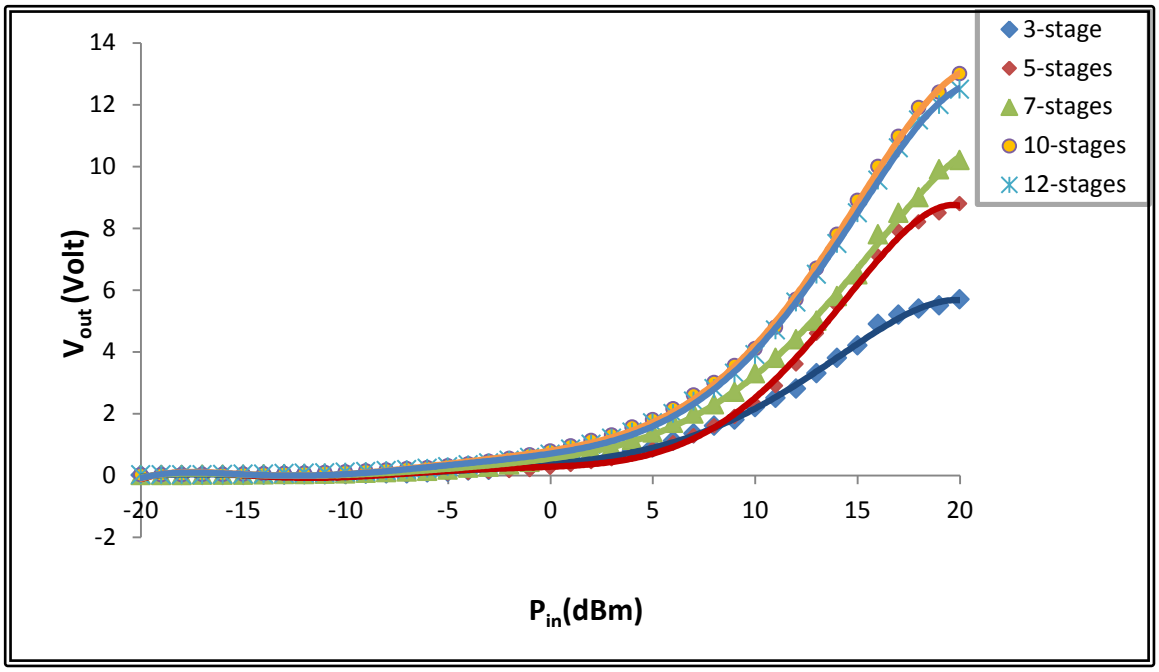


**Figure3.23: $P_{in}$ with $V_{out}$ at (700-900)MHz for 3,5,7,10 and 12 stage**

The relationship between the output voltage and the input power has been drawn for phases (3, 5, 7, 10, and 12) at (2.5) GHz. As illustrated in the diagram 3.24.

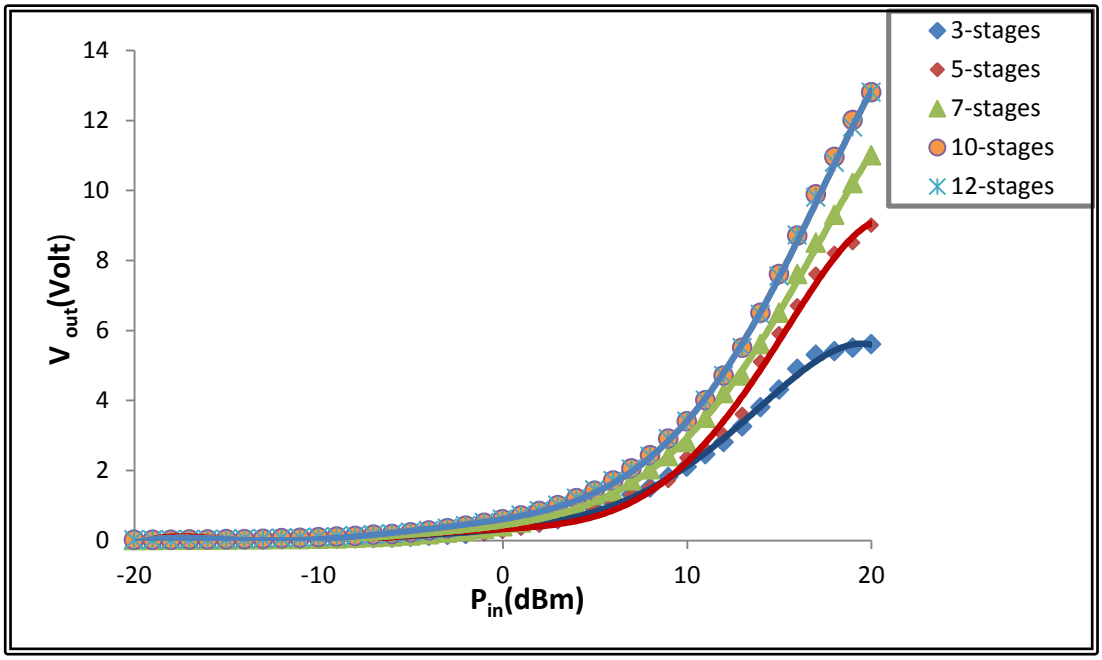


**Figure 3.24: $P_{in}$ with $V_{out}$ at (2.5) GHz for 3,5,7,10 and 12 stage**

Figures 3.22,3.23, and 3.24 show the proposed circuit's diodes and capacitors validate the circuit's role as a rectifier and multiplier of input power. At all measured input powers, it works better at all the ranges of frequency approximately. It was also shown that increasing the number of phases in the voltage doubling circuit increases the output voltage. As shown in the figures above, a ten-phase circuit produces the highest voltage (13.5,13) Volts, followed by seven-phase the highest voltage (11,10.5) Volts and finally three phases providing the highest voltage within values (5.6,5.5) Volts, for all regions of frequency, This is the same as what was described in reference [ 10, 27,93]. However, after (12) phases, the voltage begins to fall, which is ascribed to an increase in the circuit's resistance, and the circuit therefore loses its characteristic as a voltage doubling circuit.

Figures 3.25, 3.26, and 3.27 show the efficiency of the stage circuits (3, 5, 7, 10, 12) which was calculated using Eq. 2.24. The results have been plotted as a function of the input power under the frequency ranges (400-680) MHz, (700-900) MHz, and (2.5) GHz, respectively.

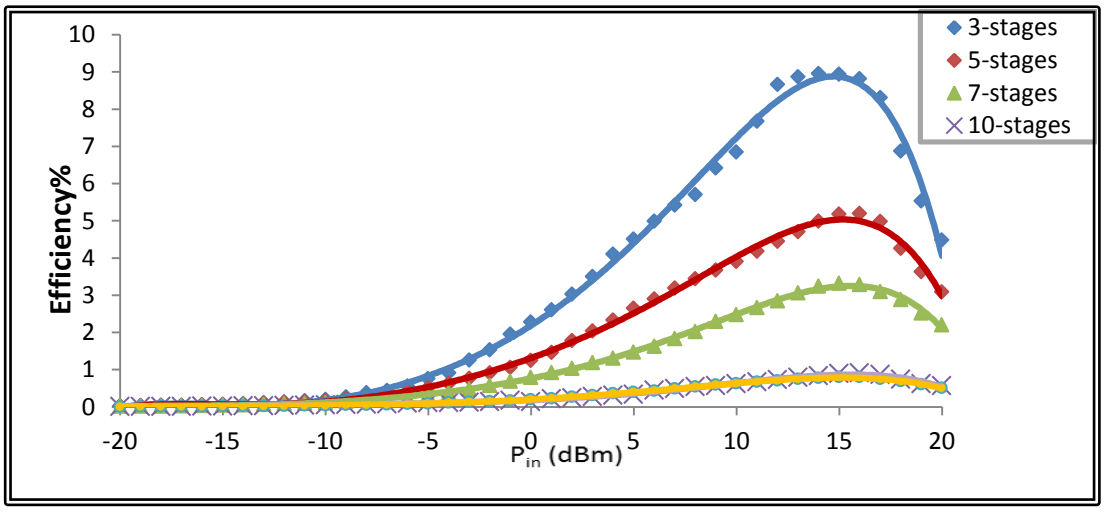


**Figure 3.25:$P_{in}$ with Efficiency at (400-680) MHz for 3,5,7,10 and 12 stages**

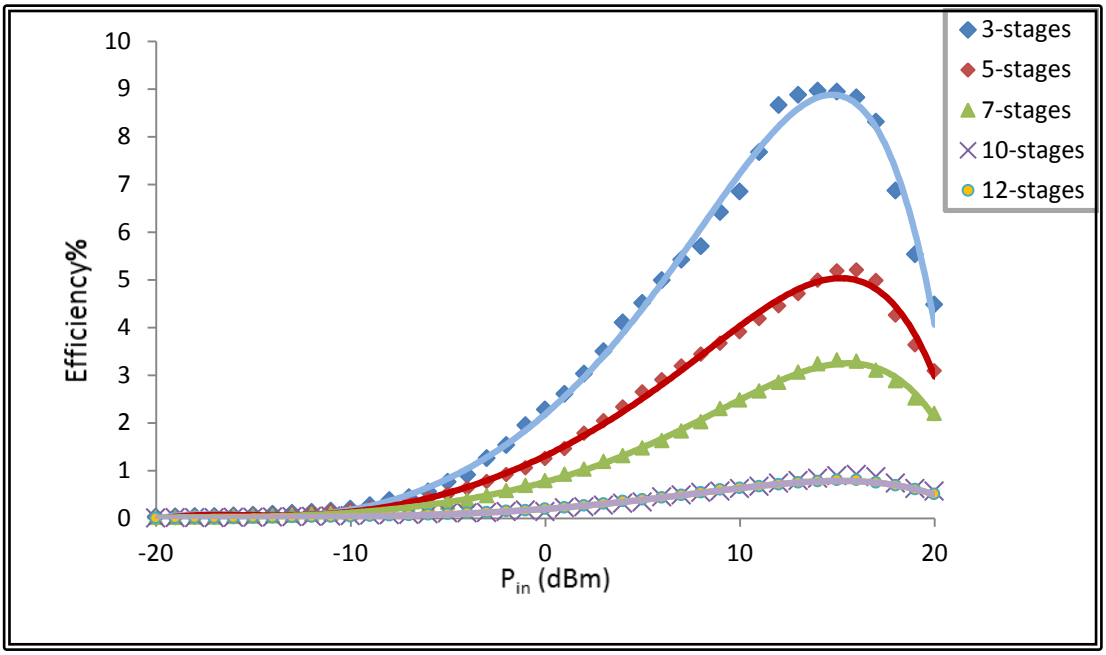


**Figure 3.26: $P_{in}$ with Efficiency at (700-900) MHz for 3,5,7,10 and 12 stages**

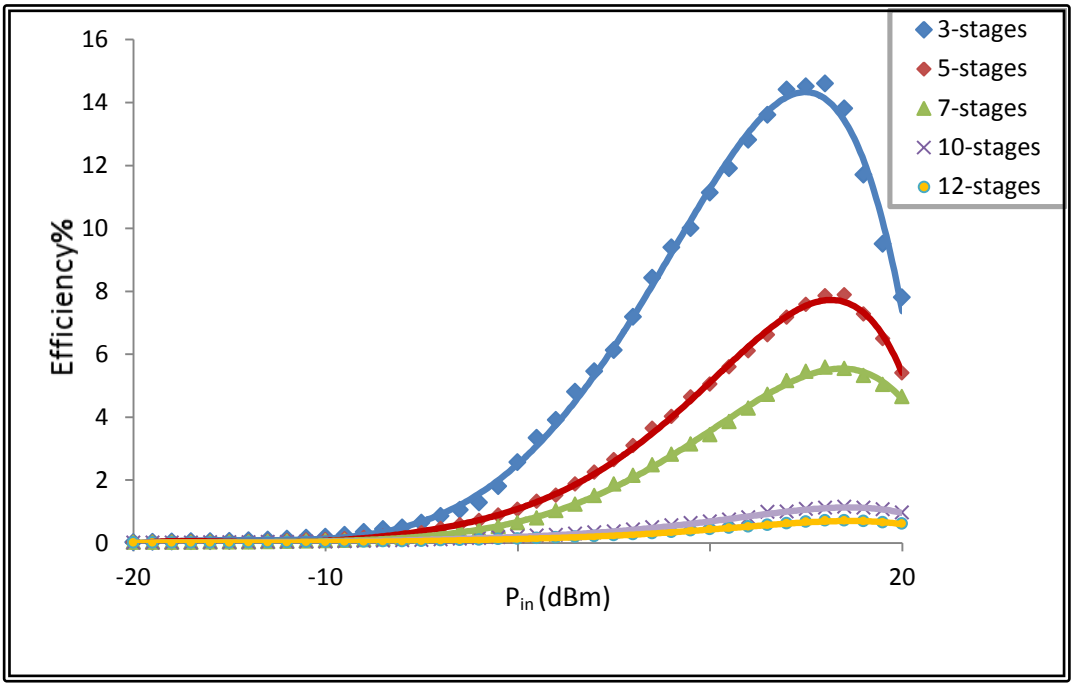


**Figure 3.27: $P_{in}$ with Efficiency at (2.5) GHz for 3,5,7,10 and 12 stages**

Demonstrate that at three stages, more efficient, with values of (8.89) % for frequency (400-680) MHz, (10.25) % for frequency (700-900) MHz, and (15.4) % for frequency (2.5) GHz at load (7,6,4) KΩ. And as the number of stage increases, the efficiency decreases. The greatest efficiency in a five-phase circuit was (3, 4, and 5 ) % for frequency ranges (400-680) MHz, (700-900) MHz, and (2.5) GHz, respectively. In a seven-phase circuit, the highest efficiency ratings were (3, 4, and 5) %. In a ten-phase and twelve-phase circuits, the efficiency is very low . The decrease in efficiency as the number of stages rises is due to parasitic effects of each stage's component capacitors, as well as an increase in the amount of load on each stage. This is the same as what was described in references [28,94].

Also, Figures 3.28, 3.29 and 3.30 illustrate the relationship between the input and output power of amplification stages (3,5,7,10,and 12) at the frequency ranges (400-680) MHz, (700-900) MHz, and (2.5) GHz, respectively.

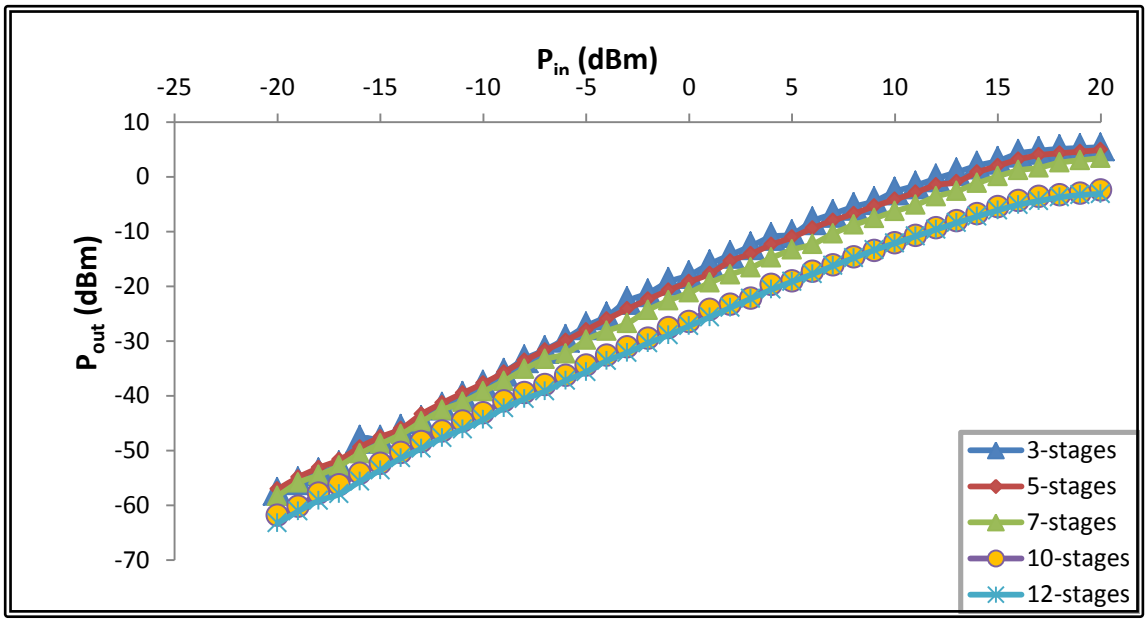


**Figure 3.28: $P_{in}$ with $P_{out}$ at (400-680) MHz for 3,5,7,10 and 12 stages**

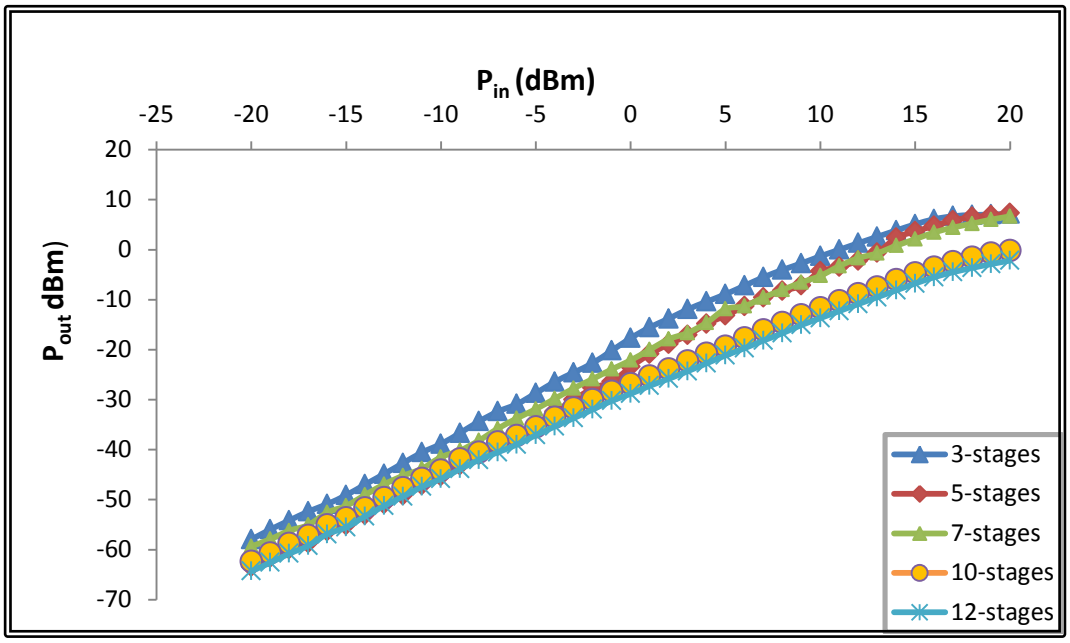


**Figure 3.29: $P_{in}$ with $P_{out}$ at (700-900) MHz for 3,5,7,10 and 12 stages**

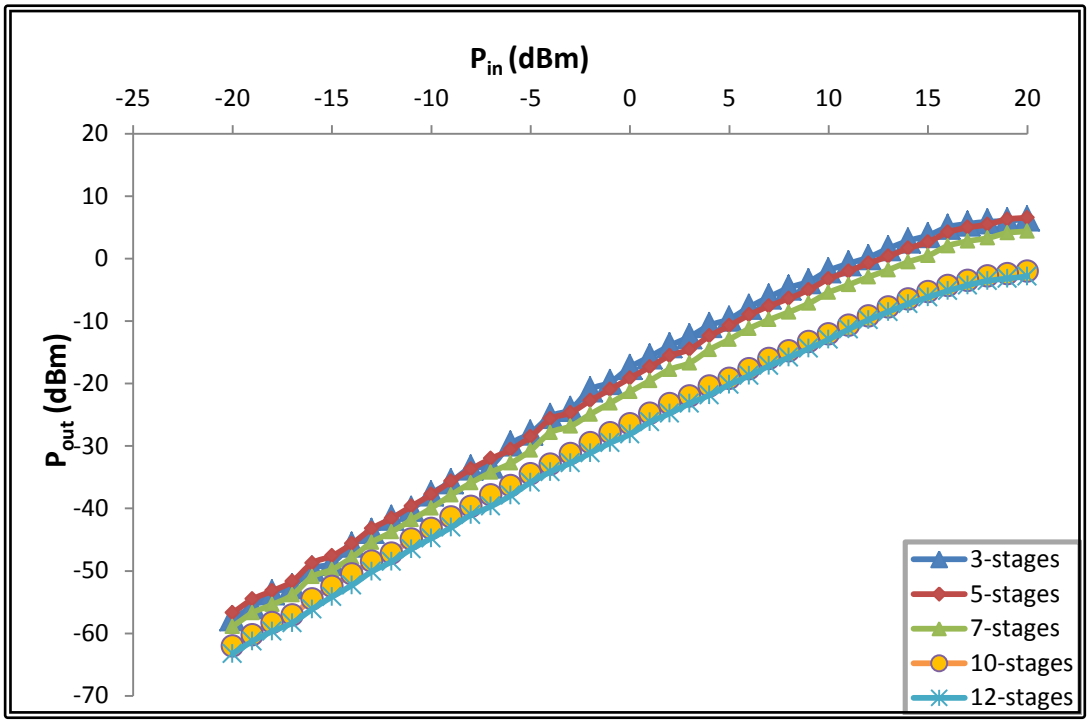


**Figure 3.30: $P_{in}$ with $P_{out}$ at (2.5)GHz for 3,5,7,10 and 12 stages**

As demonstrated in Figures 3.28, 3.29, and 3.30, the relationship between $P_{out}$t and $P_{in}$ has a high value at $P_{in}$ (20) dBm ,which is equal to

(6.5,4.9,3.4,-2.44 ,and -2.7) dBm for (three ,five , seven ,ten ,and twelve ) stages at (400-680) MHz and (7.2,5.2 , 4.4,-2 ,and -2.8) dBm for ( three ,five , seven ,ten ,and twelve) stages at (700-900) MHz and (7.8, 7.3 , 6.67,- 0.16, and -2.16) dBm for (three ,five , seven ,ten ,and twelve) stages for (2.5)GHz begins degreasing until (-20) dBm.

Figure 3.31 exhibits a relationship between $V_{out}$ and the number of amplification stages (1-12) at ($P_{in}$=20) dBm $P_{in}$ and (2.5) GHz .

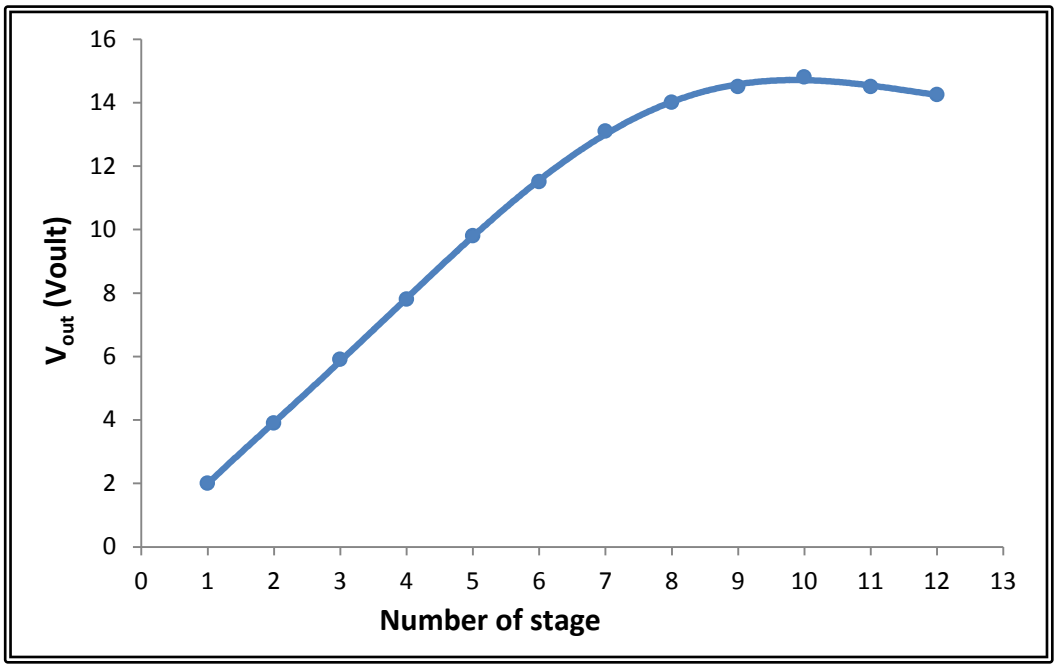


**Figure 3.31: The relationship between the output voltage and the number of amplification stages (1-12)**

The output increased as the number of rectifier stage increased. Level ten is the most effective since it can provide an optimal rectified voltage, at (11 and 12) stages, the voltage begins to fall, which is ascribed to an increase in the circuit's resistance,

and the circuit therefore loses its characteristic as a voltage doubling circuit .

To maximize the amplification circuits efficiency, a model of an energy harvesting system has been suggested as a parallel (two , three , four, five, six, seven, and eight) stages for a voltage doubling circuit with three phases ,shown in Figures (3.32- 3.38). It should be noted that the input power is set to (10) dBm, and the frequency is set to (2.5) GHz.

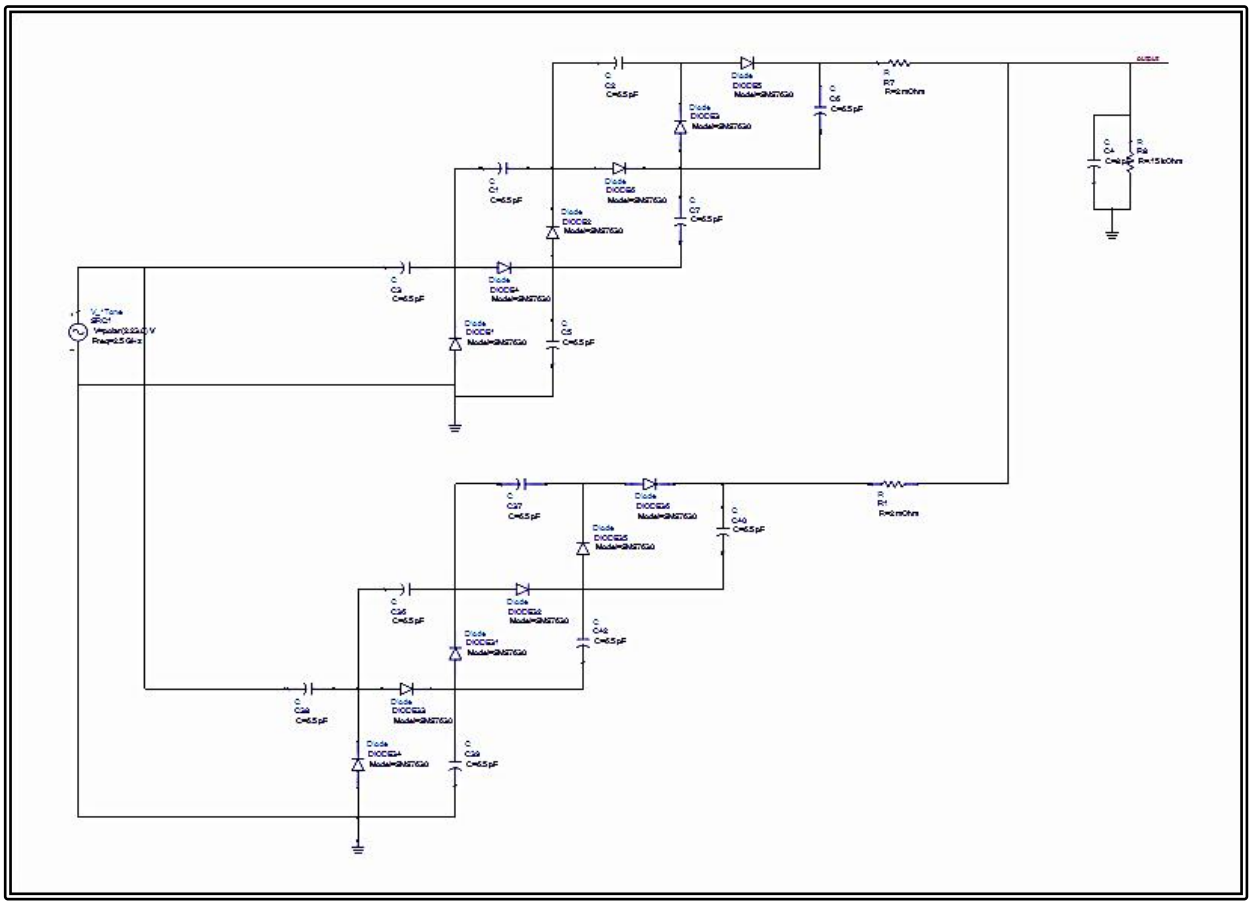

**Figure 3.32: RF energy harvesting with two parallel lines of the voltage doubling circuits for 3-stage**

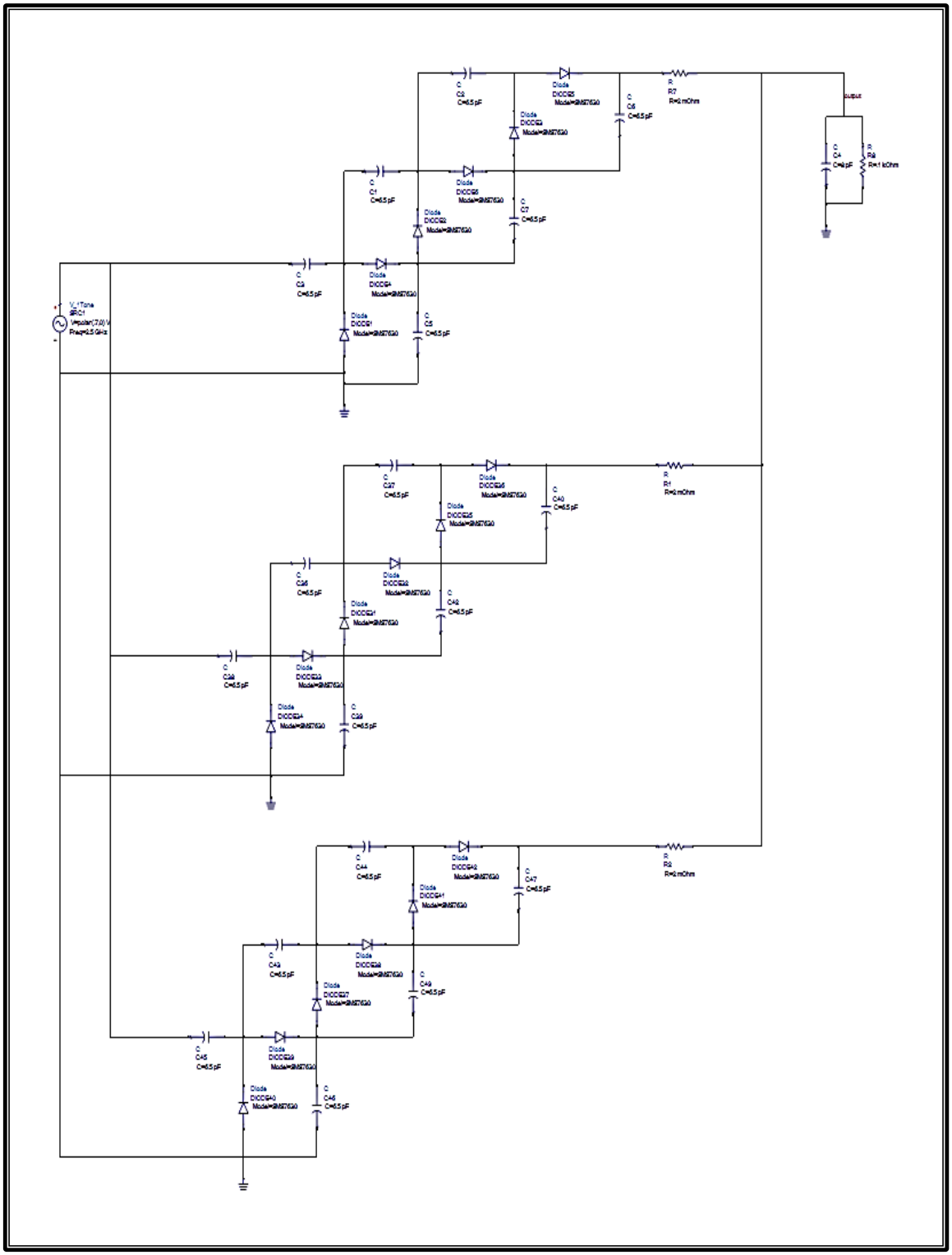

**Figure 3.33**: **RF energy harvesting with three parallel lines of the voltage doubling circuits for 3-stage**

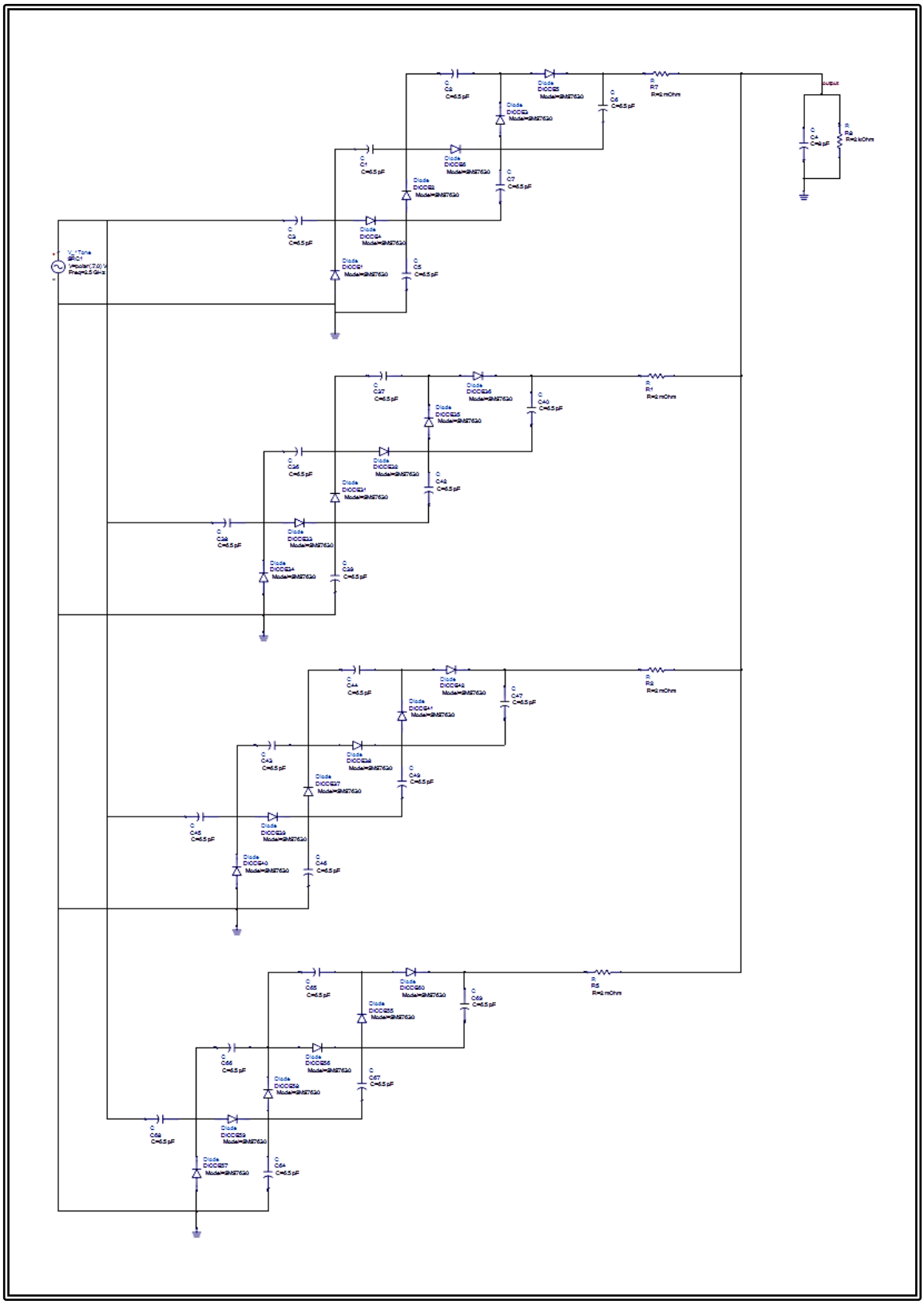

**Figure 3.34**: **RF energy harvesting with four parallel lines of the voltage doubling circuits for 3-stages**

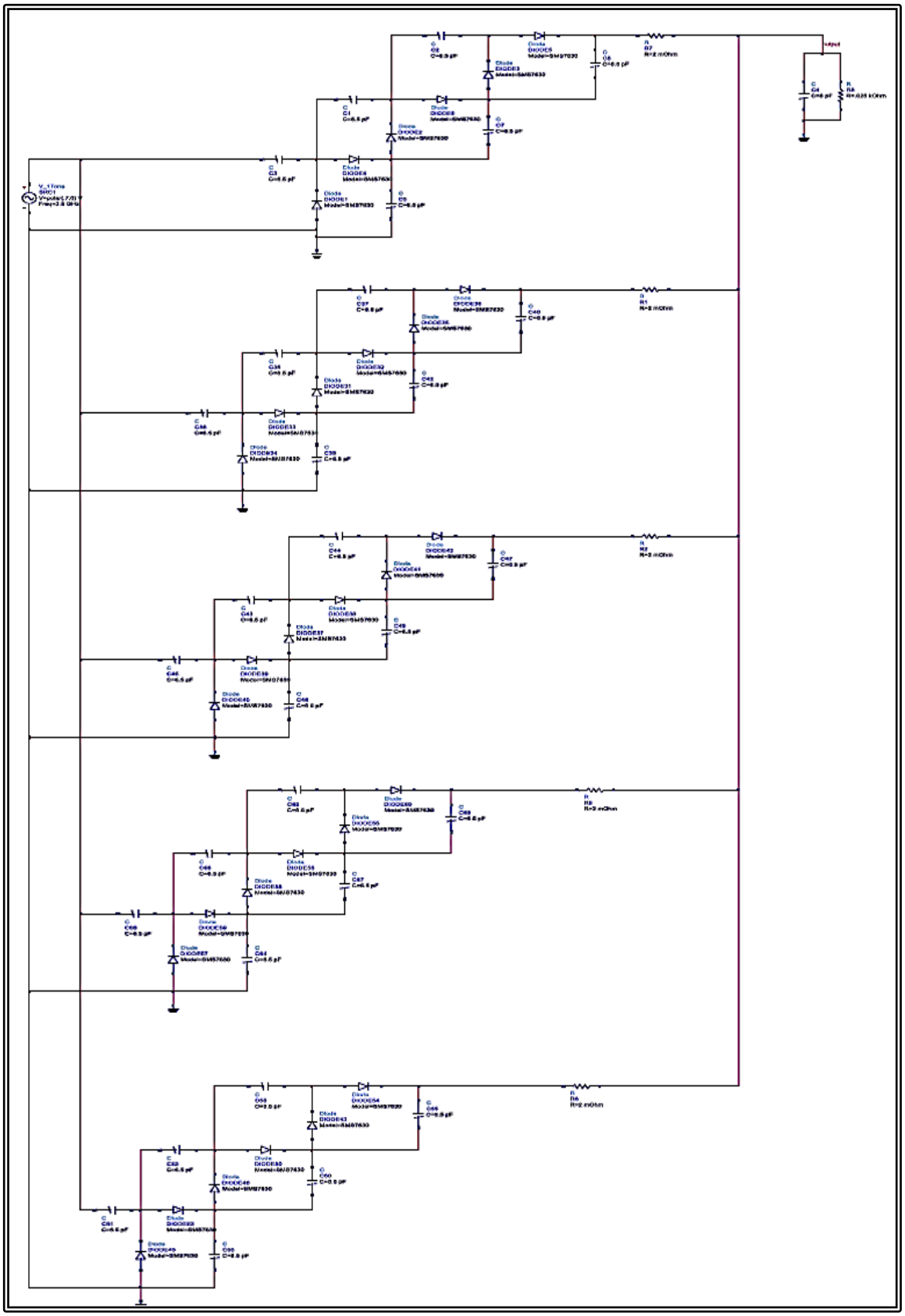

**Figure3. 35:RF energy harvesting with five parallel lines of the voltage doubling circuits for 3-stage**

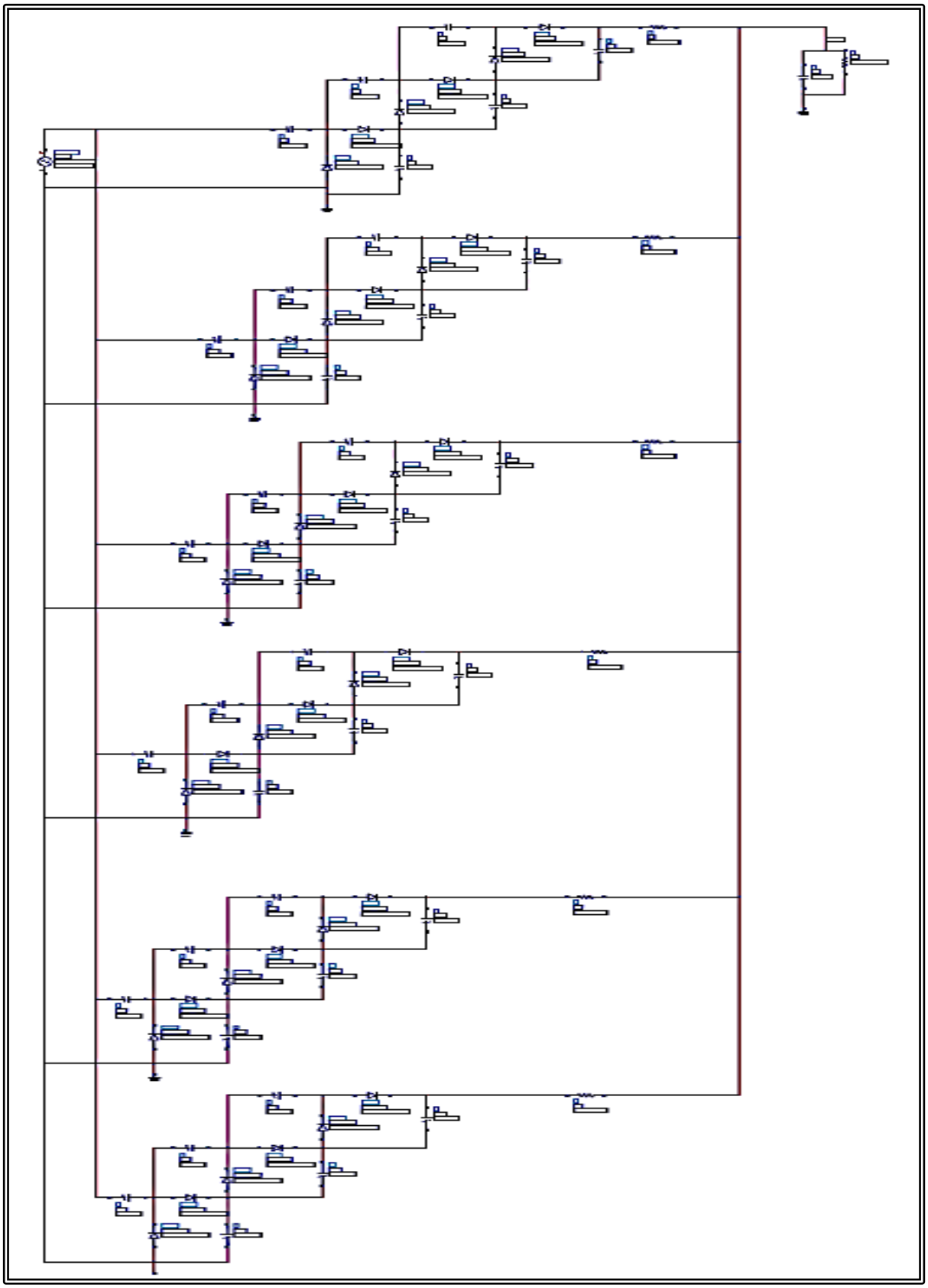

**Figure3. 36:RF energy harvesting with six parallel lines of the voltage doubling circuits for 3-stage**

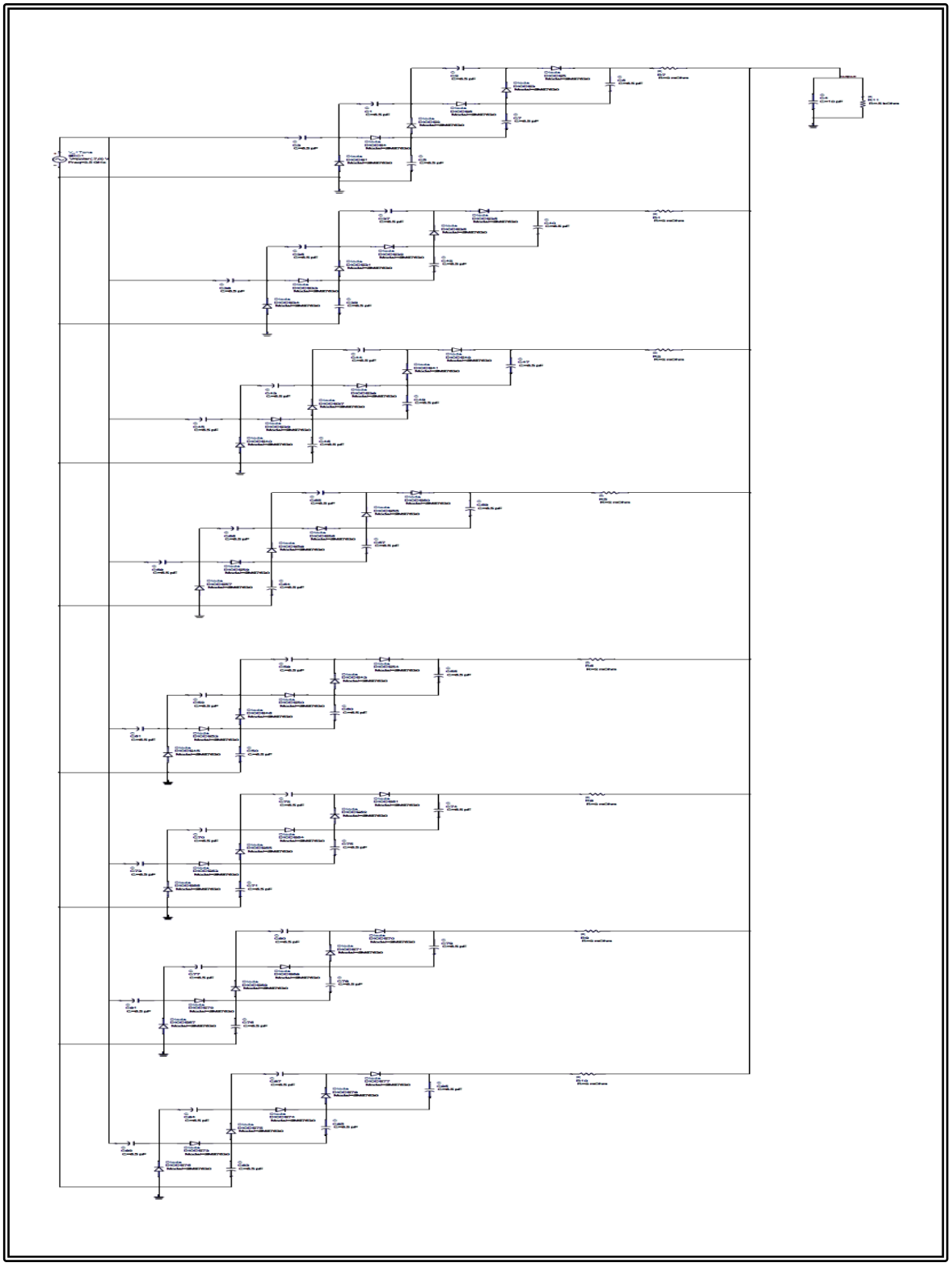

**Figure3. 37:RF energy harvesting with eight parallel lines of the voltage doubling circuits for 3-stage**

By implementing the above circuits, the efficiency was calculated with the number of stages as shown in Figure 3.38.

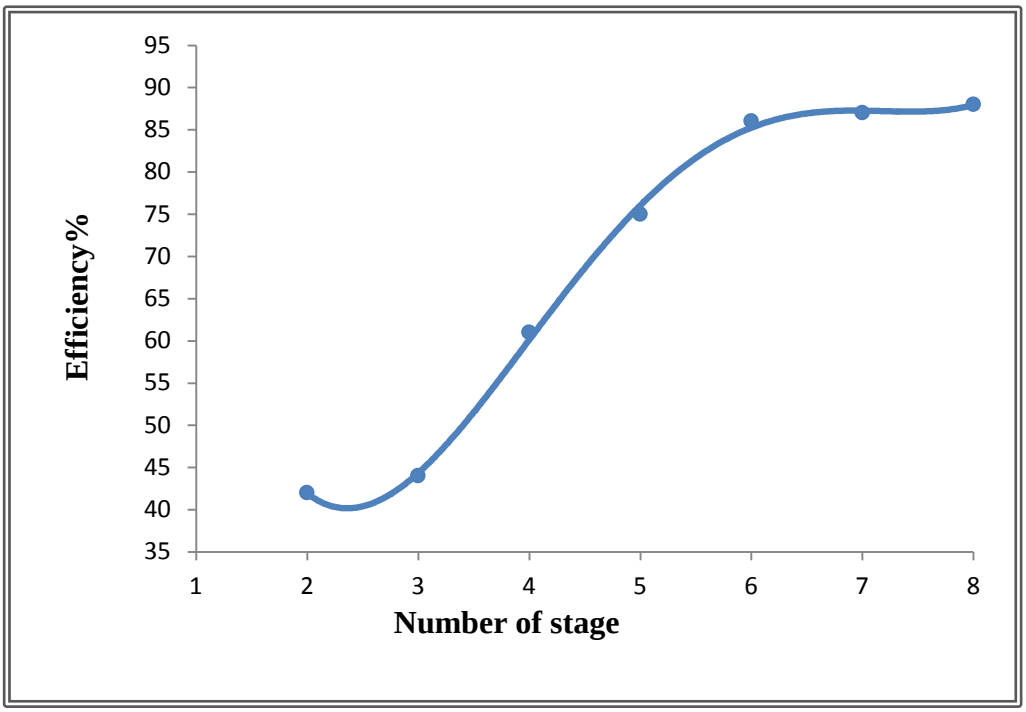


**Figure 3.38: Number of stage for (2-8) parallel lines of the voltage doubling circuits for 3-stage and efficiency percent**

Given the low efficiency of series circuits, parallel circuits were proposed to enhance the amount of efficiency. To maximize the amplification circuits efficiency, a model of an energy harvesting system has been suggested as a parallel phases (two , three , four, five , six, seven and eight) phases for a voltage doubling circuit with three phases. The circuit becomes more efficient as the parallel phases of a three-phase voltage- doubling circuit grow. This is the result of putting the current values together. As a result, the output voltage rises while the load decreases. As shown in Figure 3.38 .

# Chapter Four

# Experimental Work

## 4-1:CNC machine

The word “CNC” stands for Computer Numerical Control, CNC Machining is a process used in the manufacturing sector that involves the use of computers to control machine tools. Tools that can be controlled in this manner include lathes, mills, machines and grinders. The CNC depends on digital instructions usually made on Computer Aided Manufacturing (CAM) or Computer Aided Design (CAD) software like SolidWorks or Master CAM. The software writes G-code that the controller on the CNC machine can read. The computer program on the controller interprets the design and moves cutting tools and/or the workpiece on multiple axes to cut the desired shape from the workpiece [89-91]. Figure 4.1 depicts the CNC engraving machine.

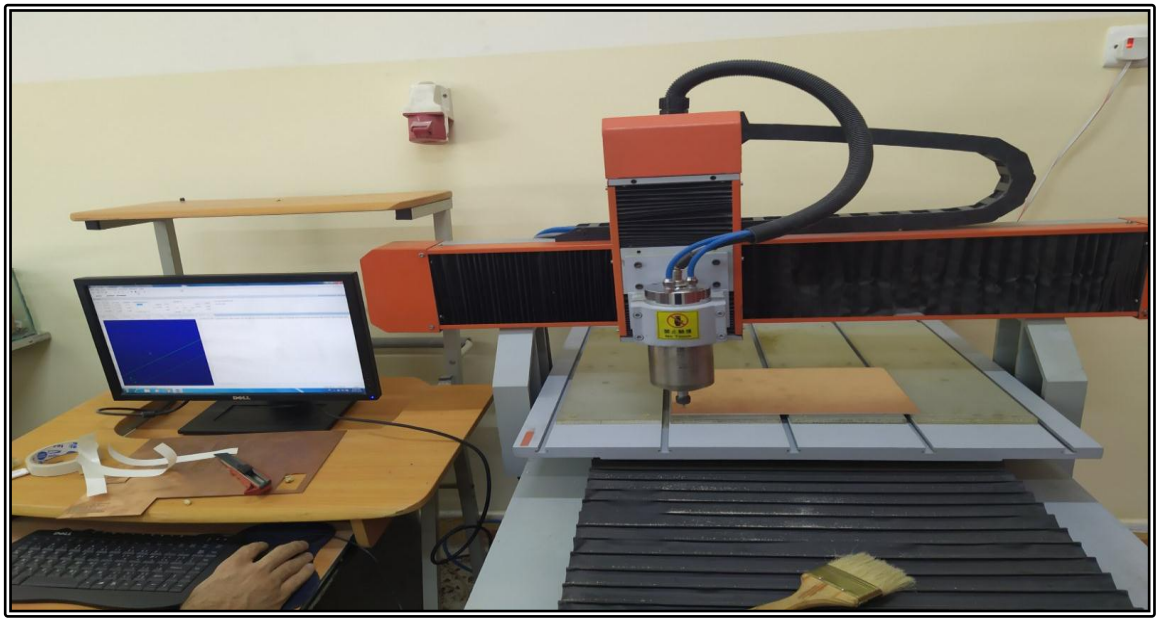

**Figure 4.1:CNC machine**

Steps of printing the circuit map using a CNC machine [91]:

1-The design is loaded into a computer connected to the CNC machine. The design is converted by the computer into a particular code numerical (0,1) that regulates how the CNC cuts and forms the material.

2- The material to be shaped is taped on to a block with double sided tape. This must be done carefully so that it does not come off the block during machining.

3- The guard is placed in position. It protects the machine operator in case the material is pulled out of the vice by the power of the cutter. For safety reasons, if the guard is not in position the motor will not start.

4- The CNC is turned on and the shape is cut from the material. When the cutter has stopped the shaped material can be removed from the clamping device.

## 4-2: Three-stages voltage multiplier circuit test

Each level of the voltage doubling circuit is a series and parallel HSMS-7630 modified voltage multiplier. For compared the empirical and theoretical outcomes Theoretical calculations were performed in the frequency bands (850-960) MHz and (2.11-2.17) GHz. In addition, the input power with range (15 to -15) dBm.

A CNC engraving machine see Figure 4.1 was used to construct a connecting circuit lines. A three-phase schematic in Figure 4. 2 has been prepared using a printed circuit board, Figure 4.3 shows the electrical components. Figure 4.4 and Figure 4.5 show the electrical components on the printed circuit board.

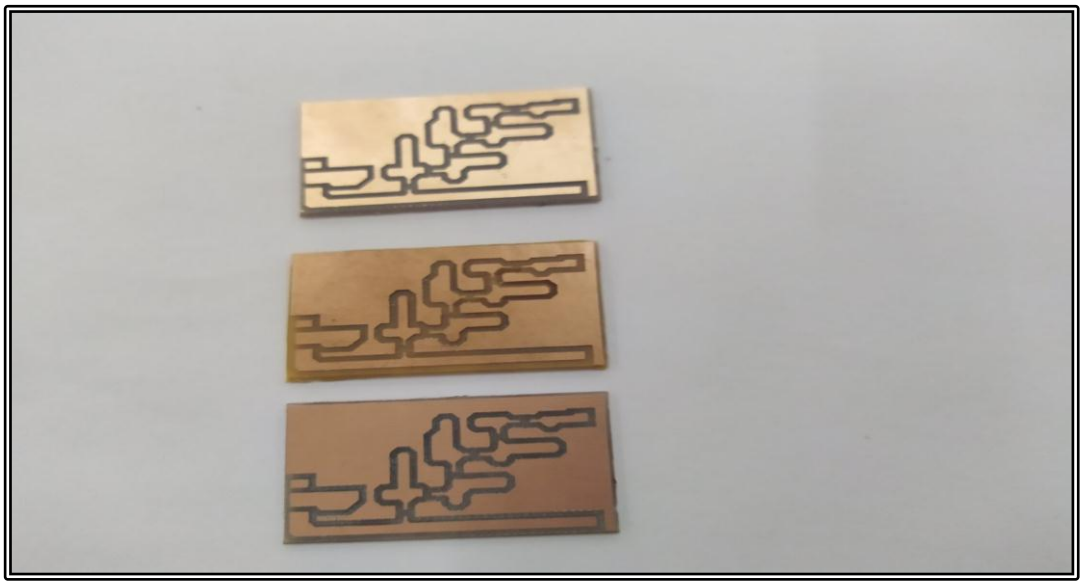

**Figure 4.2: A printed map of a three-phase circuit**

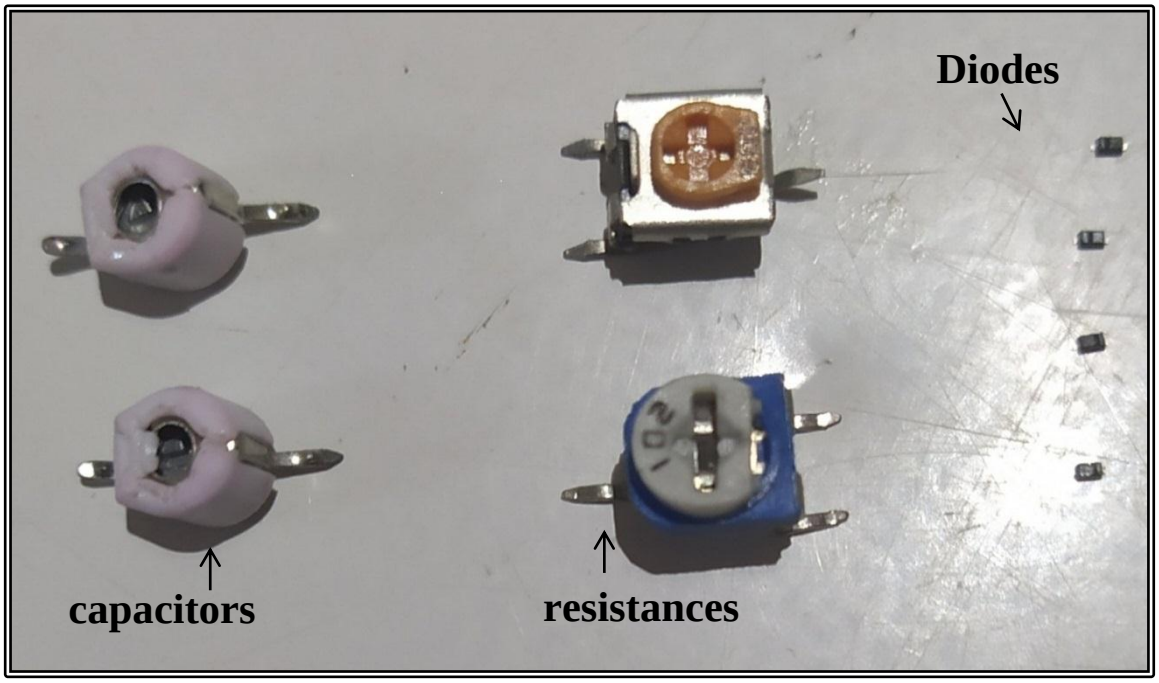


**Figure 4. 3: Electronic components**

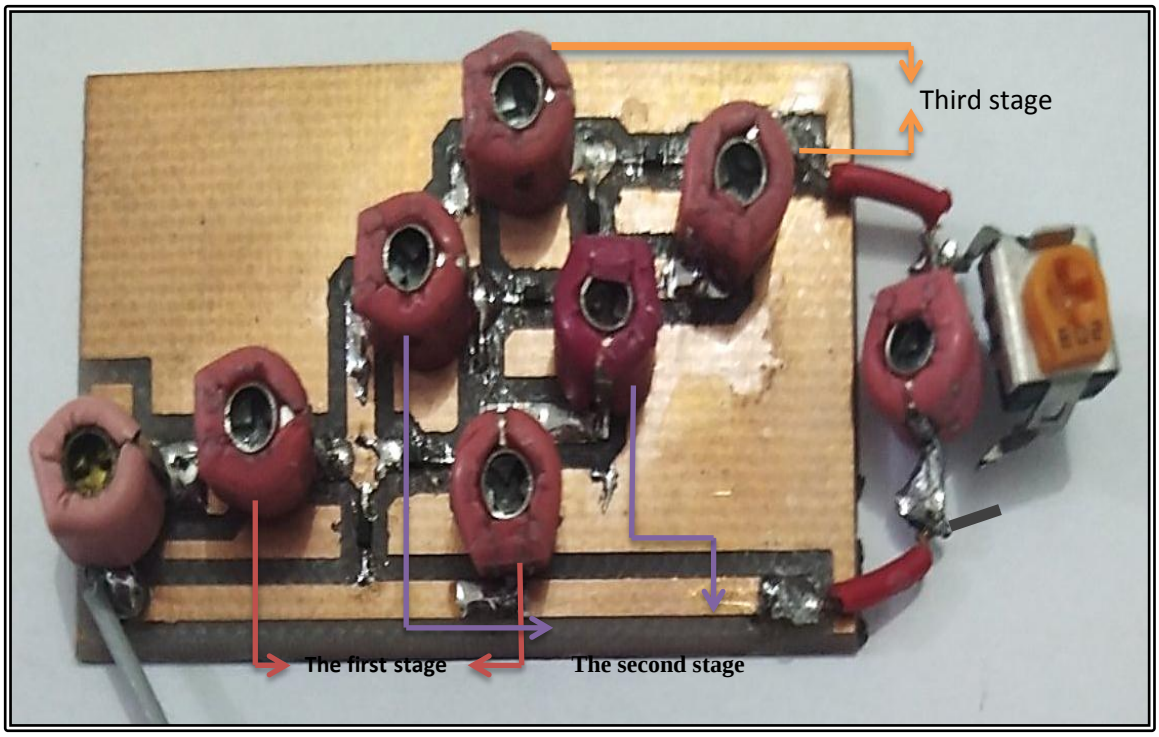


**Figure 4. 4. The electrical circuit is a three-phase series**

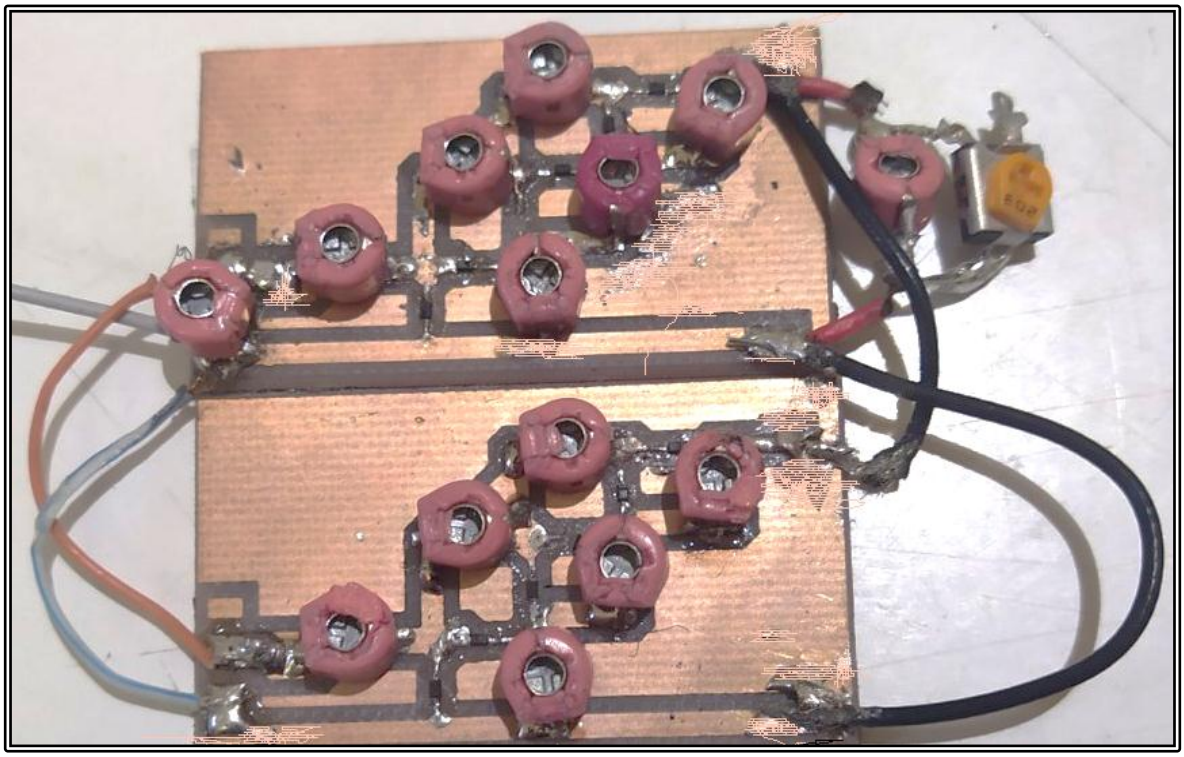

**Figure 4. 5. The electrical circuit is a three-phase parallel circuit**

## 4-3 :The DC measurements and results

The necessary measurements were taken using an experimental setup in Figure 4.6. A frequency transmitter (High power disk signal jammer for worldwide all networks ) has been implemented to obtain different frequency range start from (850 )MHz Where different colors fixed on the device gives a specific frequency range. For example red color (2.11-2.17) GHz, and so on of the other colors. A DC voltmeter has been used to measure the amount of the DC voltage which has been collected from a specific frequency range using the three stage circuit.

The design of a three- stage voltage multiplier circuit has been implemented with the filter capacitor across the load resistor. The range values of the input voltages within (1.25 -0.039 ) Volt and the output voltages of the three-phases voltage multiplier circuit have been presented in Table 4.1 under different frequencies of the waveforms (850-960)MHz, and (2.11-2.17) GHz.

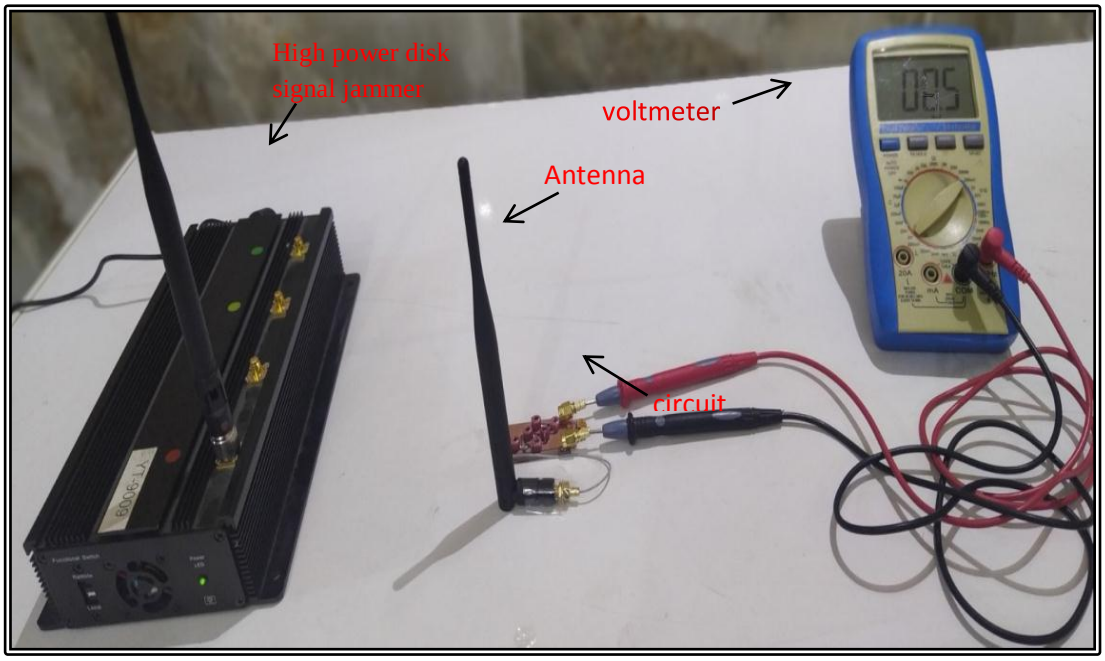


**Figure4. 6. The electrical circuit for a three-phase circuit**

**Table 4. 1:$V_{out}$ of three- stage at (850-960)MHz and (2.11-2.17)GHz**

| $V_{in}$(Volt) | Simulation results for a three-stage | | Practical results for a three-stage | |
|---|---|---|---|---|
| | (850-960)MHz | (2.11-2.17)GHz | (850-960)MHz | (2.11-2.17)GHz |
| | $V_{out}$ (Volt) | $V_{out}$ (Volt) | $V_{out}$ (Volt) | $V_{out}$ (Volt) |
| 1.25 | 4.6 | 4.6 | 2.1 | 2.3 |
| 1.12 | 3.7 | 4.2 | 2.03 | 2.07 |
| 0.89 | 3 | 3.4 | 1.4 | 1.42 |
| 0.7 | 2.3 | 2.5 | 1.21 | 1.23 |
| 0.56 | 1.8 | 1.9 | 0.7 | 0.87 |
| 0.44 | 1.3 | 1.5 | 0.52 | 0.72 |
| 0.35 | 0.97 | 1.1 | 0.29 | 0.34 |
| 0.28 | 0.65 | 0.69 | 0.25 | 0.27 |
| 0.22 | 0.45 | 0.48 | 0.19 | 0.21 |
| 0.199 | 0.35 | 0.39 | 0.12 | 0.15 |
| 0.158 | 0.25 | 0.27 | 0.07 | 0.085 |
| 0.125 | 0.14 | 0.19 | 0.039 | 0.030 |
| 0.102 | 0.1 | 0.13 | 0.026 | 0.025 |
| 0.079 | 0.055 | 0.058 | 0.019 | 0.015 |
| 0.063 | 0.04 | 0.047 | 0.01 | 0.011 |
| 0.05 | 0.025 | 0.027 | 0.008 | 0.009 |
| 0.039 | 0.015 | 0.016 | 0.0047 | 0.005 |

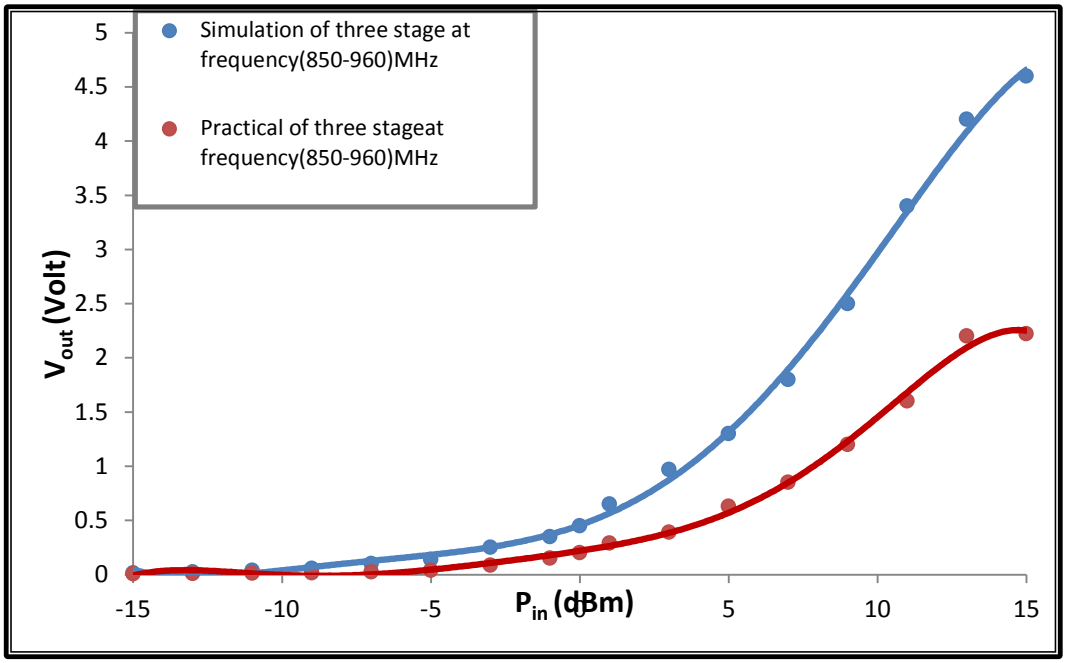


**Figure 4. 7: $P_{in}$ with $V_{out}$ at (850-960)MHz for three-stages**

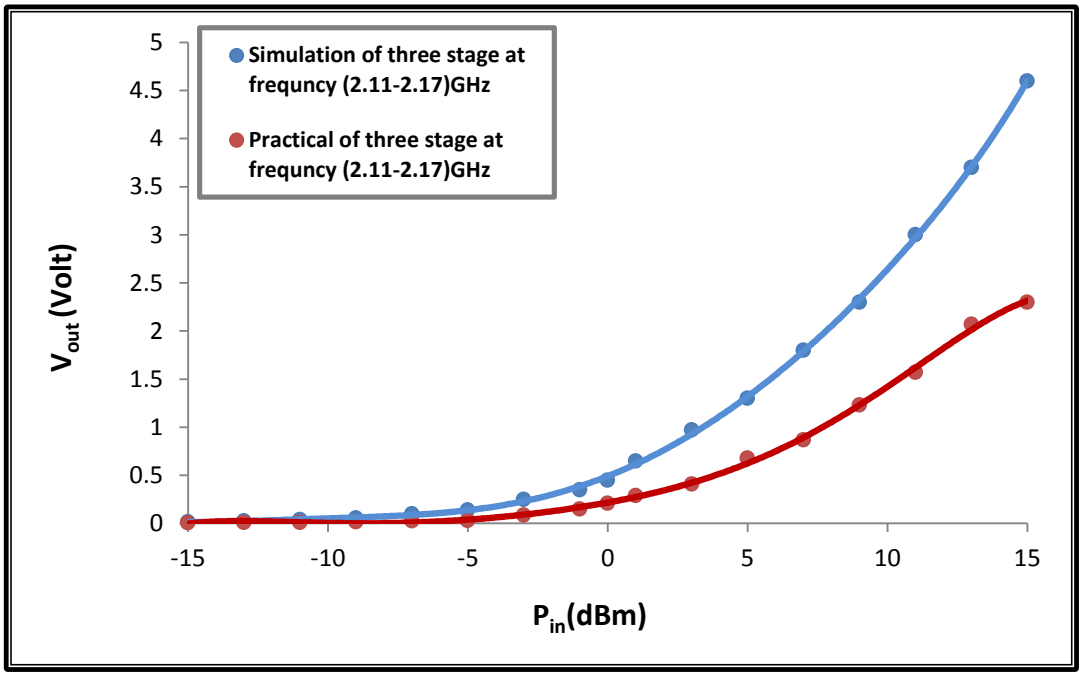


**Figure 4. 8: Pin with Vout at (2.11-2.17)GHz for three- stages**

Figure 4.7 shows a comparison curves between a simulation results and experimental measurements of the input power and the output voltage

in the frequency range (850-960) MHz. The results show the curves are almost identical at the values (-7 to -15) dBm . However, there is a clear and somewhat small Approximately difference at the values (15 to -6 ) dBm. This is, due to the practical values of the capacitors and load values that were used in the circuit and energy consumption in the connecting wires and circuit welding.

Also, calculated the output voltage for a three-phase circuit in the frequency range (2.11-2.17) GHz, then established the relationship between the output voltage and the input power has been drawn and compared it to the theoretical results. As seen in Figure 4.8.

The range values of the input voltages within (1.25-0.039 ) Volt and the output voltages of the three-phases voltage multiplier circuit have been presented in Table 4.1 under different frequencies of the waveforms (850-960) MHz, and (2.11-2.17) GHz. Figure 4.8 shows a comparison curves between a simulation results and experimental measurements of the input power and the output voltage. The results show the curves are almost identical at the values (-8 to -15) dBm. However, there is a clear and somewhat small Approximately difference at the values (15 to -7) dBm. This is, due to the practical values of the capacitors and load values that were used in the circuit and energy consumption in the connecting wires and circuit welding.

Figure 4. 9 illustrate the relationship between the input and output power of amplification stage three-phase at the frequency range (850-960) MHz. The relationship between $P_{out}$ and $P_{in}$ has a high value at $P_{in}$ (15) dBm ,which is equal to (0.34) dBm begins decreasing until (-15) dBm. The drop in power is caused by a fall in output voltage, which is caused by practical

values of the capacitors and load values employed in the circuit, as well as energy consumption in the connecting wires and circuit welding.

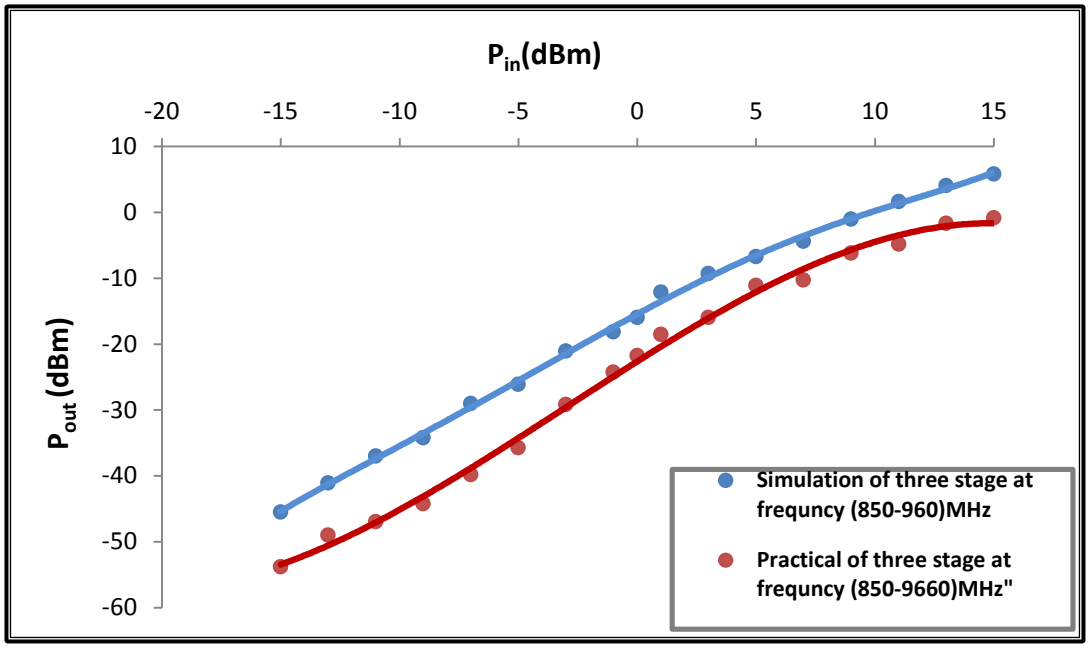


**Figure 4.9: $P_{in}$ with $P_{out}$ at (850-960)MHz for three- stages**

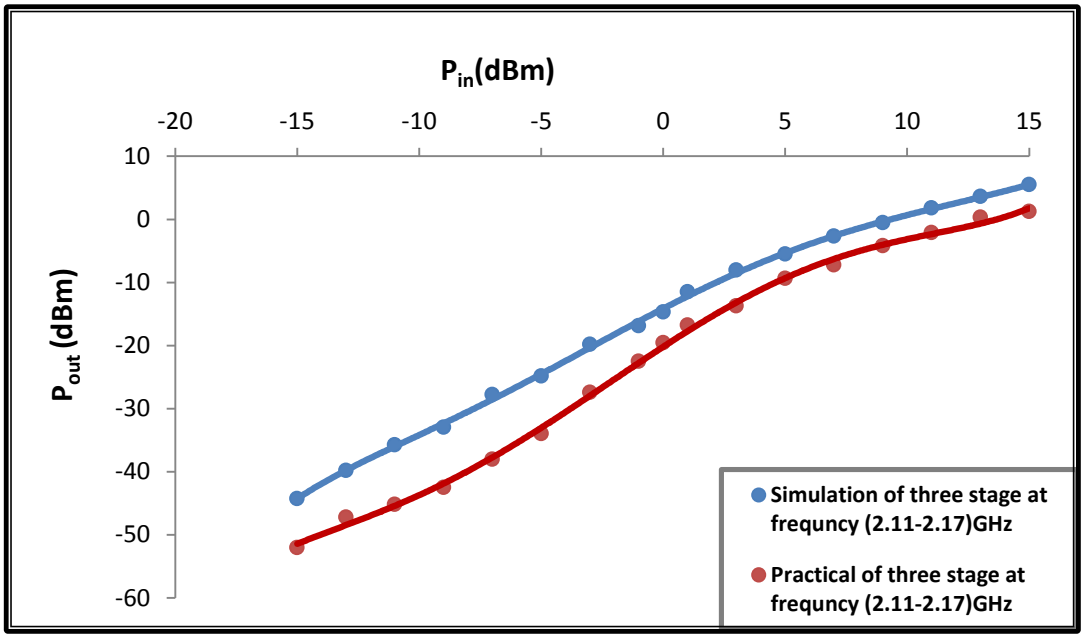


**Figure 4.10: $P_{in}$ with $P_{out}$ at (2.11-2.17) GHz for three- stages**

Figure 4. 10 depicts the relationship between the input power and output power of a three-phase amplification stage operating at a frequency of (2.11-2.17) GHz. The relationship between $P_{out}$ and $P_{in}$ has a high value at $P_{in}$ (15) dBm ,which is equal to (0.34) dBm begins decreasing until (-15) dBm. The drop in power is caused by a fall in output voltage, which is caused by practical values of the capacitors and load values employed in the circuit, as well as energy consumption in the connecting wires and circuit welding.

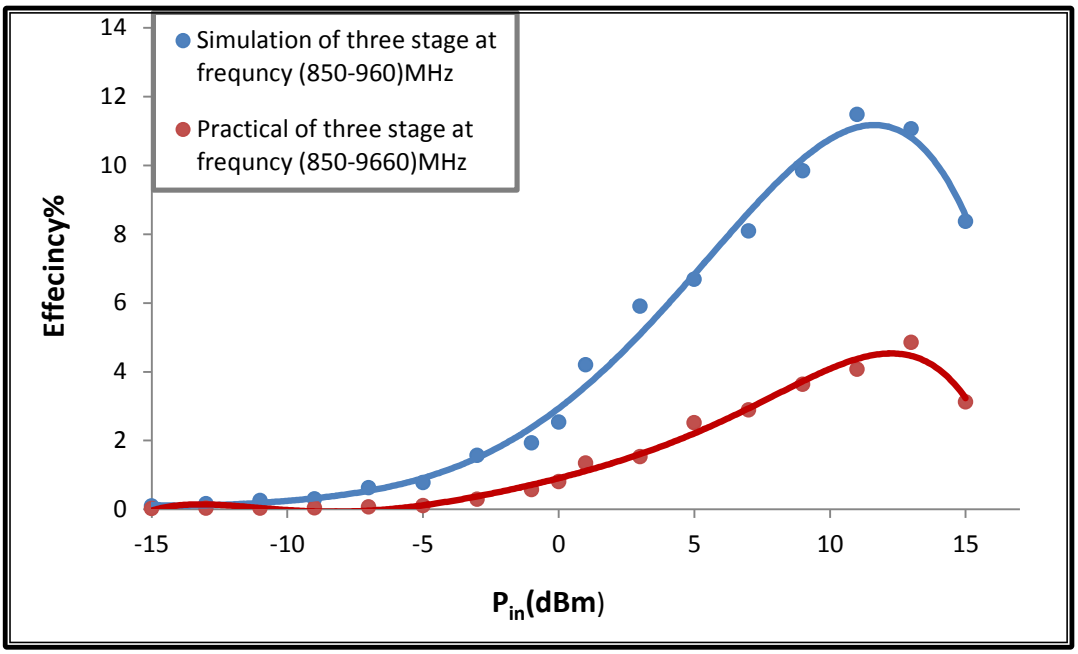


**Figure 4.11: $P_{in}$ with Efficiency at (850-960)MHz for three- stages**

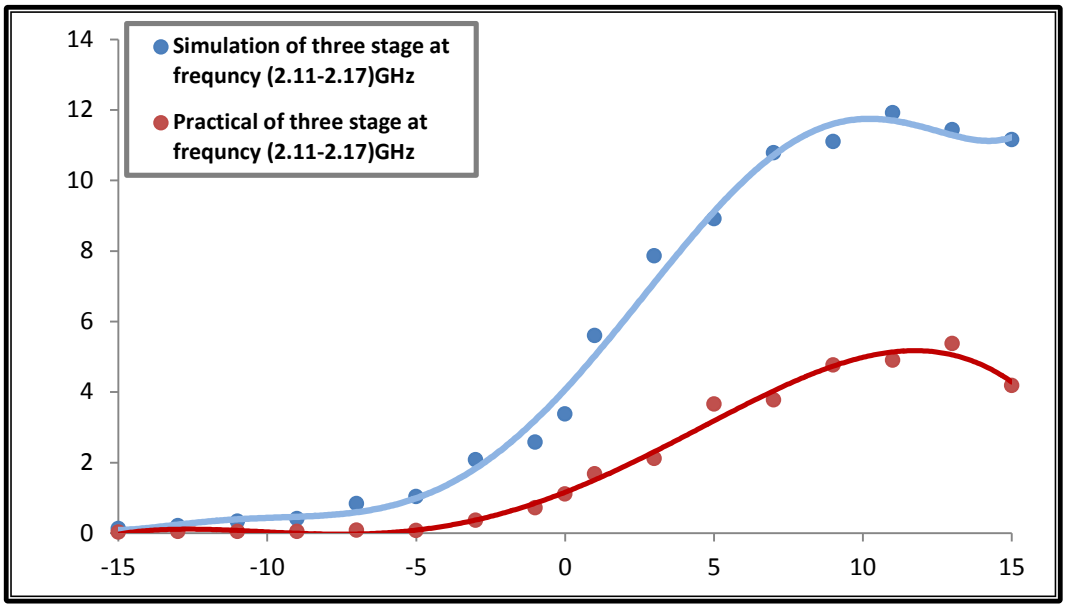


**Figure 4.12: Pin with Efficiency at (2.11-2.17)GHz for three- stages**

Figure 4.11 depicts the efficiency of a three-stage circuit determined using Eq. 2.19. The findings were shown as a function of input power over a frequency range of (850-960) MHz. The greatest efficiency value, (4.8) % was reached. The decline in efficiency value is due to the same factors discussed above.

Figure 4.12 depicts the efficiency of a three-stage circuit . The findings were shown as a function of input power over a frequency range of (2.11-2.17) GHz. The greatest efficiency value, (5.3)% was reached. The decline in efficiency value is due to the same factors discussed above.

A two-phase parallel circuit was implemented for a three-stage circuit. The circuit is shown in Figure 4.5, yielding a (26) % efficiency. It is worth noting that the input power is (10) dBm and the frequency is (2.15) GHz.

## 4-4:Simple harvesting circuit

It Presented thorough examination of the various radio frequency sources (DTV, GSM, Wi-Fi) available electromagnetic signals as renewable energy sources. Using existing commercial antennas such as TV network and dish antenna, as well as a wire antenna, then can to discover energy sources. By using experimental electronic circuit described in Figure 4.13. One can ran a number of experiments in the absence of an antenna and with various types of antennas

A model of a simple RF energy harvesting circuit is displayed in Figure 4.13. The architecture in this research focuses on the circuitry of processing, which includes filtering ($C_3$, $C_4$ and $D_1$, $D_2$), and switch mode power conversion ($C_1$, $C_2$, and $D_3$, $D_4$). $C_1$,$C_2$=100 µF, $C_3$,$C_5$=20 nF ,$D_1$,$D_2$,$D_3$,$D_4$= diodes, $C_1$,$C_2$= electrolytic capacitor and $C_3$,$C_4$=ceramic capacitor.

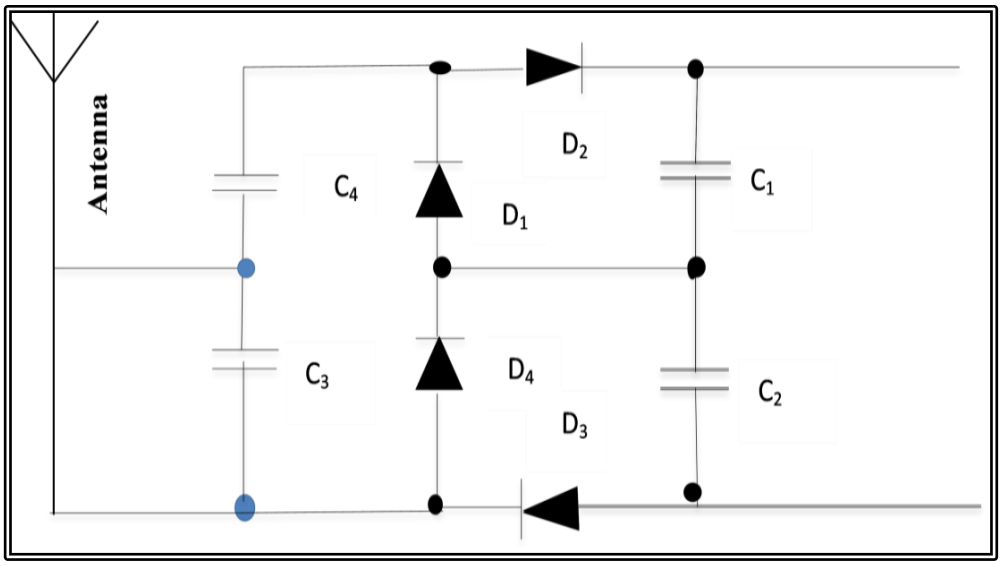


**Figure 4.13: Design of on RF energy harvesting circuit**

The circuit itself exhibits nonlinearity, because the energy harvesting circuit consists of diodes, which are nonlinear devices [95]. This

ensures that the energy harvesting circuit's impedance changes with the amount of antenna power produced. Because when the circuit is combined with the antenna, the full power transfer occurs, the impedance matching is typically achieved at the same input power. The impedance matching network converts impedance to ensure optimal power distribution [96].

### 4-3-1: Without an antenna

Figure 4.14-a shows the circuit connection without using an antenna and Figure 4.14-b,c displays the amount of energy DC. voltage on the screen of the oscilloscope at t= 0 minute and t= 3 minutes respectively.

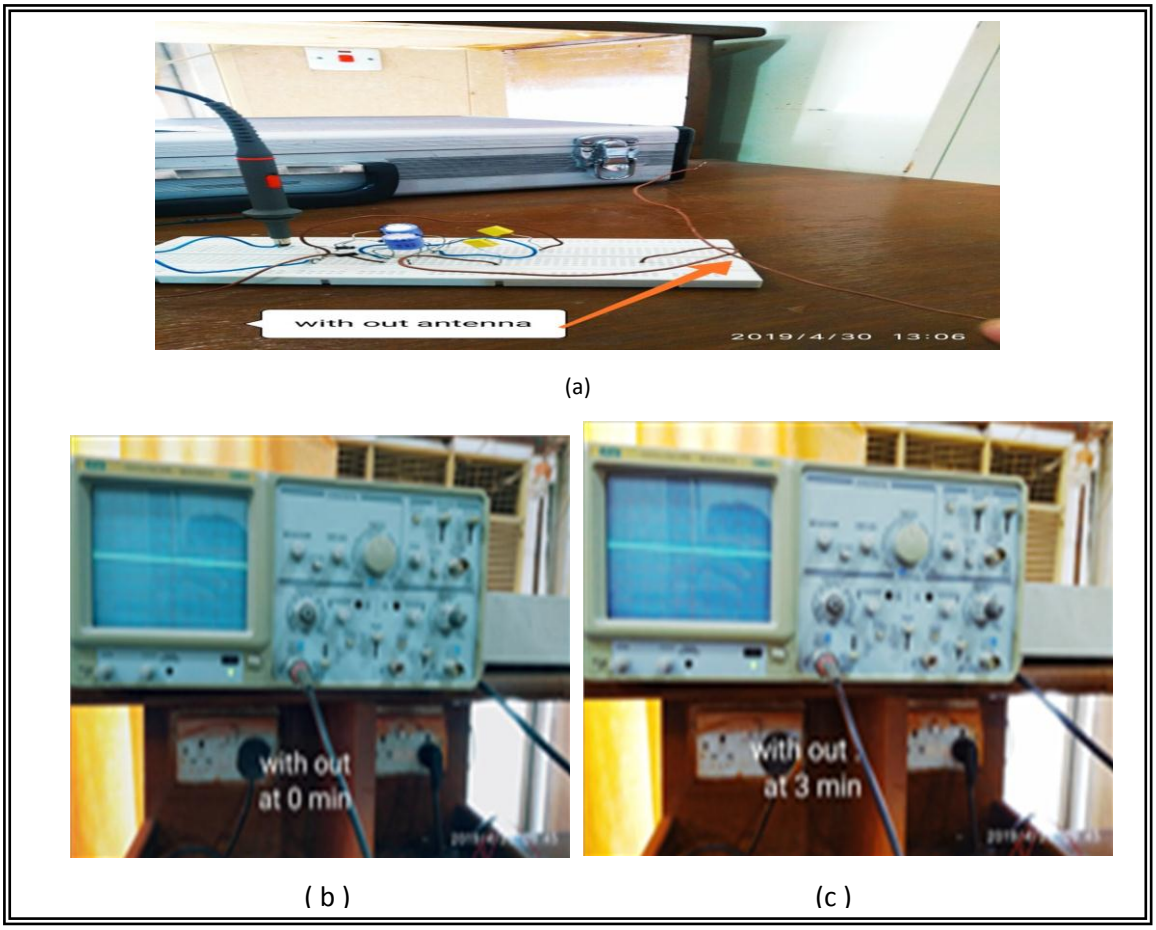


**Figure 4.14 : The circuit connection without using antenna, a- circuit design, b- the amount of voltage at t=0 min and c-the amount of voltage at t=3 min**

**Table4. 2: The amount of voltage without an antenna**

| | V(mV) | t (min ) |
|---|---|---|
| **Without antenna** | **20** | **0** |
| | **22** | **3** |

This is representative of the exponential recovery function, which is the predicted charging characteristic of the capacitor. These findings show the RF energy harvester's proof-of-concept, as well as validating the processing circuitry's ability to rectify the RF signal received. These findings, however, indicate that the circuit cannot work as planned. The circuit was desigened to output a voltage of approximately 5V, which is far higher than the real voltage calculated through the capacitor. The potential explanation why it does not produce the desired output is that the RF energy harvester is unable to reach this threshold, insufficient power received poor power transfer.

### 4-3-2: With wire antenna

To extract more energy from the RF signal, a wire an antenna (dipole antenna) of has been proposed. Figure 4.15-a shows the circuit design, and the amount of the DC voltage on the oscilloscope screen at time (0,3) minute is shown in Figure 4. 15- b and c respectively, and Table 4.3.

The wire antenna has been suggested to get more energy from RF signal. Although the input power obtained from the antenna varies over time, the RF energy harvester will have to sustain a voltage level of at least (625) mV at the input even though the threshold is exceeded

**Table 4.3 : The amount of voltage for wire antenna**

| | V(mV) | t (min ) |
|---|---|---|
| **Wire antenna** | **50** | **0** |
| | **75** | **3** |

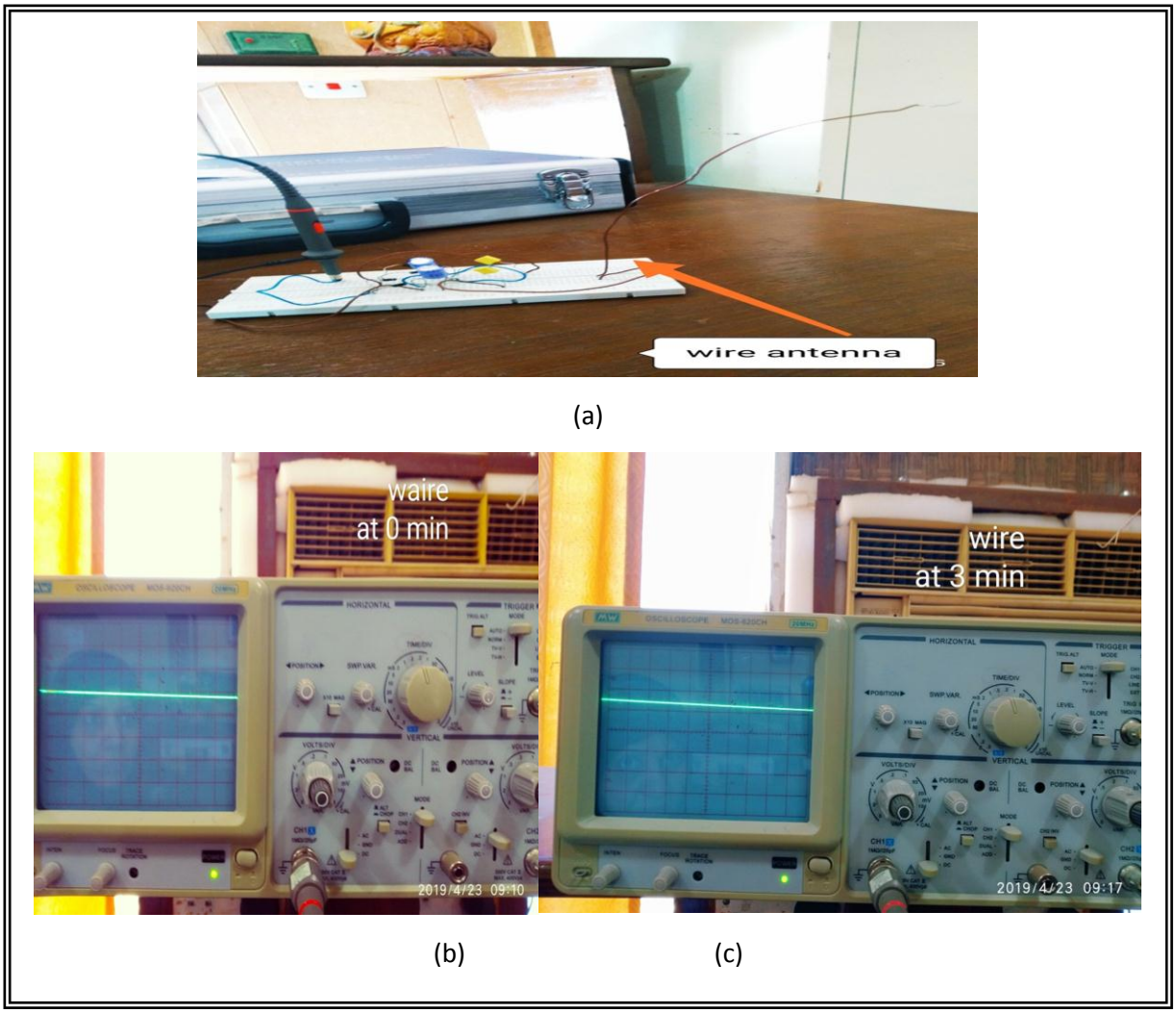


**Figure 4.15: The circuit and the amount of the DC voltage on the oscilloscope screen are :a- circuit design, b- at time 0 minute, and c- after 3 minute**

Using an electrolytic capacitor for research is an added challenge that may restrict the maximum output voltage reached by the circuit. In a low

power application like the one discussed here, the leakage current of the capacitor may have a substantial negative effect on the output voltage. If the output current decreases to a degree equivalent to the capacitor's leakage current, Then the capacitor will no longer receive a charge.

**4-4-3:With air antenna**

The results of the air antenna (type of yagi antenna) recorded at t= (0, 3) min. are shown in Figure 4.16 and Table 4.4.

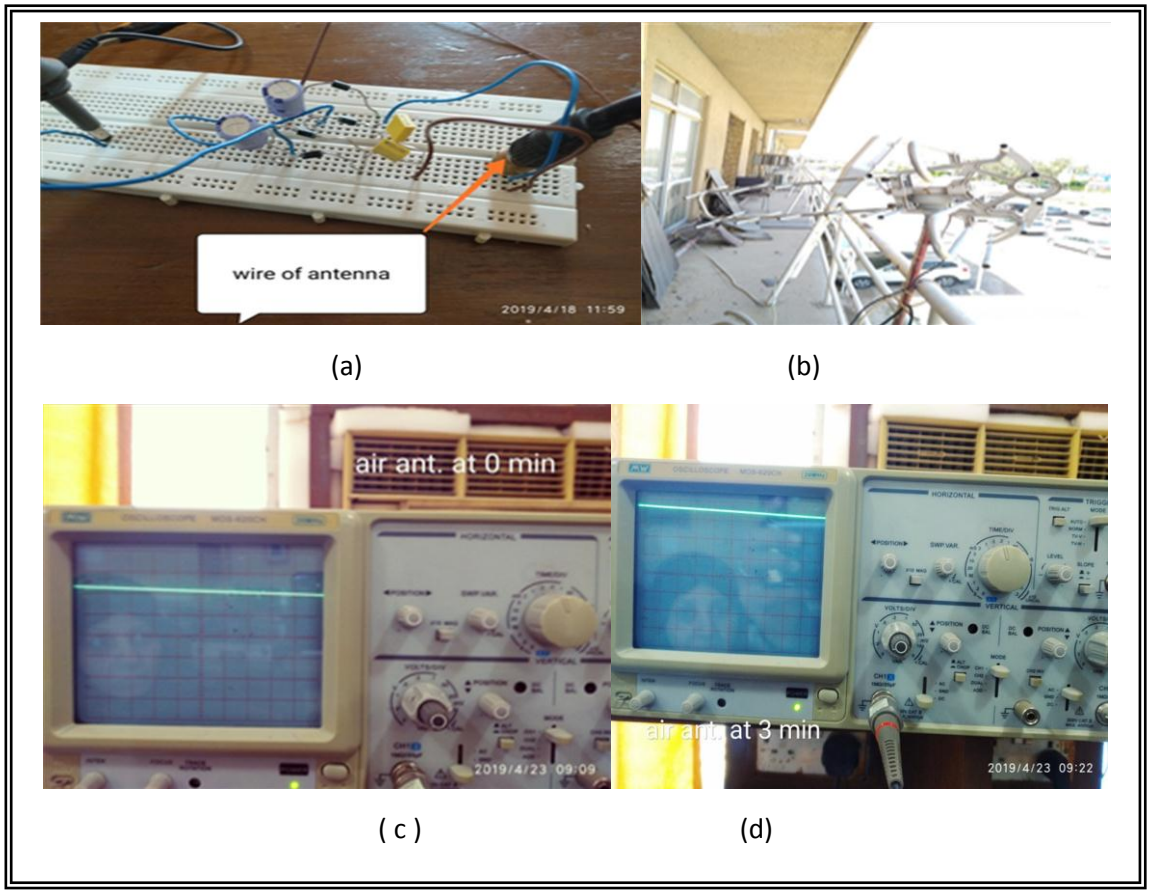


**Figure 4.16 : The circuit and the amount of the DC voltage on the oscilloscope screen: a- circuit design, b- air antenna , c- the amount of voltage at time 0 minute, and d- the amount of voltage after 3 minutes**.

The amount of voltage has been increased up to (400) mV at t=0, and (700) mV at t=3min. That's because the air antenna has an ability to capture the ambient E.M. waves more than the wire antenna.

**Table 4.4 : The amount of voltage for air antenna**

| | V(mV) | t (min ) |
|---|---|---|
| **Air antenna** | **400** | **0** |
| | **700** | **3** |

### 4-4-4: With dish antenna

The results of the dish antenna(type of reflector antenna have been recorded at t = (0, 3) min. as shown in Figure 4.17 and Table 4.5.

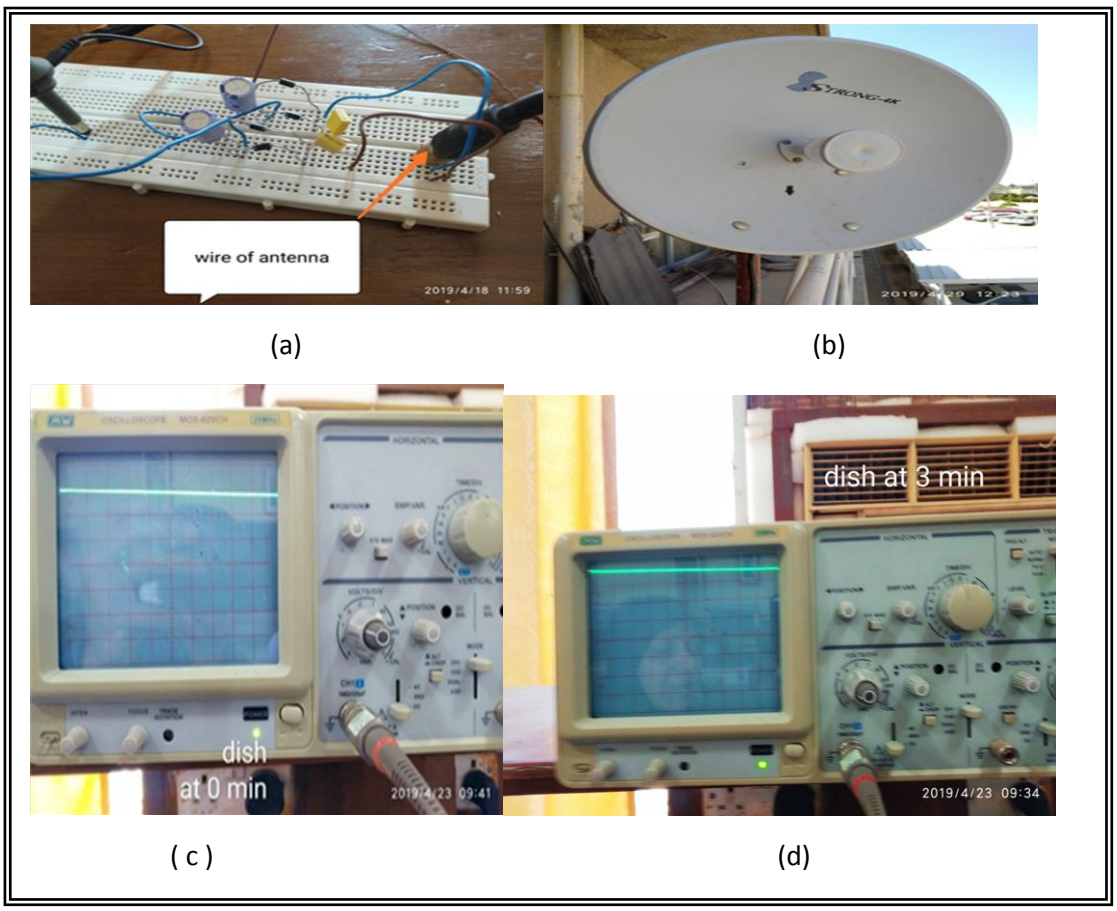


**Figure 4.17: The circuit and the amount of the DC voltage on the oscilloscope screen: a- circuit design, b- dish antenna, c- the amount of voltage at time 0 minute, and d- the amount of voltage after 3 minutes**

**Table4. 5 : The amount of voltage for dish antenna**

| | V(mV) | t (min ) |
|---|---|---|
| **Dish antenna** | **280** | **0** |
| | **800** | **3** |

The amount of voltage increased up to (800) mV at t=3min. Obviously, the value of the energy gain in this case is higher than the energy gain in the case of air antenna. It may be referred to the size of the dish antenna larger as compared to the size of the air antenna.

# Chapter Five

# Conclusions and Recommendations

This chapter includes the conclusions, which are extracted from the present study and recommendations for future studies.

## 5-1: Conclusions

1. The number of rectifier stages has a major influence on the output voltage of the energy harvesting circuit.
2. The results have shown that the voltage amount that can be obtained from the three steps, five steps, seven , ten and twelve steps voltage multiplier circuits are approximately the expected and valuable amount.
3. The circuit yields higher efficiency at three stage and decreases with the number of stages increasing, due to the parasitic effect of the constituent capacitors of each stage, and finally it becomes negligible.
4. The circuit yields higher efficiency with the increase in parallel phases of a three phase voltage doubling circuit due to the output power to being increased while the load is reduced.
5. The ambient RF frequencies are a considerable, powerful, and promising source of energy.
6. The amount of the DC. voltage that is collected from the RF frequencies without an antenna can be considered and employed after using an amplifier circuit.
7. The wire antenna gives a significant improvement in the value of DC. Voltage as compared with the kinds of antenna.
8. Although the air antenna raised the DC. power to a higher level, the shape and the large size of the antenna could be limited to its use.

9. The amount of the DC. power that is obtained using a dish antenna is approximately the same as the energy that is collected using an air antenna.
10. The amount of the DC. Power could be controlled by the charging time (RC) of the capacities.

## 5-2: Future works

1. Using a different shapes of antenna design.
2. Using different frequencies as a source for the RF circuits.
3. Designing a multiple RF (energy harvesting - system using different capacitance) and inductance values.
4. Using a transistor, construct an energy collecting circuit.
5. Using several types of matching networks and comparing their performance.

# Supervisor's Certification

We Certify that this Thesis titled **(Design and Implementation of Energy Harvesting from an Ambient Radio Frequencies)** was prepared by **(Ibtesam Omran Radi Hamadi)** under our supervision at Department of Physics, College of Science, University of Babylon, as a partial fulfillment of the requirements for the degree of doctor of philosophy science in physics.

**Signature:**
**Supervisor: Dr. Samira Adnan Mahdi**

**Title: Asst. Prof**
**Address: Department of Physics, College of Science, University of Babylon**

**Date : / / 2022**

**Signature:**
**Supervisor: Dr. Hassan Jassim Motlak**

**Title : Proffesor**
**Address: Department of Electrical Engineering ,College of Engineering ,University of Babylon**

**Date : / / 2022**

## Certification of the Head of the Department

In view of the available recommendation, I forward this proposal of thesis for debate by the examination committee.

**Signature:**
**Name: Dr. Abdulazeez O. Mousa Al-Ogaili**
**Title: Professor**
**Address: Head of Physics Department,**
**College of Science, University of Babylon.**

**Date: / / 2022**

## References

[1] Inbaraj, D., Kailasam, M., and Sankararajan, R. (2018). Statistical analysis on ambient RF energy harvesting for low-power wireless applications. *International Journal of Communication Systems*, *31*(8), e3538.

[2] Ostaffe, H. (2017). RF-based wireless charging and energy harvesting enables new applications and improves product design. Powercast Corporation.

[3] Md Din, N., Chakrabarty, C. K., Bin Ismail, A., Devi, K. K. A., and Chen, W. Y. (2012). Design of RF energy harvesting system for energizing low power devices. Progress In Electromagnetics Research, 132, 49-69.

[4] Srinivasu, G., Sharma, V. K., and Anveshkumar, N. (2019). A Survey on Conceptualization of RF Energy Harvesting. *Journal of Applied Science and Computations (JASC)*, *6*(2), 791-800.

[5] Sivaramakrishnan, A., and Jegadishkumar, K. J. (2011). A highly efficient power management system for charging mobile phones using RF energy harvesting. *International Journal of Information Technology Convergence and Services*, *1*(5), 21.

[6] Bouchouicha, D., Dupont, F., Latrach, M., and Ventura, L. (2010, March). Ambient RF energy harvesting. In *International Conference on Renewable Energies and Power Quality* (Vol. 13, pp. 2-6).

[7] Ojaroudi, M., Yazdanifard, S., Ojaroudi, N., and Naser-Moghaddasi, M. (2010). Small square monopole antenna with enhanced bandwidth by using inverted T-shaped slot and conductor-backed plane. *Transactions on Antennas and Propagation*, *59*(2), 670-674.

[8] Mikeka, C., Arai, H., Georgiadis, A., and Collado, A. (2011, September). DTV band micropower RF energy-harvesting circuit architecture and performance analysis. In *2011 IEEE International Conference on RFID-Technologies and Applications* (pp. 561-567).

[9] Arrawatia, M., Baghini, M. S., and Kumar, G. (2011, January). RF energy harvesting system from cell towers in 900MHz band. In *2011 National Conference on Communications (NCC)* (pp. 1-5).

[10] Nintanavongsa, P., Muncuk, U., Lewis, D. R., and Chowdhury, K. R. (2012). Design optimization and implementation for RF energy harvesting circuits. *Journal on emerging and selected topics in circuits and systems*, *2*(1), 24-33.

[11] Hong, S. S. B., Ibrahim, R. B., Khir, M. H. M., Zakariya, M. A. B., and Daud, H. (2013). WI-FI energy harvester for low power RFID application. *Progress In Electromagnetics Research C*, *40*, 69-81.

[12] Barroca, N., Saraiva, H. M., Gouveia, P. T., Tavares, J., Borges, L. M., Velez, F. J., and Balasingham, I.. (2013, September). Antennas and circuits for ambient RF energy harvesting in wireless body area networks. In *2013 IEEE 24th annual international symposium on personal, indoor, and mobile radio communications (PIMRC)* (pp. 532-537).

[13] Ali, E. M., Yahaya, N. Z., Perumal, N., and Zakariya, M. A. (2014). Design of RF to DC rectifier at GSM band for energy harvesting applications. A Journal of Engineering, Science and Society, 10(2), 15-22.

[14] Akter, N., Hossain, B., Kabir, H., Bhuiyan, A. H., Yeasmin, M., and Sultana, S. (2014). Design and performance analysis of 10-stage voltage doublers RF energy harvesting circuit for wireless sensor network. Journal of Communications Engineering and Networks, 2(2), 84-91.

[15] Siddhesh, S., Jagdale, and Roshan, L. K.(2015, May) RF Energy Harvesting for 2110MHz -2170MHzBand. *International Journal of Engineering Research and Technology (IJERT), Vol. 4 Issue 05,* ISSN: 2278-0181*.*

[16] Lee, T. J., Patil, P., Hu, C. Y., Rajabi, M., Farsi, S., and Schreurs, D. M. P. (2015, January). Design of efficient rectifier for low-power wireless energy harvesting at 2.45 GHz. In 2015 IEEE Radio and Wireless Symposium (RWS) (pp. 47-49).

[17] Zeng, M., Andrenko, A. S., Liu, X., Zhu, B., Li, Z., and Tan, H. Z. (2016, September). Differential topology rectifier design for ambient wireless energy harvesting. In 2016 IEEE International conference on RFID technology and applications (RFID-TA) (pp. 97-101).

[18] Bakkali, A., Pelegrí-Sebastiá, J., Sogorb, T., Llario, V., and Bou-Escriva, A. (2016). A dual-band antenna for RF energy harvesting systems in wireless sensor networks. Journal of Sensors, 2016.

[19] Shen, S., Chiu, C. Y., and Murch, R. D. (2017, July). A broadband L-probe microstrip patch rectenna for ambient RF energy harvesting. In 2017 IEEE International Symposium on Antennas and Propagation & USNC/URSI National Radio Science Meeting (pp. 2037-2038).

[20] Song, C., Huang, Y., Zhou, J., and Carter, P. (2017, May). A novel compact and frequency-tunable rectenna for wireless energy harvesting. In 2017 IEEE Wireless Power Transfer Conference (WPTC) (pp. 1-3).

[21] Amjad, O., Munir, S. W., Imeci, S. T., and Ercan, A. Ö. (2018). Design and implementation of dual band microstrip patch antenna for WLAN energy harvesting system. Applied Computational Electromagnetics Society Journal.

[22] Sedeek, A., Tammam, E., and Hasaneen, E. S. (2018, December). High efficiency 2.45 GHz low power hybrid junction rectifier for RF energy harvesting. In 2018 International Japan-Africa Conference on Electronics, Communications and Computations (JAC-ECC) (pp. 147-150).

[23 Filiz, S. A. R. I., and Yunus, U. Z. U. N. (2019). A Comparative Study: Voltage Multipliers for Rf Energy Harvesting System. Communications Faculty of Sciences University of Ankara Series A2-A3 Physical Sciences and Engineering, 61(1), 12-23.

[24] Park, S., Yang, J., and Rivas-Davila, J. (2019). A hybrid Cockcroft–Walton/Dickson multiplier for high voltage generation. IEEE Transactions on Power Electronics, 35(3), 2714-2723.

[25] Nguyen, C. V., Nguyen, M. T., Quyen, T. V., Le, A. M., Masaracchia, A., Nguyen, H. T., and Nguyen, V. Q. (2020). Hybrid solar-RF energy harvesting systems for electric operated wheelchairs. Electronics, 9(5), 752.

[26] Tafekirt, H., Pelegri-Sebastia, J., Bouajaj, A., and Reda, B. M. (2020). A sensitive triple-band rectifier for energy harvesting applications. IEEE Access, 8, 73659-73664.

[27] Ali, E. M., Yahaya, N. Z., Saraereh, O. A., Assaf, A. H. A., Alqasem, B. H., Iqbal, S., and Patel, A. V. (2021). Power Conversion Using Analytical Model of Cockcroft–Walton Voltage Multiplier Rectenna. Electronics, 10(8), 881.

[28] Yalcin, A. B., and Filiz, S. A. R. I. (2021). Efficiency Analysis for Triple Band RF Energy Harvesting. Aksaray University Journal of Science and Engineering, 5(1), 36-45.

[29] Surender, D., Halimi, M. A., Khan, T., Talukdar, F. A., Koul, S. K., and Antar, Y. M. (2022). 2.45 GHz Wi-Fi band operated circularly polarized rectenna for RF energy harvesting in smart city applications. Journal of Electromagnetic Waves and Applications, 36(3), 407-423.

[30] Roy, S., Tiang, J. J., Roslee, M. B., Ahmed, M., Kouzani, A. Z., & Mahmud, M. A. (2022). Design of a Highly Efficient Wideband Multi-Frequency Ambient RF Energy Harvester. *Sensors*, *22*(2), 424.

[31] Shariati, N. (2015). Sensitive ambient RF energy harvesting. *RMIT University*.

[32] Reddy, D. S.(2012). RF Energy Harvesting for Low Power Devices. *International Journal of Advanced Research in Electrical, Electronics and Instrumentation Engineering*., Vo l. 1. 77-82.

[33] Surendar, P., Pramodh, S., and Kannan, M. R. (2016). Wireless charging using RF energy. *International Research Journal of Engineering and Technology* .Vol.03. 1870-1872.

[34] Ungan, T., and Reindl, L. M. (2008, May). Harvesting low ambient RF-sources for autonomous measurement systems. In 2008 IEEE Instrumentation and Measurement Technology Conference (pp. 62-65).

[35] Ramachandran, M., Ramanadhan, I., Elavazhagan, S. R., and Shanmugham, B. (2017). Rectenna design of GSM band signal for energy harvesting. Int. J. Sci. Technol. Eng., 3(10), 221-226.

[36] Votis, C. I., Kostarakis, P., and Alexandridis, A. A. (2010). Design, analysis, and measurements of an antenna structure for 2.4 GHz wireless applications. International Journal of Antennas and Propagation, 2010.

[37] Mossberg, C. (2019). Energy harvesting from ambient WiFi energy: A method of harvesting and measuring ambient WiFi energy.

[38] Stutzman, W. L., and Thiele, G. A. (2012). Antenna theory and design. John Wiley and Sons.

[39] Mishra, D., De, S., Jana, S., Basagni, S., Chowdhury, K., and Heinzelman, W. (2015). Smart RF energy harvesting communications: Challenges and opportunities. IEEE Communications Magazine, 53(4), 70-78.

[40] Erol-Kantarci, M., and Mouftah, H. T. (2012). Suresense: sustainable wireless rechargeable sensor networks for the smart grid. IEEE Wireless Communications, 19(3), 30-36.

[41] Erol-Kantarci, M., and Mouftah, H. T. (2012, December). DRIFT: Differentiated RF power transmission for wireless sensor network deployment in the smart grid. In 2012 IEEE Globecom Workshops (pp. 1491-1495).

[42] Flint, I., Lu, X., Privault, N., Niyato, D., and Wang, P. (2014, December). Performance analysis of ambient RF energy harvesting: A stochastic geometry approach. In 2014 IEEE Global Communications Conference (pp. 1448-1453).

[43] Zhang, R., and Ho, C. K. (2013). MIMO broadcasting for simultaneous wireless information and power transfer. IEEE Transactions on Wireless Communications, 12(5), 1989-2001.

[44] Yan, H., Montero, J. M., Akhnoukh, A., De Vreede, L. C., and Burghartz, J. (2005, November). An integration scheme for RF power harvesting. In Proc. STW Annual Workshop on Semiconductor Advances for Future Electronics and Sensors (Vol. 2005, pp. 64-66).

[45] Nintanavongsa, P., Muncuk, U., Lewis, D. R., and Chowdhury, K. R. (2012). Design optimization and implementation for RF energy harvesting circuits. IEEE Journal on emerging and selected topics in circuits and systems, 2(1), 24-33.

[46] Bird, J. (2007). *Electrical circuit theory and technology*. Routledge.

[47] Jang, M., Kim, Y., Shin, J., and Lee, S. (2005). Characterization of erbium-silicided Schottky diode junction. IEEE electron device letters, 26(6), 354-356..

[48] Karris, S. T. (2008). *Electronic Devices and Amplifier Circuits: With Matlab Applications*. Orchard Publications.

[49] Cory, R., and Solutions, S. (2009). Schottky Diodes. *Microwave Product Digest*, 1-5.

[50] Solutions, S. (2016). Surface Mount Mixer and Detector Schottky Diodes.

[51] Schauwecker, B. (2016). Design of processing circuitry for an RF energy harvester.

[52] Ahmed, A. E., Abdullah, K., Habaebi, M. H., Ramli, H. A., and Asnawi, A. L. (2021). Rf energy harvesting wireless networks: Challenges and opportunities. Indonesian Journal of Electrical Engineering and Informatics (IJEEI), 9(1), 101-113..

[53] Jabbar, H., Song, Y. S., and Jeong, T. T. (2010). RF energy harvesting system and circuits for charging of mobile devices. IEEE Transactions on Consumer Electronics, 56(1), 247-253.

[54] Song, C., Huang, Y., Zhou, J., Carter, P., Yuan, S., Xu, Q., and Fei, Z. (2016). Matching network elimination in broadband rectennas for high-efficiency

wireless power transfer and energy harvesting. IEEE Transactions on Industrial Electronics, 64(5), 3950-3961.

[55 Kissick, W. A. (2001). Antenna System Guide (Vol. 202). US Department of Justice, Office of Justice Programs, National Institute of Justice..

[56] Raju, G. S. N. (2019). *Antennas and wave propagation*. Pearson Education India.

[57] Balanis, C. A. (2015). *Antenna theory: analysis and design*. John wiley and sons.

[58] *Nisha S.,and Madhuri S.( March 2015). Antenna and Its Application(Vol. 6,). Dept. of Computer Application, TES College of Arts and Technology, Amritsar, Punjab, India ,Dept. of Physics, Sri Sai University, Palampur, Himachal, Pradesh, India.*

[59] Carr, J. J., and George, W. (2012). *Practical antenna handbook*. McGraw-Hill Education.

[60] Wang, C., & Keech, T. (2012). Antenna models for electromagnetic compatibility analyses. US department of commerce NTIA, Tech. Rep.

[61] Weiner, M. M. (2003). *Monopole antennas*. CRC Press.

[62] Dhande, P. (2009). Antennas and its Applications. DRDO Science Spectrum, 66-78.

[63] He, Y. (2016). *Ultra-low profile VHF antennas for M2M communications via satellite* (Doctoral dissertation, University of British Columbia).

[64] Starck, P. (2018). Energy harvesting of ambient radio waves (Doctoral dissertation, Uppsala University).

[65] SRINIVAS, M. S. S. (2019). Design and development of EBG structured compact antenna for wireless applications..

[66] Fatthi Alsager, A. (2011). Design and analysis of microstrip patch antenna arrays.

[67] Penella-López, M. T., and Gasulla-Forner, M. (2011). Radiofrequency energy harvesting. In Powering Autonomous Sensors, 125-147. Springer, Dordrecht.

[68] Barnett, R. E., Liu, J., and Lazar, S. (2009). A RF to DC voltage conversion model for multi-stage rectifiers in UHF RFID transponders. IEEE Journal of solid-state circuits, 44(2), 354-370.

[69] Anchustegui Echearte, I., Jimenez Lopez, D., Gasulla Forner, M., Giuppi, F., and Georgiadis, A. (2013). A high-efficiency matching technique for low power levels in RF harvesting. In PIERS 2013 Stockholm-Progress In Electromagnetics Research Symposium. Proceedings (pp. 1806-1810). The Electromagnetics Academy.

[70] Assogba, O., Mbodji, A. K., and Diallo, A. K. (2020, February). Efficiency in RF energy harvesting systems: A comprehensive review. In 2020 IEEE International Conf on Natural and Engineering Sciences for Sahel's Sustainable Development-Impact of Big Data Application on Society and Environment (IBASE-BF) (pp. 1-10).

[71] Agrawal, S., Pandey, S. K., Singh, J., and Parihar, M. S. (2014, March). Realization of efficient RF energy harvesting circuits employing different matching technique. In Fifteenth international symposium on quality electronic design (pp. 754-761). IEEE.

[72] Mossberg, C. (2019). Energy harvesting from ambient WiFi energy: A method of harvesting and measuring ambient WiFi energy..

[73] Hameed, Z., and Moez, K. (2017). Design of impedance matching circuits for RF energy harvesting systems. *Microelectronics Journal*, *62*, 49-56.

[74] Hagerty, J. A., Helmbrecht, F. B., McCalpin, W. H., Zane, R., and Popovic, Z. B. (2004). Recycling ambient microwave energy with broad-band rectenna

arrays. IEEE Transactions on Microwave Theory and Techniques, 52(3), 1014-1024.

[75] Ghovanloo, M., and Najafi, K. (2004). Fully integrated wideband high-current rectifiers for inductively powered devices. IEEE Journal of solid-state circuits, 39(11), 1976-1984.

[76] Song, C., Huang, Y., Zhou, J., Zhang, J., Yuan, S., and Carter, P. (2015). A high-efficiency broadband rectenna for ambient wireless energy harvesting. IEEE Transactions on Antennas and Propagation, 63(8), 3486-3495.

[77] Tran, L. G., Cha, H. K., and Park, W. T. (2017). RF power harvesting: a review on designing methodologies and applications. Micro and Nano Systems Letters, 5(1), 1-16.

[78] Curty, J. P., Declercq, M., Dehollain, C., and Joehl, N. (2006). Design and optimization of passive UHF RFID systems. Springer Science and Business Media.

[79] De Vita, G., and Iannaccone, G. (2005). Design criteria for the RF section of UHF and microwave passive RFID transponders. IEEE Transactions on microwave theory and techniques, 53(9), 2978-2990.

[80] Lu, X., Wang, P., Niyato, D., Kim, D. I., and Han, Z. (2014). Wireless networks with RF energy harvesting: A contemporary survey. IEEE Communications Surveys & Tutorials, 17(2), 757-789.

[81] Mariun, N., Ismail, D., Anayet, K., Khan, N., and Amran, M. (2006). Simulation, design and construction of high voltage DC power supply at 15 kV output using voltage multiplier circuits. American Journal of applied sciences, 3(12), 2178-2183.

[82] Hameed, Z., and Moez, K. (2014). Hybrid forward and backward threshold-compensated RF-DC power converter for RF energy harvesting. IEEE Journal on Emerging and Selected Topics in Circuits and Systems, 4(3), 335-343.

[83] Boylestad, R. L., & Nashelsky, L. (2012). *Electronic devices and circuit theory*. Prentice Hall.

[84] Mazaheri, M., Scaini, V., and Veerkamp, W. E. (2003). Cause, effects, and mitigation of ripple from rectifiers. IEEE Transactions on Industry Applications, 39(4), 1187-1192.

[85] Doval-Gandoy, J., Castro, C., and Martínez, M. C. (2003). Line input AC-to-DC conversion and filter capacitor design. IEEE Transactions on Industry Applications, 39(4), 1169-1176.

[86] Rashid, M. H. (Ed.). (2017). *Power electronics handbook*. Butterworth-Heinemann.

[87] Pyakuryal, S., and Matin, M. (2013). Filter design for AC to DC converter. International Refereed Journal of Engineering and Science, 2(6), 42-49.

[88] Dinesh, k. and Veeramani R.(2016) harvesting microwave signal power from the ambient environment.*International Journal of communication and computer Technologies*, 2278-9723.

[89] Madekar, K. J., Nanaware, K. R., Phadtare, P. R., and Mane, V. S. (2016). Automatic mini CNC machine for PCB drawing and drilling. International Research Journal of Engineering and Technology (IRJET), 3(02), 1107-1108.

[90] Valentino, J., and Goldenberg, J. (2008). Introduction to computer numerical control (CNC). Prentice Hall.

[91] Choudhary, R., Titus, S. D., Akshaya, P., Mathew, J. A., and Balaji, N. (2017, August). CNC PCB milling and wood engraving machine. In 2017 International Conference On Smart Technologies For Smart Nation (SmartTechCon) (pp. 1301-1306).

[92] Ramesh, V., and Srinivasulu, M. (2016). Study on computer numerical control (CNC) machines. International Journal of Advanced Scientific Research.

[93] Selim, K. K., Wu, S., Saleeb, D. A., and Ghoneim, S. S. (2021). A Quad-Band RF Circuit for Enhancement of Energy Harvesting. Electronics, 10(10), 1160.

[94] Song, C., Huang, Y., Carter, P., Zhou, J., Yuan, S., Xu, Q., and Kod, M. (2016). A novel six-band dual CP rectenna using improved impedance matching technique for ambient RF energy harvesting. IEEE Transactions on Antennas and Propagation, 64(7), 3160-3171.

[95] Ma, Z., and Vandenbosch, G. A. (2013). Wideband harmonic rejection filtenna for wireless power transfer. IEEE Transactions on Antennas and Propagation, 62(1), 371-377.

[96] Ladan, S., Ghassemi, N., Ghiotto, A., and Wu, K. (2013). Highly efficient compact rectenna for wireless energy harvesting application. IEEE microwave magazine, 14(1), 117-122..